---- *Supporting Information* ----

The solvent determines the product in the hydrogenation of aromatic ketones using unligated RhCl₃ as catalyst precursor

Soumyadeep Chakrabortty,[a] Nils Rockstroh,[a] Stephan Bartling,[a] Henrik Lund,[a] Bernd H. Müller,[a] Paul C. J. Kamer,[a] † Johannes G. de Vries *[a]

[a] Leibniz−Institut für Katalyse e.V.

Albert-Einstein-Straße 29a, 18059 Rostock, Germany

Johannes.deVries@catalysis.de

Table of Contents

1. General considerations

The metal salts and aromatic ketones were purchased from commercial sources - Sigma Aldrich, TCI chemicals, Fluorochem and Alfa Aesar. The metal salt $RhCl_3$ (98%) used in the catalytic reaction was bought from Sigma Aldrich and TCI (for comparison of the catalytic activity) and directly used. The solvents were degassed prior to catalysis.

For GC analysis an Agilent HP6890 instrument with FID detector and a column HP530 m x 250 mm x 0.25 μm was used. GC Method details: $T_0 = 30°C$, ramp = 8°C/ min, $T_1 = 280°C$, $t_{hold} = 10$ min, $T_1 = 280°C$, ramp = 8°C/ min, $T_2 = 320°C$, $t_{hold} = 10$ min, $T_2 = 280°C$, ramp = 8°C/ min, $T_3 = 320°C$, $t_{hold} = 5$ min (T_0 is the injection temperature, then the column is heated to T_1 (ramp), t_{hold} is the holding time after heating to a certain temperature, similarly T_2 and T_3 are the temperature heated consecutively with specified ramp rate). GC-MS analysis was carried out with the same methods as described. NMR spectra were recorded on Avance 400 (^1H: 400, ^{13}C: 100 MHz) instruments operating at the denoted spectrometer frequency given in Megahertz (MHz) for the specified nucleus using $CDCl_3$ as solvent.

XRD powder patterns were recorded on a Panalytical X'Pert θ/2θ -diffractometer equipped with Xcelerator detector using automatic divergence slits and Cu Kα1/α2 radiation (40 kV, 40 mA; λ= 0.15406 nm, 0.154443 nm). Cu beta-radiation was excluded using a nickel filter foil. The measurements were performed with $0.021°s^{-1}$. Samples were mounted on silicon zero background holders. Obtained intensities were converted from automatic to fixed divergence slits (0.25°) for further analysis. Peak positions and profile were fitted with Pseudo-Voigt function using the HighScore Plus software package (Panalytical). Phase identification was done by using the database of the International Center of Diffraction Data (ICDD).

The XPS (X-ray Photoelectron Spectroscopy) measurements were performed on an ESCALAB 220iXL (Thermo Fisher Scientific) with monochromated Al Kα radiation (E = 1486.6 eV). Samples are prepared on a stainless-steel holder with conductive double-sided adhesive carbon tape. The electron binding energies were obtained with charge compensation using a flood electron source and referenced to the C 1s core level of carbon at 284.8 eV (C-C and C-H bonds). For quantitative analysis, the peaks were deconvoluted with Gaussian-Lorentzian curves using the software Unifit 2021. The peak areas were

normalized by the transmission function of the spectrometer and the element specific sensitivity factor of Scofield[1].

Scanning transmission electron microscopy (STEM) measurements were conducted at 200 kV with an aberration corrected transmission electron microscope (JEM-ARM200F, JEOL Ltd.). The microscope is further equipped with a JED-2300 energy dispersive X-ray spectrometer (JEOL) having a silicon drift detector (dry SD60GV). For general imaging, a high-angle annular dark field (HAADF) and an annular bright field (ABF) detector were used. Sample loading was done by dry deposition of the recovered catalyst nanoparticles on a holey carbon supported Cu grid (mesh 300), which was then transferred into the microscope. In the case of reaction solutions, preparation of the grids was done by transfer of a drop of the solution onto the grid and subsequent evaporation of the solvent under ambient atmosphere without any external auxiliaries applied.

Dynamic light scattering (DLS) measurements have been measured at 25°C on a Malvern Zetasizer Ultra-Red equipped with a He-Ne laser ($\lambda = 633$ nm).

2. General procedure for hydrodeoxygenation experiments

All the hydrodeoxygenation experiments were conducted in a stainless-steel autoclave (PARR Instrument Company) charged with an insert suitable for up to eight reaction vials (4mL) with teflon mini stirring bars. In a typical experiment, a reaction vessel is charged with the desired mol% of the Rh-metal salt and stirred for 10-15 min in the appropriate solvent (1-1.5 mL). Then the desired substrates (0.2 mmol) were added to the reaction vessel and the vessels were placed in a high-pressure autoclave. First the autoclave was purged once with nitrogen and two times with hydrogen. Finally, it was pressurized at 50 bar of H_2 pressure at a specific temperature. After the desired reaction time, the autoclave was depressurized, and the products were analyzed by GC-MS and GC-FID analysis using tetradecane as internal standard. The reaction mixtures were centrifuged and passed through a short silica pad in order to separate the NPs and the products were separated by the slow evaporation of the solvent and isolated as liquid at room temperature.

## 3. General procedure for hydrogenations in water

All the hydrogenation experiments were conducted in a stainless-steel autoclave (PARR Instrument Company) charged with an insert suitable for upto eight reaction vials (4mL) with teflon mini stirring bars. In a typical experiment, a reaction vessel was charged with the desired mol% of Rh-metal salt and stirred for 10-15 min in water (2 mL). Then the desired substrates (0.3 mmol) were added to the reaction vessel and the vessels were placed in a high-pressure autoclave. The autoclave was purged once with nitrogen and then two times with hydrogen. Finally, it was pressurized at 50 bar of H_2 pressure at the specified temperature. After the desired reaction time, the autoclave was depressurized, and the products were analyzed by GC-MS and GC-FID analysis using tetradecane as internal standard. The reaction mixtures were extracted in ethyl acetate and passed through a short silica pad followed by drying. All the cyclohexane-alcohols were isolated as sticky liquid at room temperature.

4. Isolation of RhNPs

The in situ formed Rh nanoparticles were isolated following the optimized reaction condition (substrate: acetophenone, solvent: TFE). The RhNPs were separated via centrifugation, washed (2 mL of TFE), and dried well (with vacuum) and submitted for spectroscopic analysis.

5. Metal precursor screening

Table S1 Different Rh-metal precursor in HDO (Heptane)
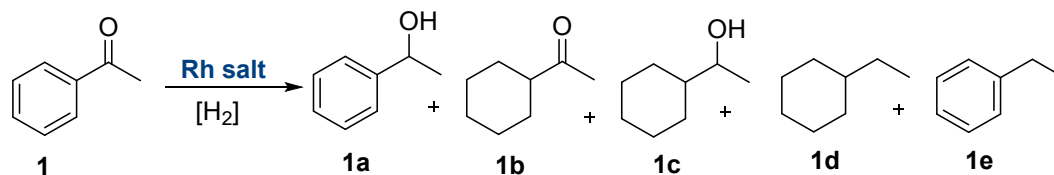
Entry	Metal salt	Conversion (%)	1b	1c	1d	1e
1	RhCl$_3$	>99	8	23	69	-
2	Rh(H)(CO)(PPh$_3$)$_3$	*No reaction*				
3	RhCl$_3$.xH$_2$O	>99	10	20	70	-

4	[Rh(acac)(COD)]	>99	28	72	-	
5	[Rh(Cl)(COD)]$_2$	>99		65	35	-
6	-	*No reaction*				

[a] Reaction condition: Rh-salt (1 mol%), substrate (0.2 mmol), H$_2$ (50 bar), **Heptane as solvent**, 10 hr, temperature (100°C). [b] Product distribution determined by GC-MS and GC-FID using internal standard.

Table S2 Different Rh-metal precursors in HDO (Trifluoroethanol)

Entry	Metal salt	Conversion (%)[b]	1b	1c	1d	1e
1	**RhCl$_3$**	**>99**			**>99**	-
2	Rh(H)(CO)(PPh$_3$)$_3$	*No reaction*				
3	RhCl$_3$.xH$_2$O	>99		<10	>90	-
4	[Rh(acac)(COD)]	>99	40	60	-	-
5	[Rh(Cl)(COD)]$_2$	>99	10	15	<75	-
6	-	*No reaction*				

[a] Reaction condition: Rh-salt (1 mol%), substrate (0.2 mmol), H$_2$ (50 bar), **TFE as solvent**, 10 h, temperature (100°C). [b] Conversion and Product distribution determined by GC-MS and GC-FID using internal standard.

6. Effect of catalyst loading in the hydrodeoxygenation of aromatic ketones
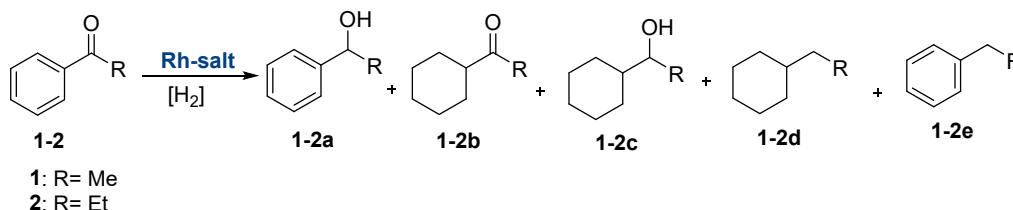
Table S3 Catalyst loading vs selectivtiy in HDO
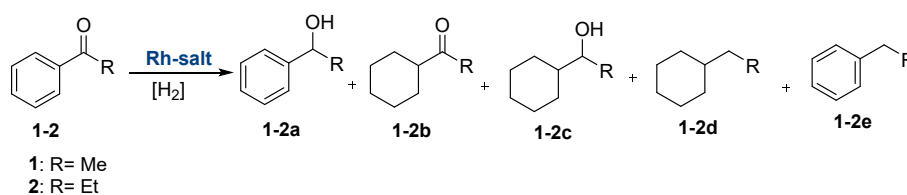
Entry	Catalyst loading (%)	Conversion (%)	1b 2b	1c 2c	1d 2d	1e 2e
1	2 mol%	>99%	-	-	>99%	-
		>99%	-	-	>99%	-
2	1.5 mol%	>99%	-	-	>99%	-
		>99%	-	-	>99%	-
3	1.0 mol%	>99%	-	-	>99%	-
		>99%	-	-	>99%	-
4	0.67 mol%	>99%	-	-	>99%	-
		>99%	-	-	>99%	-
5	0.5 mol%	>99%	>30%	-	69%	-
		>99%	>28%	-	71%	-
6	0.4 mol%	>99%	>30%	-	69%	-
		>99%	>28%	-	71%	-

7. Effect of temperature in the hydrodeoxygenation of aromatic ketones

Table S4 Selectivity at different temperatures in HDO

1-2

1: R= Me
2: R= Et

Entry	Temperature (°C)	Conversion (%)	1b 2b	1c 2c	1d 2d	1e 2e
1	100°C	>99%	-	-	>99%	-
		>99%	-	-	>99%	-
2	90°C	>99%	-	-	>99%	-
		>99%	-	-	>99%	-
3	80°C	>99%	-	-	>99%	-
		>99%	-	-	>98%	-
4	70°C	>99%	>35%	-	64%	-
		>99%	>32%	-	66%	-

[a] Reaction condition: RhCl$_3$ (1 mol%), substrate , H$_2$ (50 bar), **TFE as solvent**, 10 h, temperature (specified in the table). [b] Conversion and Product distribution determined by GC-MS and GC-FID using internal standard

8. Upscaling of HDO experiments

The upscaling of hydrodeoxygenation experiments were conducted in a stainless-steel autoclave (PARR Instrument Company) charged with an insert suitable for upto reaction vials (10mL) with teflon mini stirring bars. In a typical experiment, a reaction vessel is charged with desired mol% of defined Rh-metal salt and stirred for 10-15 mins in the appropriate solvent (6-7 mL). Then the desired substrates (10 mmol) were added to the reaction vials and the vessels were placed in a high-pressure autoclave. First the autoclave was purged once with nitrogen and two times with hydrogen. Finally, it was pressurized at 50 bar of H$_2$ pressure at specific temperature. After the desired reaction time, the autoclave was depressurized, and the products were analyzed by GC-MS and GC-FID analysis using tetradecane.
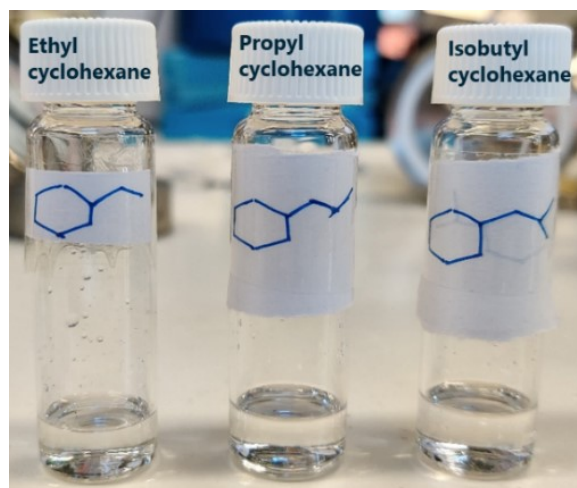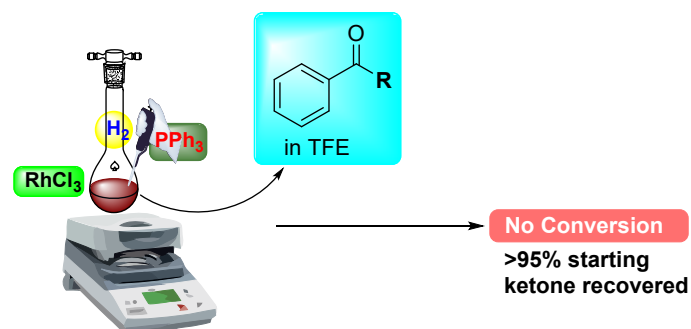
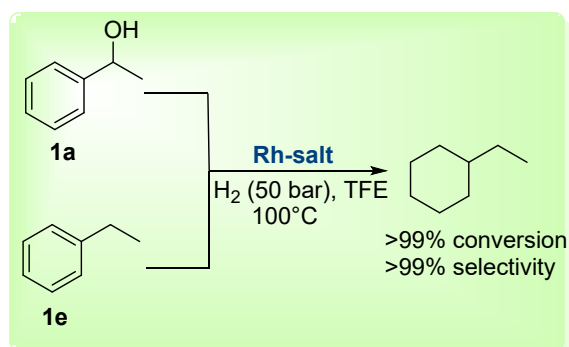*Figure S1* Isolated cyclohexane derivatives from the 10 mmol scale reactions

9. Phosphine addition experiment

[a]Reaction condition: RhCl$_3$ (1 mol%), substrate (0.3 mmol) , 0.2 eqv. of PPh$_3$, H$_2$ (50 bar), **TFE as solvent**, 10 h, temperature (100°C).

Figure S2 Phosphine addition test.[a]

## 10. Screening of other substrates (possible intermediates) in HDO

Scheme S1 Employing the optimized reaction condition on **1a** and **1e**.[a]

[a]Reaction condition: RhCl$_3$ (1 mol%), substrate (0.2 mmol) , H$_2$ (50 bar), **TFE as solvent**, 10 h, temperature (100°C). Conversion and Product distribution determined by GC-FID using internal standard

11. Recycling experiments

The catalyst recycling experiment was carried out following the hydrodeoxygenation (HDO) reaction condition. The *in-situ* formed NPs were isolated upon centrifugation after the 1st run and washed with trifluoroethanol twice and then used for the next run.

1st run: >99% selectivity
2nd run: >80% selectivity
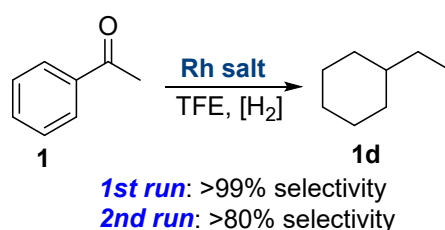
Scheme S 2 *Recycling experiment in hydrodeoxygenation using acetophenone as substrate* [a]

[a] Reaction condition: Rh-salt (1 mol%), substrate (2.0 mmol), H_2 (50 bar), **Trifluoroethanol (TFE) as solvent**, 10 hr, temperature (100°C). [b] Product distribution determined by GC-MS and GC-FID using internal standard. For 2nd run full conversion of acetophenone was observed.

12. PXRD of RhNPs
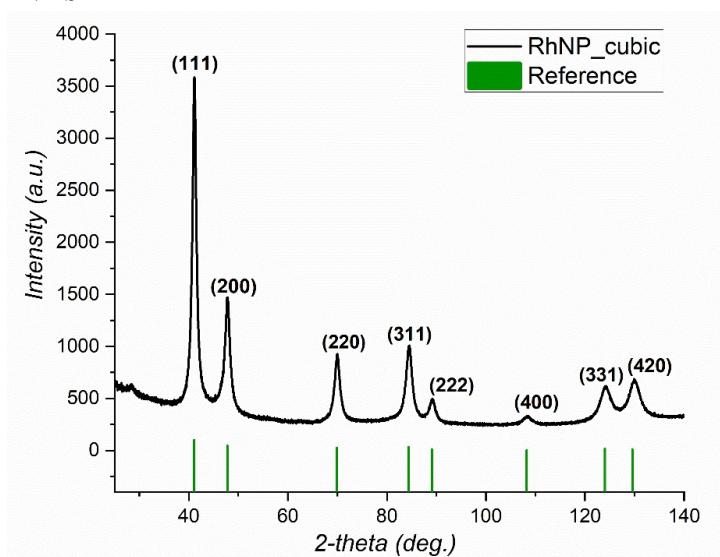
Figure S3 PXRD pattern of isolated Rh nanoparticle (Cu radiation).

Scherrer-Working-Sheet

K(beta)	1,07470						
Lamda	1,54056						

sample	d	λ/2d	h k l	theta [°]	theta [rad]	cos(theta)	beta	beta [rad]	size [nm]	average [nm]
	2,19539	0,35086	1 1 1	20,540	0,358	0,936	1,43127	0,025	7	6
	1,90264	0,40485	2 0 0	23,882	0,417	0,914	1,82385	0,032	6	
	1,34444	0,57294	2 2 0	34,955	0,610	0,820	2,0884	0,036	6	
	1,14681	0,67167	3 1 1	42,196	0,736	0,741	2,28761	0,040	6	
	1,09808	0,70148	2 2 2	44,546	0,777	0,713	2,06995	0,036	6	

Figure S 4 Crystallite size is calculated by applying the Scherrer equation using the integral breadth under the assumption of spherically shaped crystallites. K is set to 1.0747. Sizes were calculated of the (111), (200), (220), (311) and (222) Bragg peak and the mean value is presented, respectively.
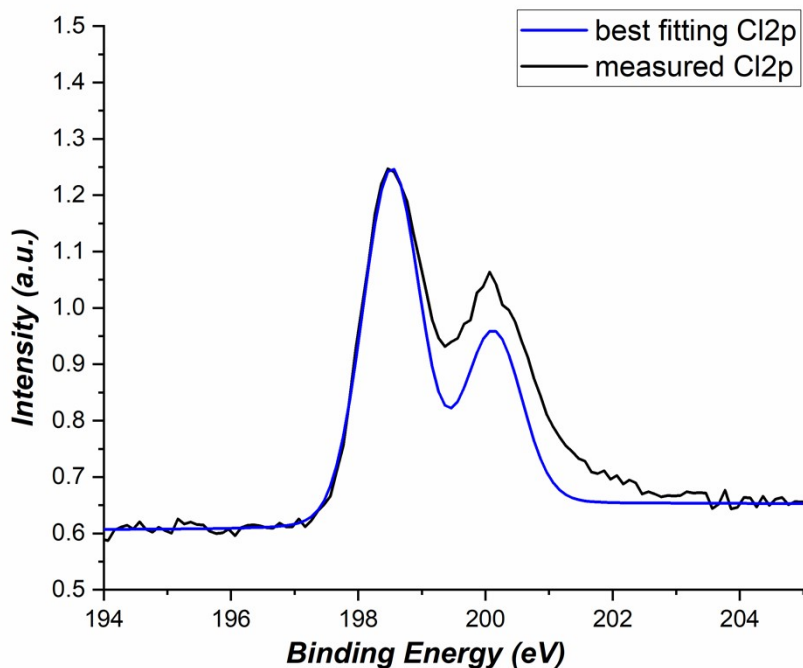
13. XPS and EDX

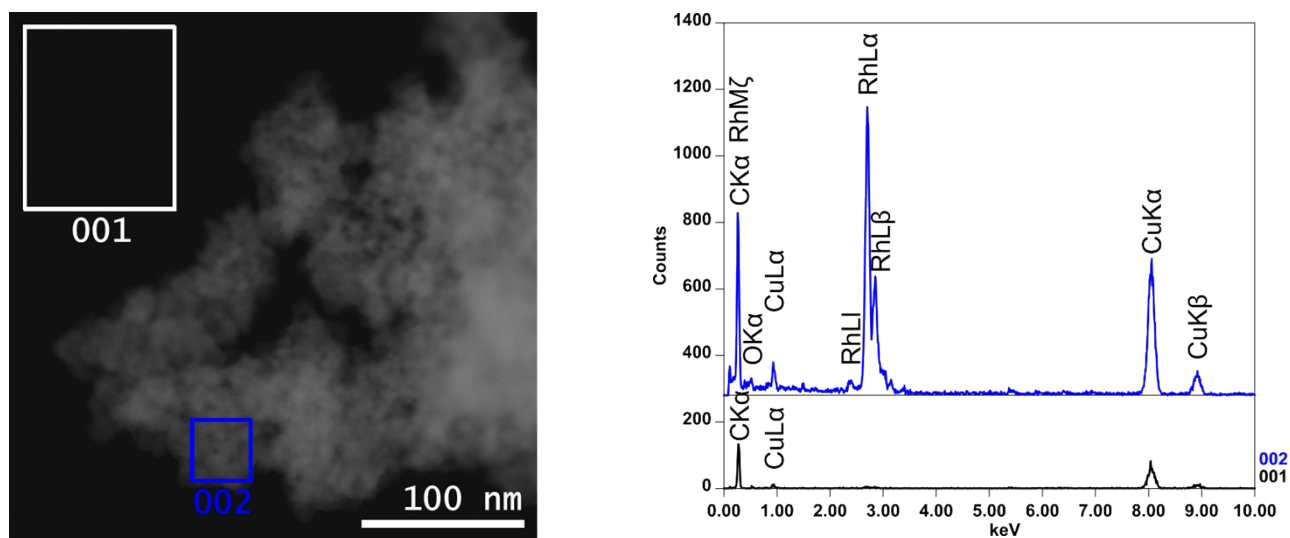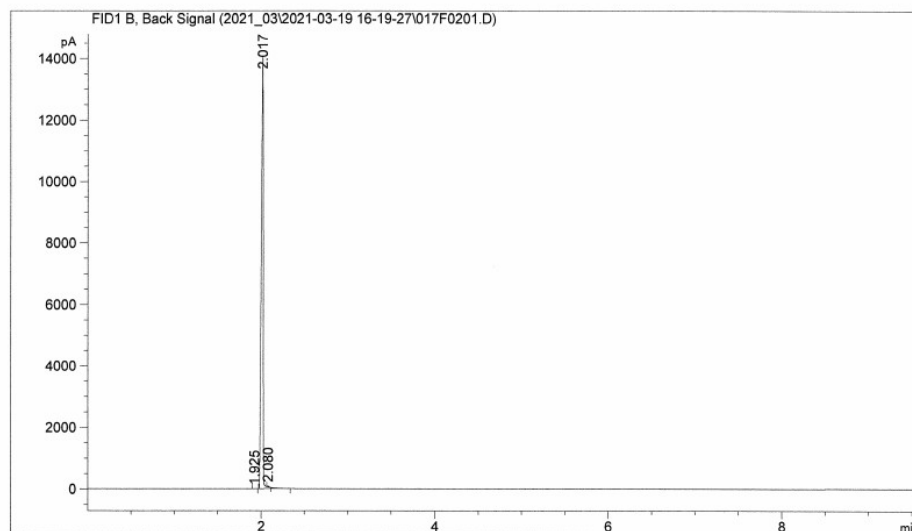***Figure S5*** XP spectrum of Cl 2p.

Figure S6 Selected EDX spectra of the marked areas of Rh nanoparticles (left) are shown on the right. Spectrum 001 shows the background (carbon of the grid) while in spectrum 002 almost exclusively metallic rhodium can be seen. Just note that the location of the peaks of Cl⁻ is almost the same (2.621 and 2.815 keV) as those from Rh so that the presence of Cl⁻ cannot be proven with this method. Comparison with spectra from Cl rich materials (see 19.) however implies no or only negligible amounts of Cl⁻ here.

14.GC Chromatogram and GC-MS

```
================================================================
Acq. Operator    : SYSTEM                     Seq. Line :    2
Acq. Instrument  : GC Lab 2.229               Location  : Vial 17
Injection Date   : 3/19/2021 4:45:24 PM          Inj :    1
                                              Inj Volume : 1 µl
Method           : C:\CHEM32\1\DATA\2021_03\2021-03-19 16-19-27\PIM5.M (Sequence
                   Method)
Last changed     : 3/19/2021 4:19:27 PM by SYSTEM
Method Info      : HP5;30mx0.32/0.25: 80/2/10-160/0/15-240/0/15-30/10; 1.5mL/min const
                   .flow; 280i/320d; Split70
```



```
================================================================
                     Area Percent Report
================================================================


Sorted By           :        Signal
Multiplier          :        1.0000
Dilution            :        1.0000
Use Multiplier & Dilution Factor with ISTDs


Signal 1: FID1 B, Back Signal

Peak RetTime Type  Width     Area        Height     Area
 #   [min]        [min]    [pA*s]        [pA]        %
----|-------|----|-------|----------|----------|--------|
  1   1.925 BB    0.0219    3.02799     2.08957   0.01400
  2   2.017 BB S  0.0266 2.15771e4   1.43134e4  99.77796
  3   2.080 BB X  0.0170   44.98775    40.26681   0.20803

Totals :                 2.16252e4   1.43557e4


================================================================
                    *** End of Report ***
================================================================
```

Figure S7 GC Chromatogram of Trifluoroethanol (TFE) used in all the catalytic reactions

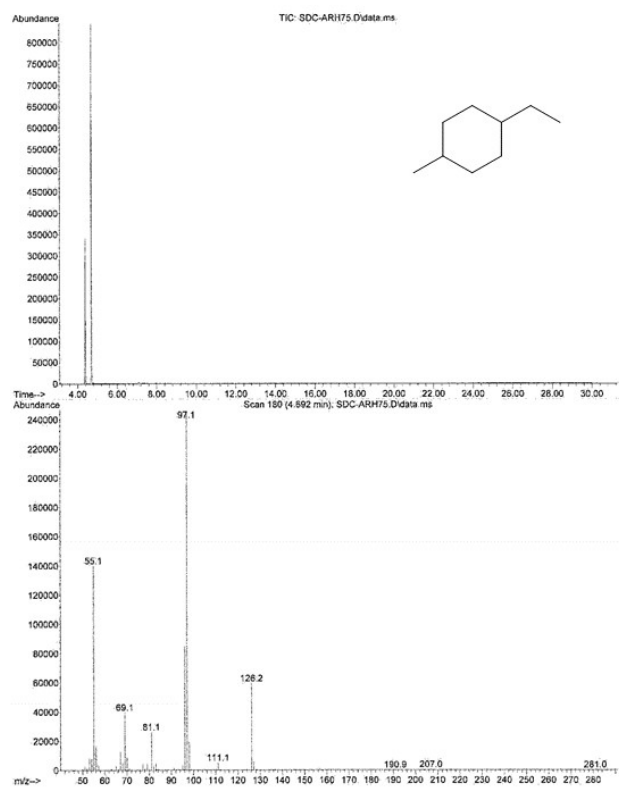- **Few prototypical Gas Chromatography-Mass Spectrometry (GC-MS)**
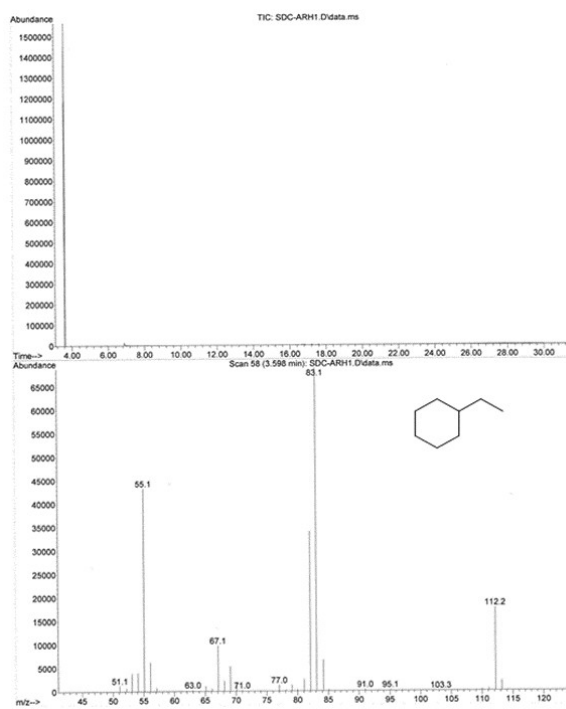
Figure S8 GC-MS spectrum of **1d**.
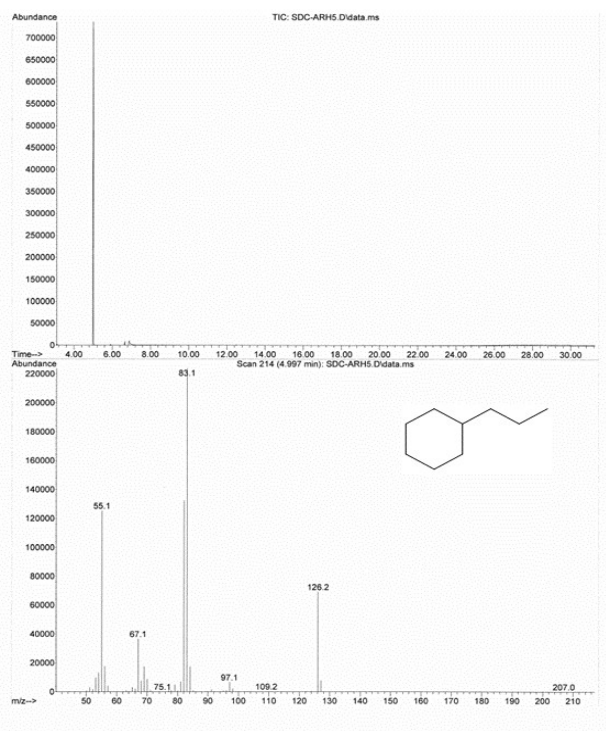
Figure S9 GC-MS spectrum of **2d**
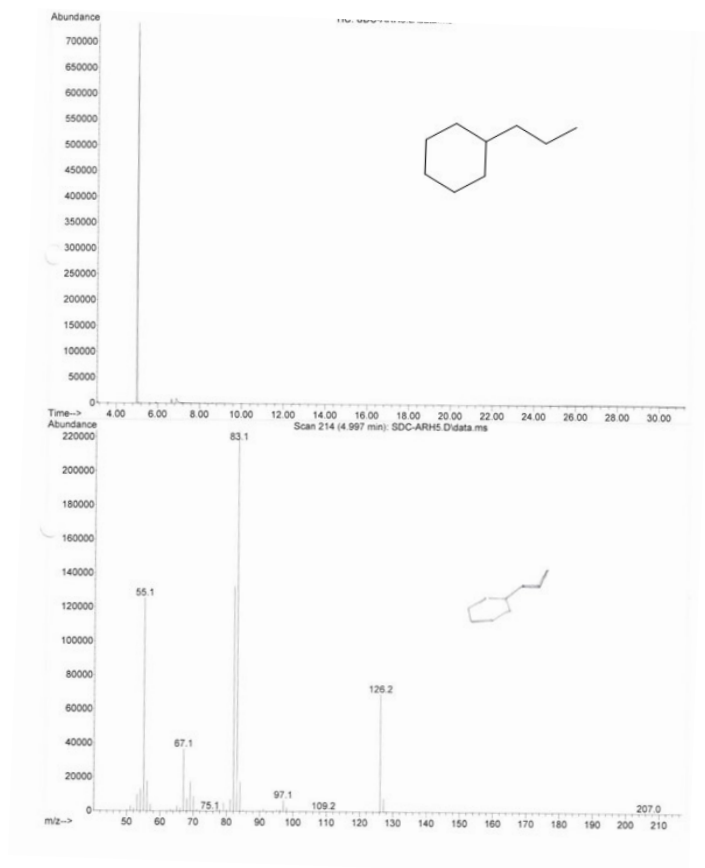
Figure S10 GC-MS spectrum of **2d**

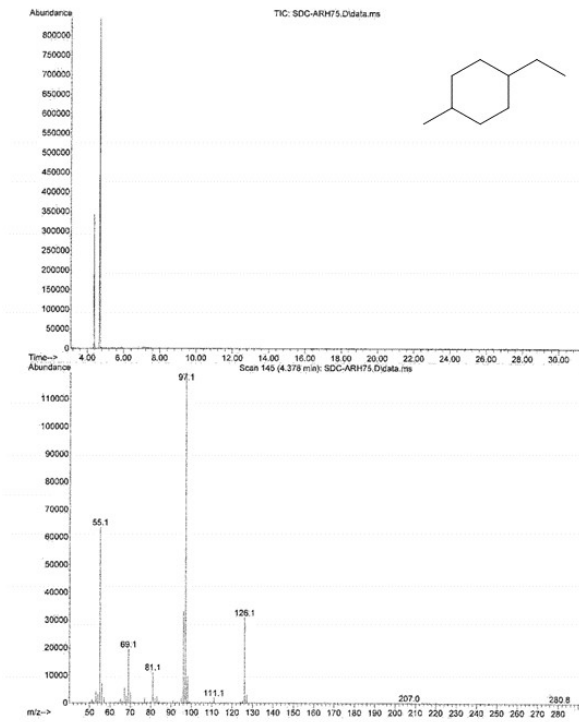***Figure S11*** GC-MS spectrum of **9d**
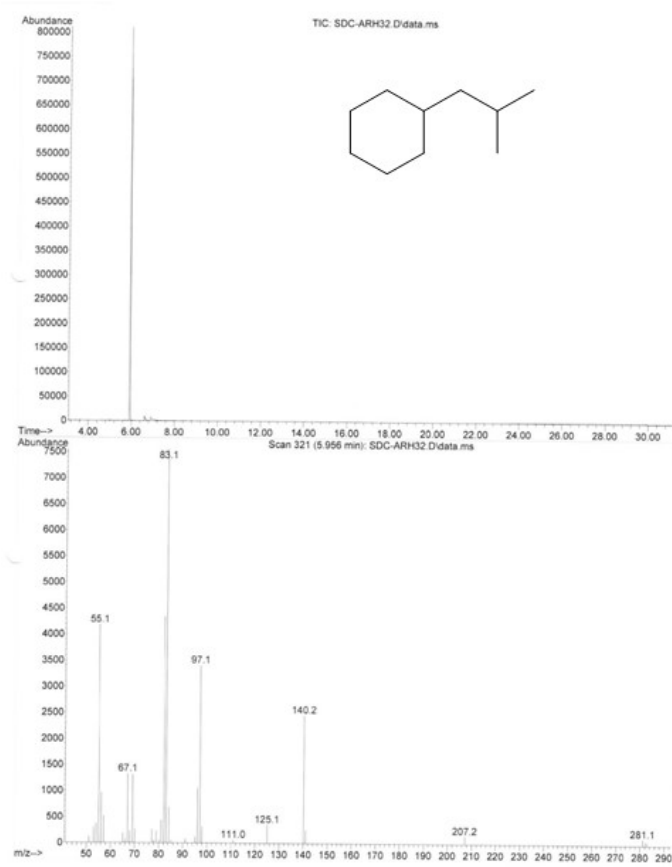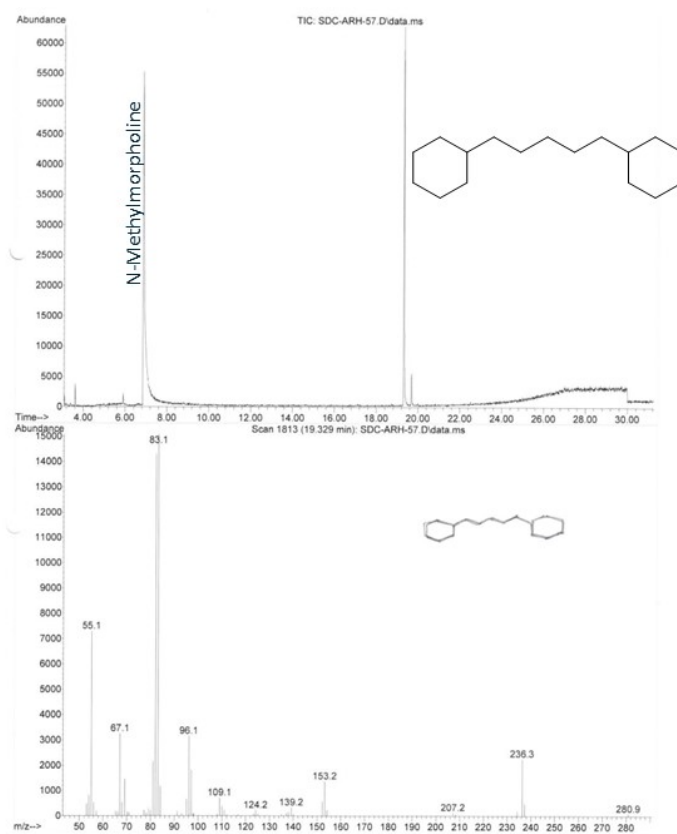
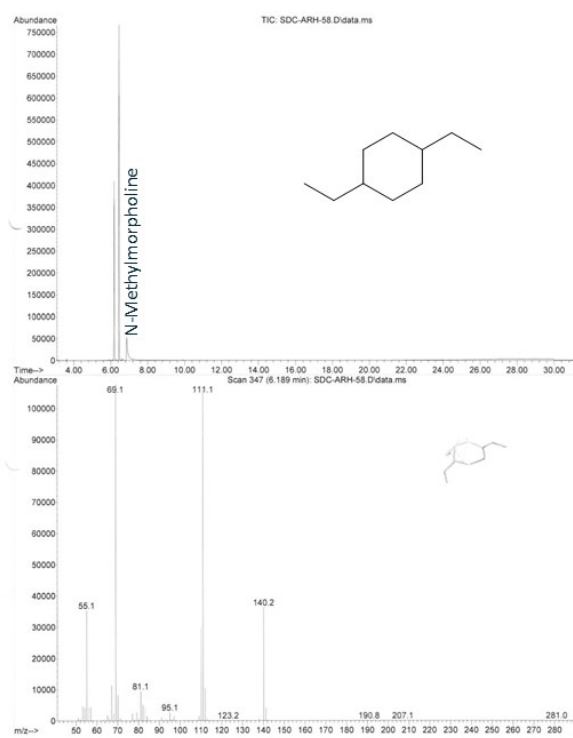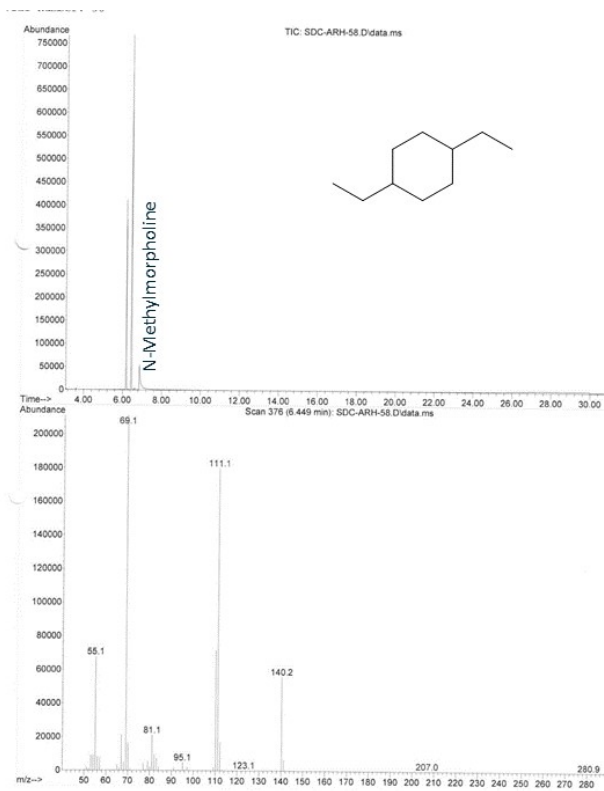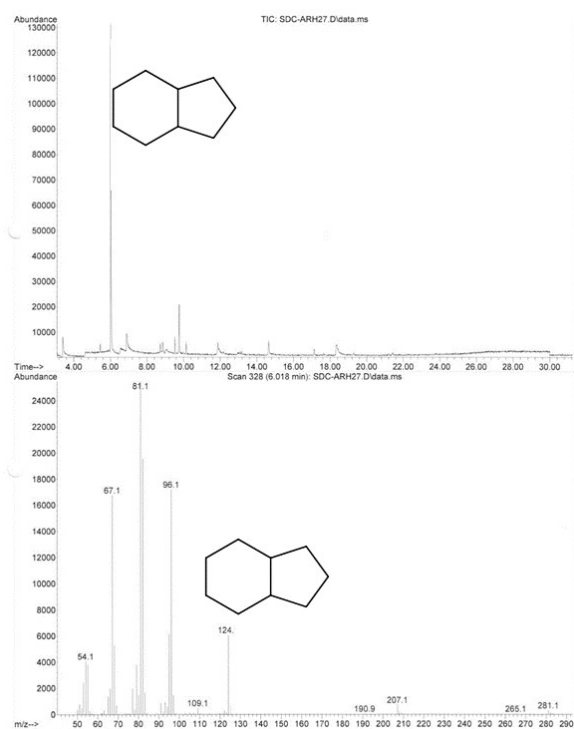***Figure S12*** GC-MS spectrum of **9d**

Figure S13 GC-MS spectrum of **3d**

Figure S14 GC-MS spectrum of **28d**
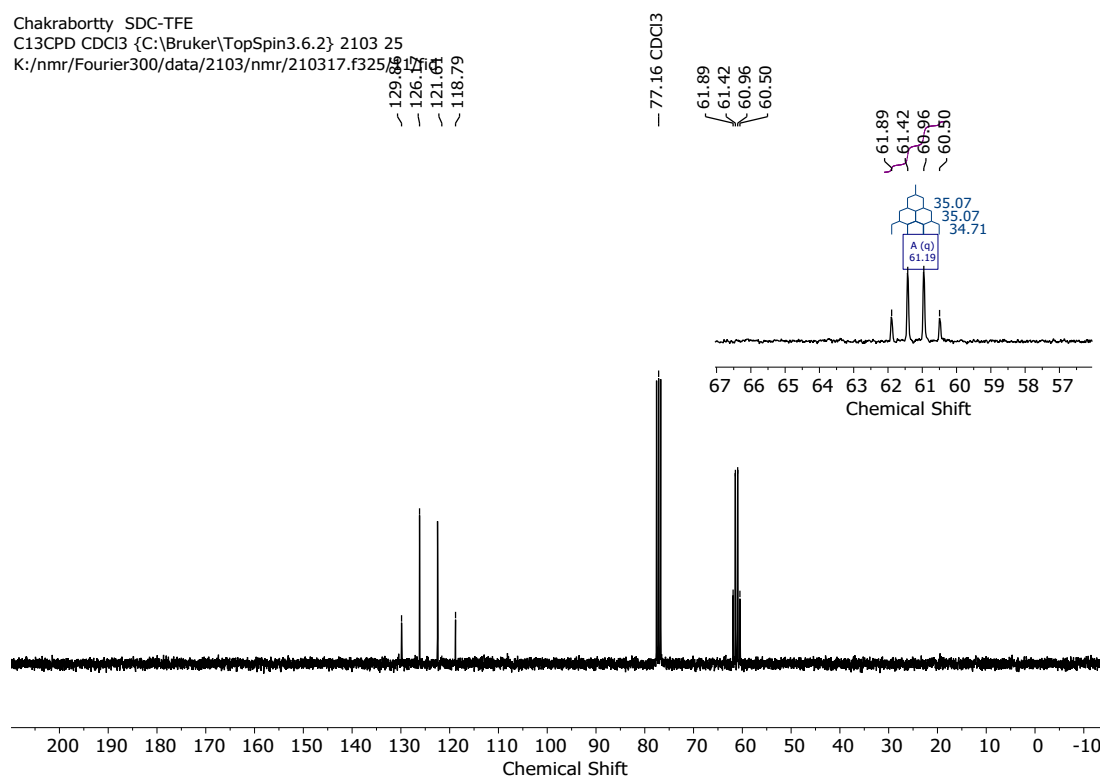

Figure S15 GC-MS spectrum of **8d**

Figure S16 GC-MS spectrum of **8d**

Figure S17 GC-MS spectrum of **10d**

15. NMR spectra

—7.26 CDCl3

3.96
3.93
3.90
3.88

8.76
8.70
8.70

A (q)
3.92

4.4 4.3 4.2 4.1 4.0 3.9 3.8 3.7 3.6 3.5
Chemical Shift

2.05
1.00

16 15 14 13 12 11 10 9 8 7 6 5 4 3 2 1 0 -1 -2 -3
Chemical Shift
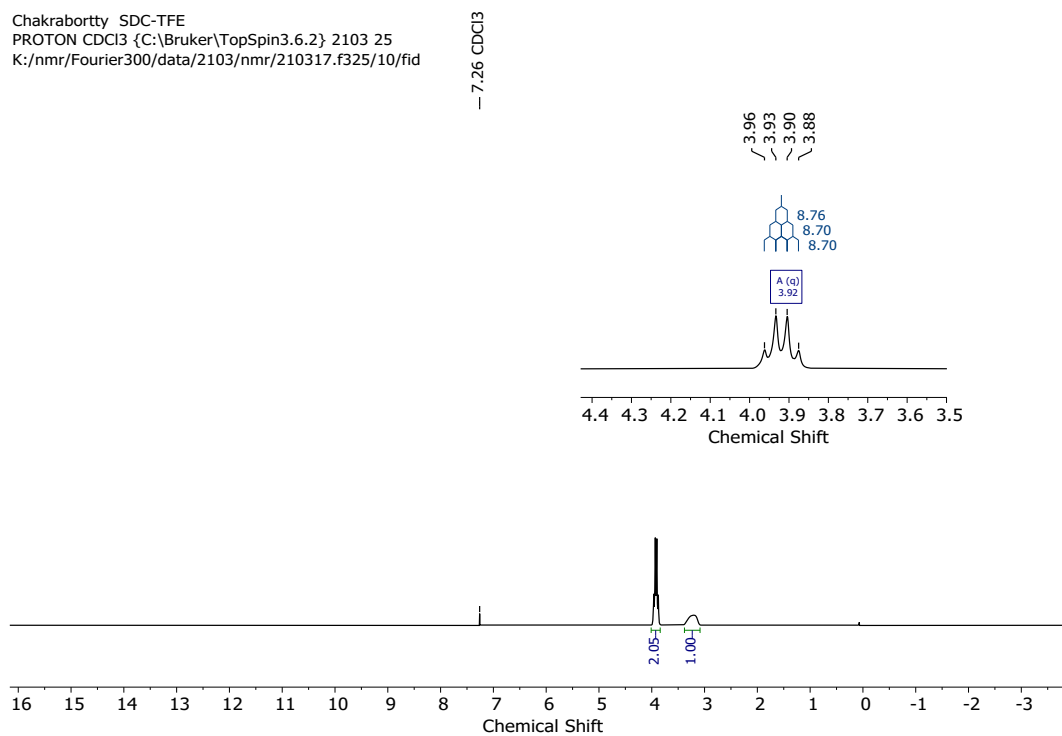
Figure S18 ^{1}H NMR of Trifluroethanol (TFE) used in all the catalytic reaction (CDCl$_3$, 400 MHz)

129.86
126.17
121.61
118.79

—77.16 CDCl3

61.89
61.42
60.96
60.50

61.89
61.42
60.96
60.50

35.07
35.07
34.71

A (q)
61.19

67 66 65 64 63 62 61 60 59 58 57
Chemical Shift

200 190 180 170 160 150 140 130 120 110 100 90 80 70 60 50 40 30 20 10 0 -10
Chemical Shift

Figure S19 ^{13}C NMR of Trifluroethanol (TFE) used in all the catalytic reaction (CDCl$_3$, 100 MHz)

16

SDC-ArH-60

— 7.26 CDCl3

1.75
1.60
1.27
1.12
0.89
0.87
0.84

— 0.89
— 0.87
— 0.84

1.00   0.90   0.80   0.70   0.60
Chemical Shift

6.03
6.05
3.18

16 15 14 13 12 11 10 9 8 7 6 5 4 3 2 1 0 -1 -2 -3
Chemical Shift
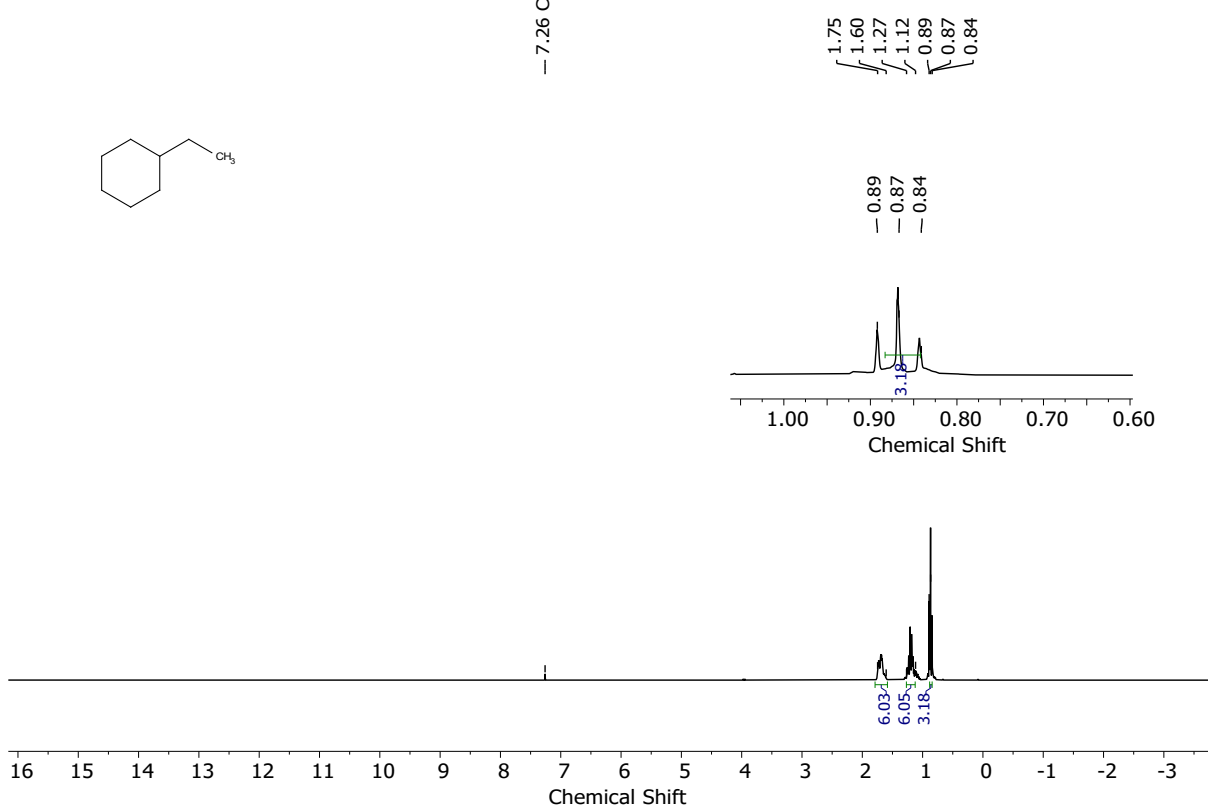
Figure S20 ¹H NMR of **1d** (CDCl₃, 400 MHz)

SDC-ArH-60

— 77.16 CDCl3

39.68
33.22
30.28
26.97
26.64

— 11.57

20 210 200 190 180 170 160 150 140 130 120 110 100 90 80 70 60 50 40 30 20 10 0 -10
Chemical Shift
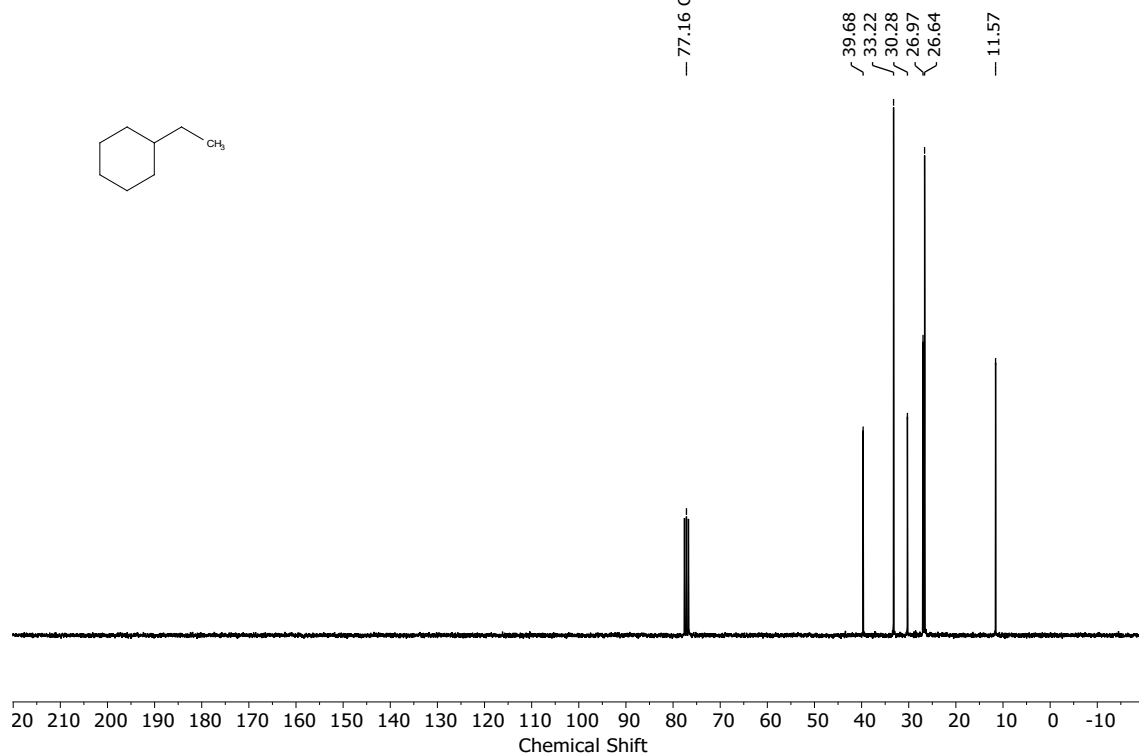
Figure S21 ¹³C NMR of **1d** (CDCl₃, 100 MHz)

17

SDC-ArH-61

— 7.26 CDCl3

1.76
1.62
1.38
1.11
0.91
0.88
0.86

0.91
0.88
0.86

3.27

1.00 0.95 0.90 0.85 0.80 0.75 0.70
Chemical Shift

5.61
3.28
5.39
3.27

16 15 14 13 12 11 10 9 8 7 6 5 4 3 2 1 0 -1 -2 -3
Chemical Shift
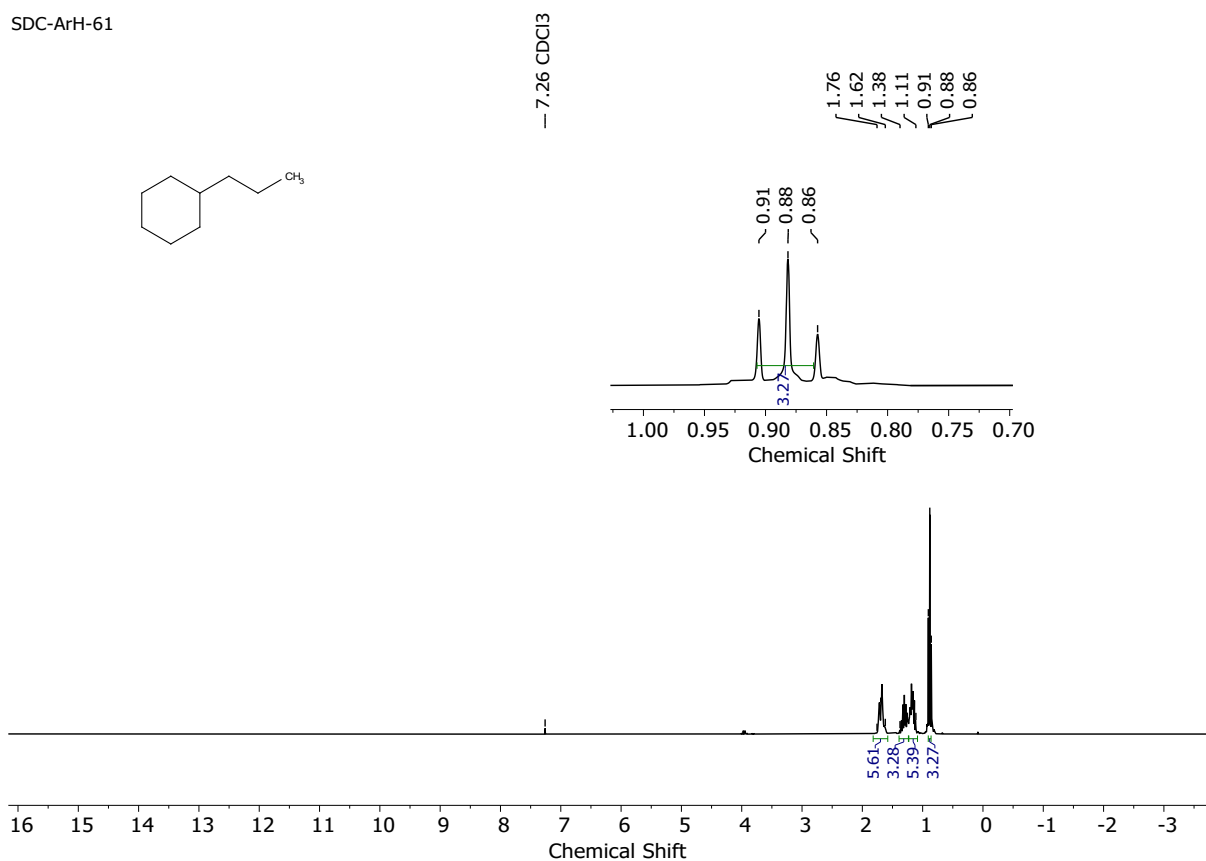
Figure S22 ^1H NMR of **2d** (CDCl$_3$, 400 MHz)

SDC-ArH-61

— 77.16 CDCl3

40.09
37.61
33.64
26.98
26.67
19.64
14.56

210 200 190 180 170 160 150 140 130 120 110 100 90 80 70 60 50 40 30 20 10 0 -10
Chemical Shift
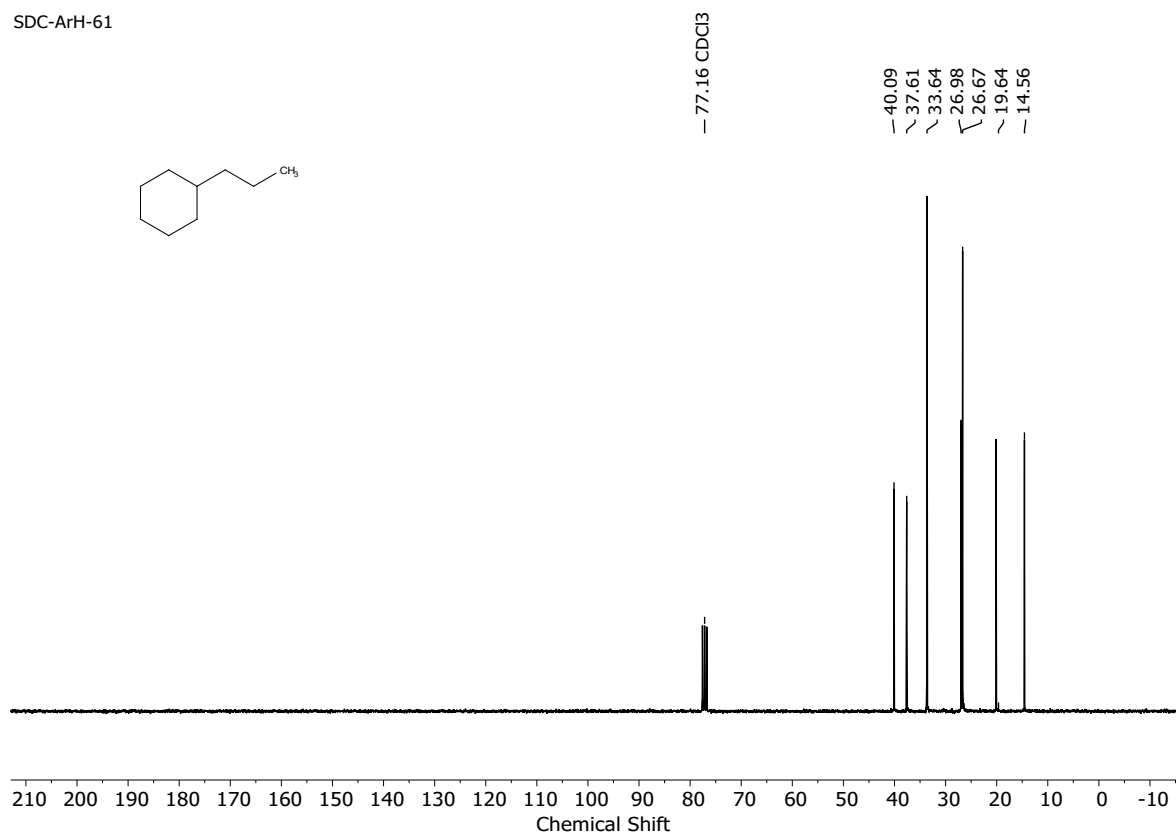
Figure S23 ^{13}C NMR of **2d** (CDCl$_3$, 100 MHz)

SDC-ArH-77
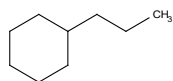
7.26 CDCl3

1.73
1.65
1.36
1.11
0.90
0.88
0.85

5.50
0.15
8.51
3.84

16 15 14 13 12 11 10 9 8 7 6 5 4 3 2 1 0 -1 -2 -3
Chemical Shift
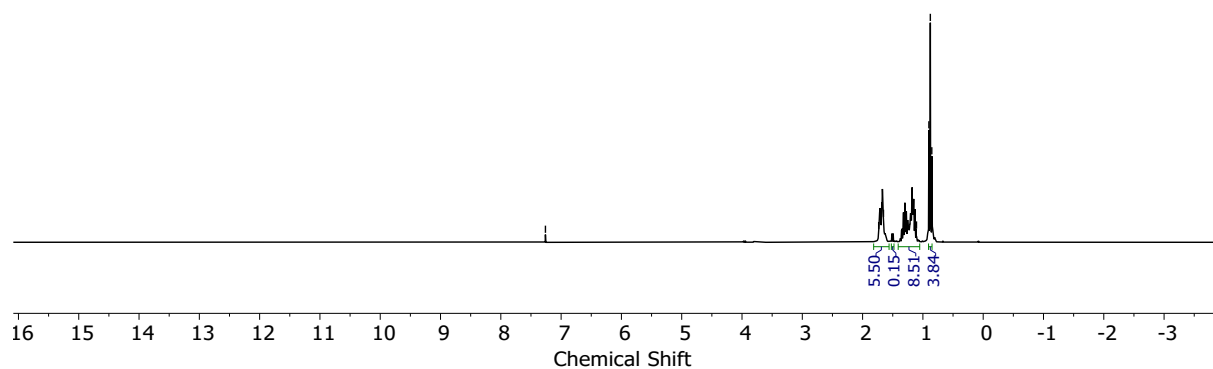
Figure S24 [superscript]1[/superscript]H NMR of **2d** (CDCl$_3$, 400 MHz) (from non-benzylic ketone **25**)

SDC-ArH-77
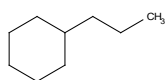
77.16 CDCl3

40.07
37.59
33.62
26.96
26.65
20.60
14.56

270 250 230 210 190 170 150 130 110 90 70 50 30 10 -10
Chemical Shift
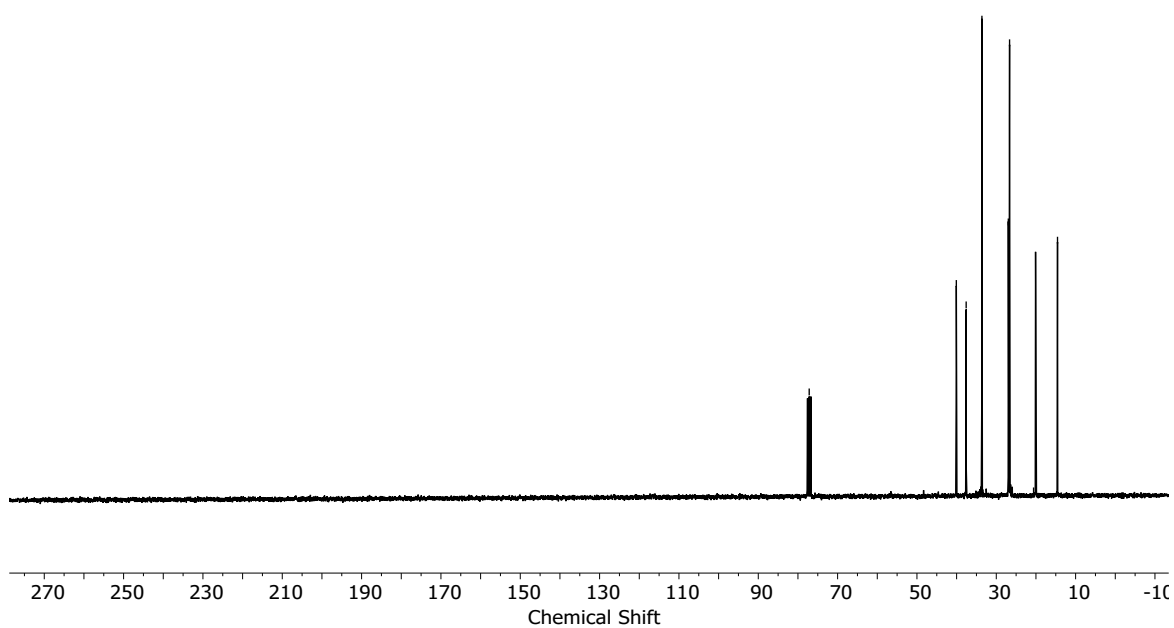
Figure S25 [superscript]13[/superscript]C NMR of **2d** (CDCl$_3$, 100 MHz) (from non-benzylic ketone **25**)

19

SDC-ArH-62

—7.26 CDCl3

1.74
1.61
1.31
1.12
1.06
1.04
1.01
0.87
0.85

0.95 0.90 0.85 0.80 0.75 0.70
Chemical Shift

TFE

6.39
4.50
2.31
6.31

16 15 14 13 12 11 10 9 8 7 6 5 4 3 2 1 0 -1 -2 -3
Chemical Shift
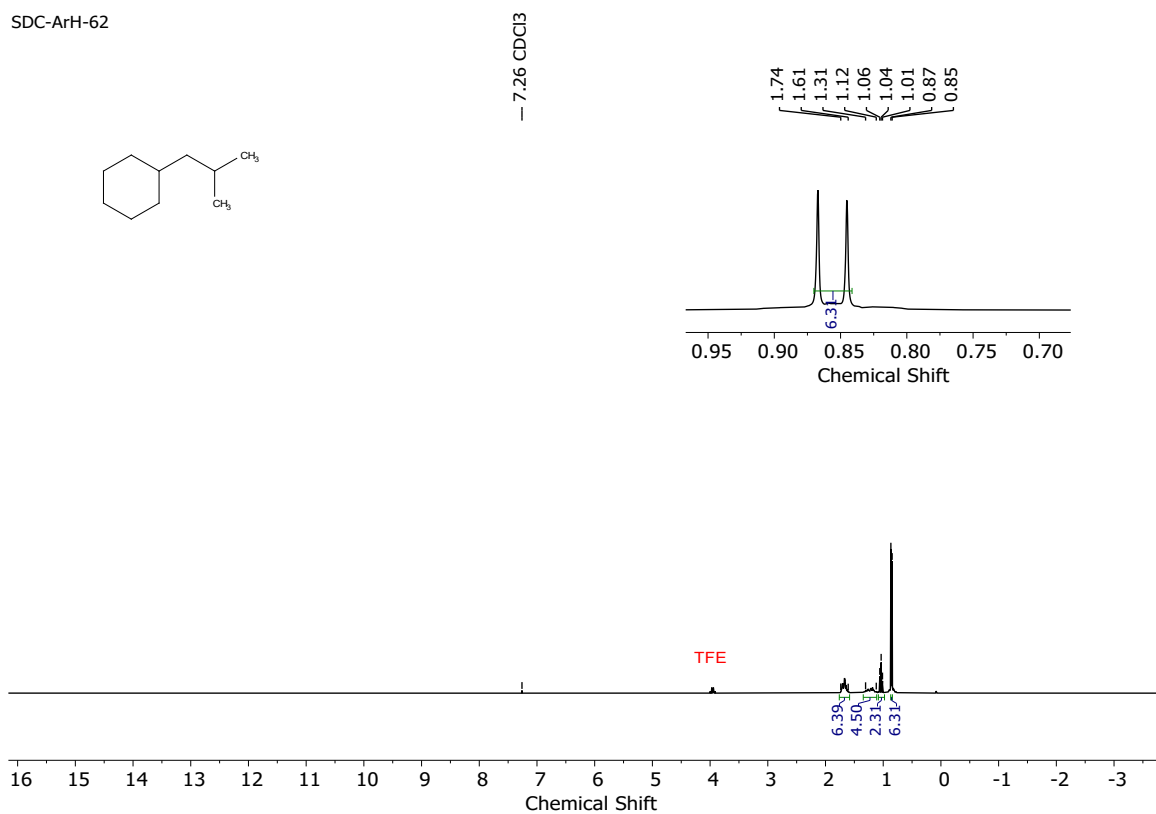
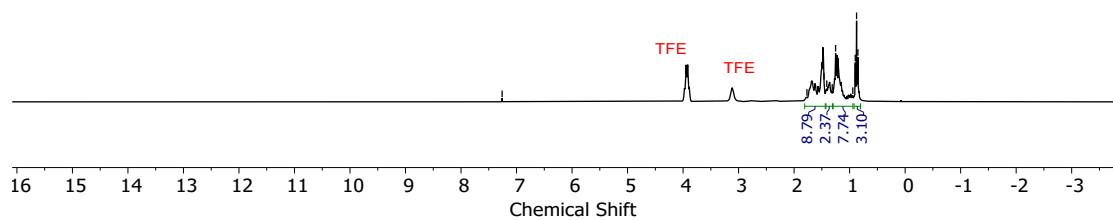*Figure S26* ¹H NMR of **3d** (CDCl₃, 400 MHz)

SDC-ArH-62

—77.16 CDCl3

—47.33

35.76
33.86
27.00
26.66
24.83
23.07

20 210 200 190 180 170 160 150 140 130 120 110 100 90 80 70 60 50 40 30 20 10 0 -10
Chemical Shift
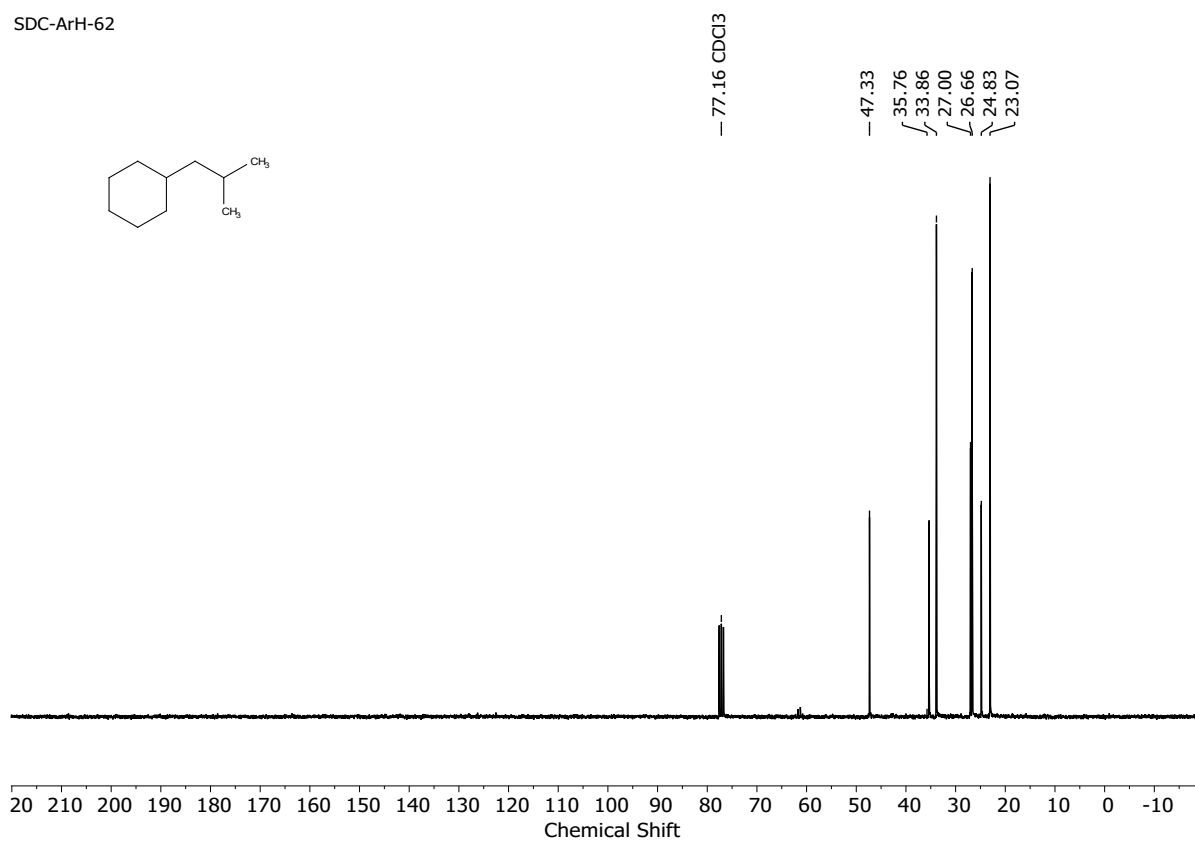
Figure S27 ¹³C NMR of **3d** (CDCl₃, 100 MHz)

20

SDC-ArH-84

— 7.26 CDCl3

2.74
2.54
1.73
1.53
1.28
1.07
0.91
0.83

TFE

4.17
4.35
7.81
3.67

16 15 14 13 12 11 10 9 8 7 6 5 4 3 2 1 0 -1 -2 -3

Chemical Shift
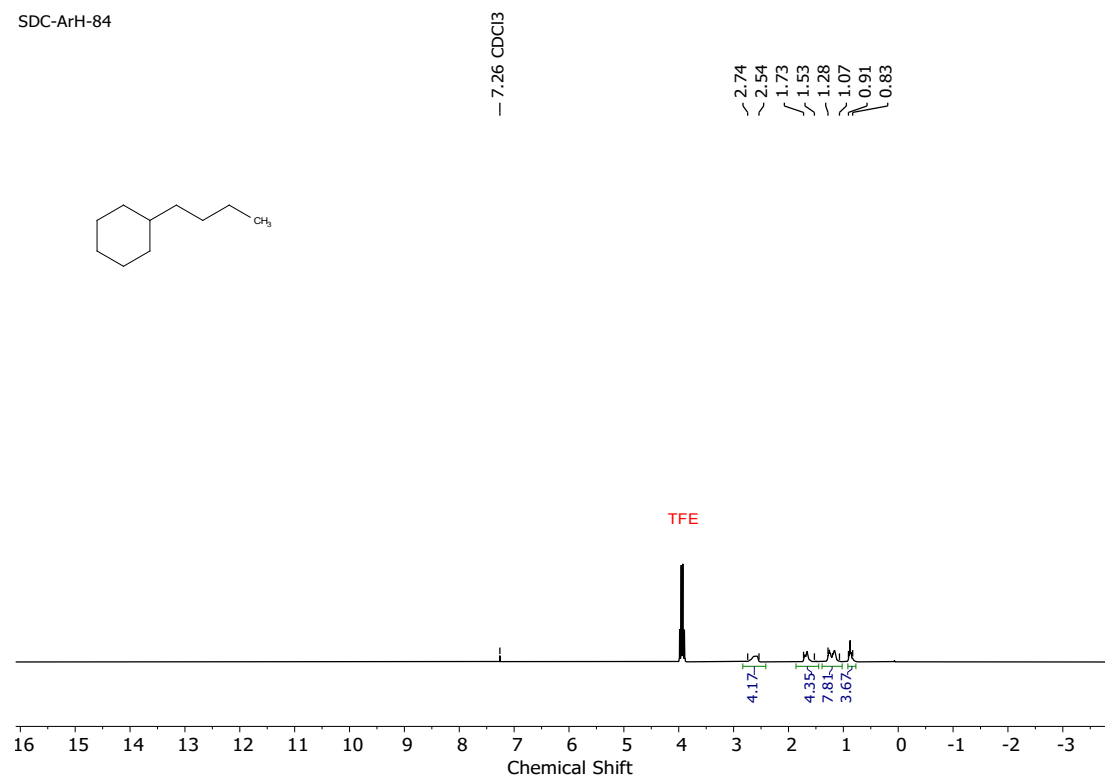
Figure S28 ^{1}H NMR of **4d** (CDCl$_3$, 400 MHz)

SDC-ArH-84

— 77.16 CDCl3

37.83
37.41
33.62
29.29
26.93
26.62
23.16
14.26

37.83
37.41
33.62
29.29
26.93
26.62
23.16
14.26

40 35 30 25 20 15 10

Chemical Shift

TFE

TFE

270 250 230 210 190 170 150 130 110 90 70 50 30 10 -10

Chemical Shift
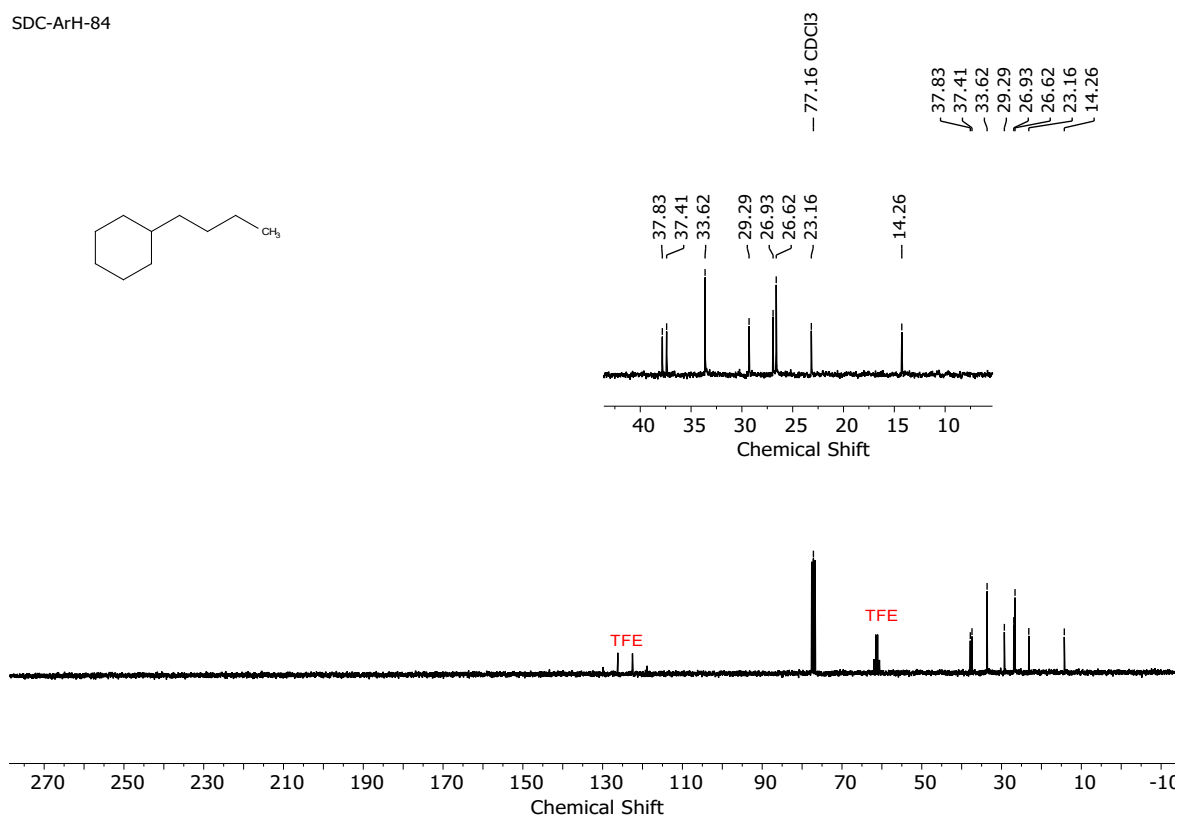
Figure S29 ^{13}C NMR of **4d** (CDCl$_3$, 100 MHz)

SDC-ArH-63

−7.26 CDCl3

1.73
1.64
1.38
1.14
1.08
1.06
1.03
0.92
0.83

TFE

10.28
8.01
2.00
3.70

16 15 14 13 12 11 10 9 8 7 6 5 4 3 2 1 0 -1 -2 -3
Chemical Shift
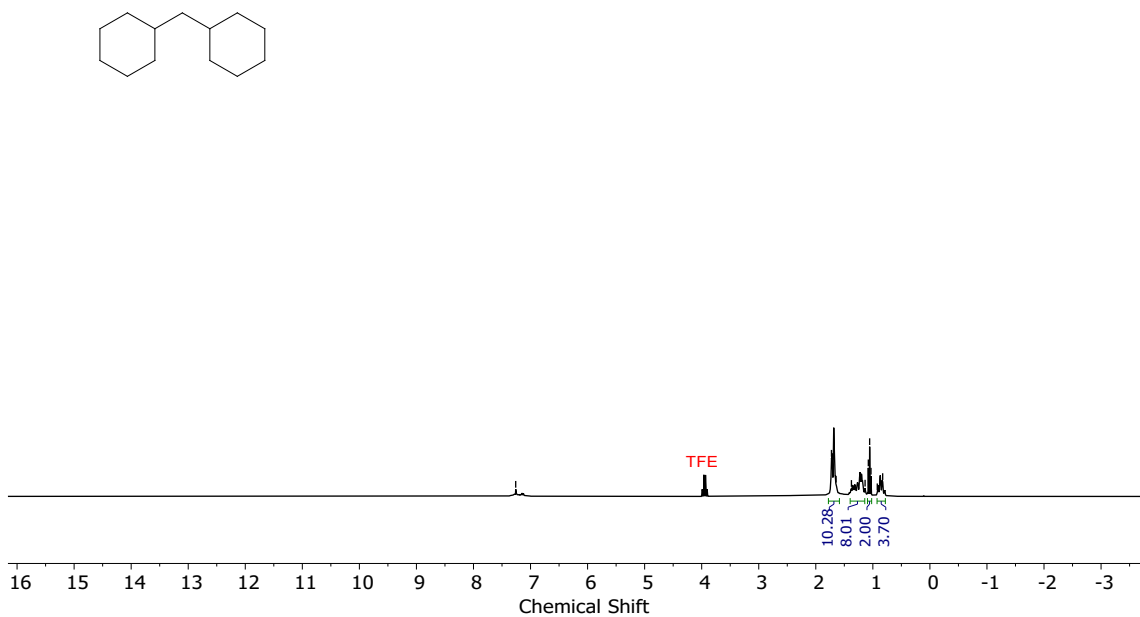
Figure S30 ^{1}H NMR of **5d** (CDCl$_3$, 400 MHz)

SDC-ArH-63

−77.16 CDCl3

−45.78

34.53
33.95
26.98
26.66

200 190 180 170 160 150 140 130 120 110 100 90 80 70 60 50 40 30 20 10 0 -10
Chemical Shift
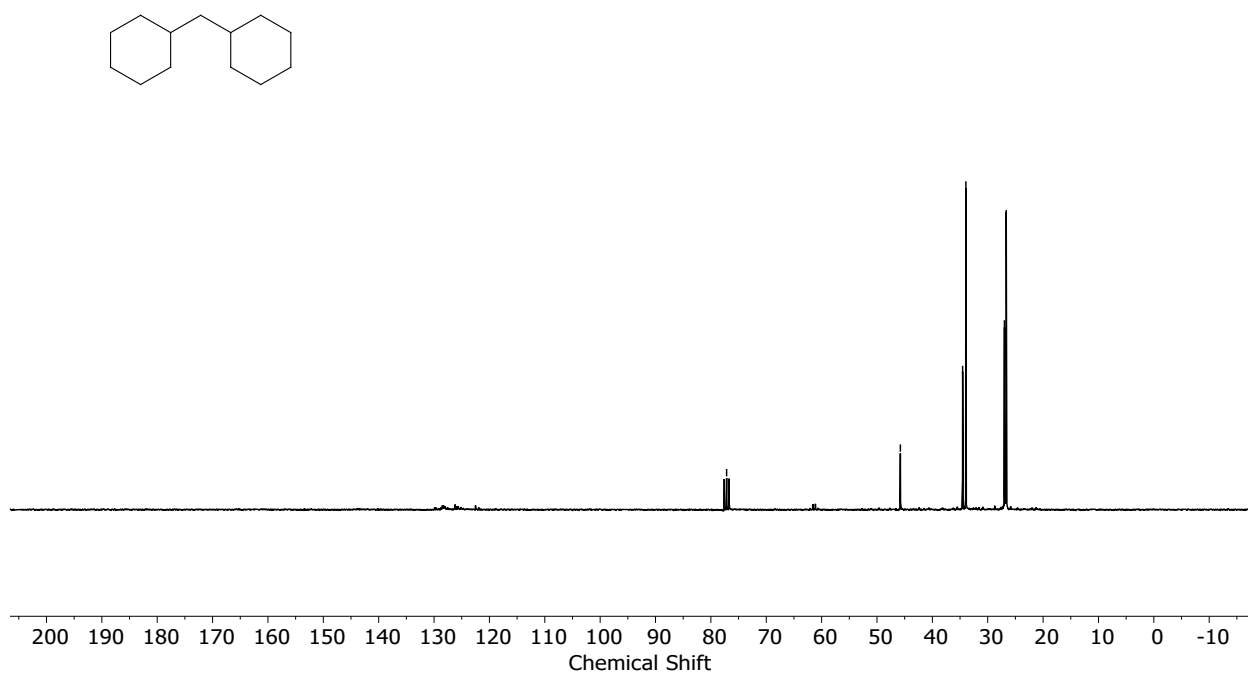
Figure S31 ^{13}C NMR of **5d** (CDCl$_3$, 100 MHz)

— 7.26 CDCl3

1.77
1.46
1.41
1.31
1.25
0.94
0.90
0.87
0.86
0.85

3.01

0.90 0.86 0.82 0.78 0.74
Chemical Shift

TFE

TFE

8.79
2.37
7.74
3.10

16 15 14 13 12 11 10 9 8 7 6 5 4 3 2 1 0 -1 -2 -3
Chemical Shift
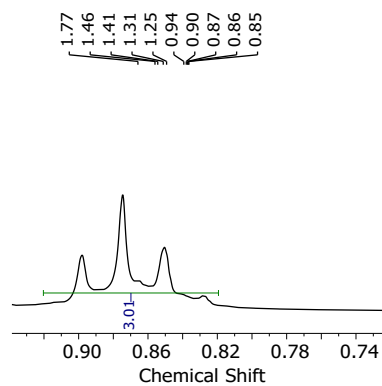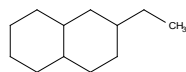
Figure S32 ^{1}H NMR of **6d** (CDCl$_3$, 400 MHz)
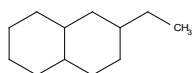
— 77.16 CDCl3

40.42
36.28
32.55
30.42
27.56
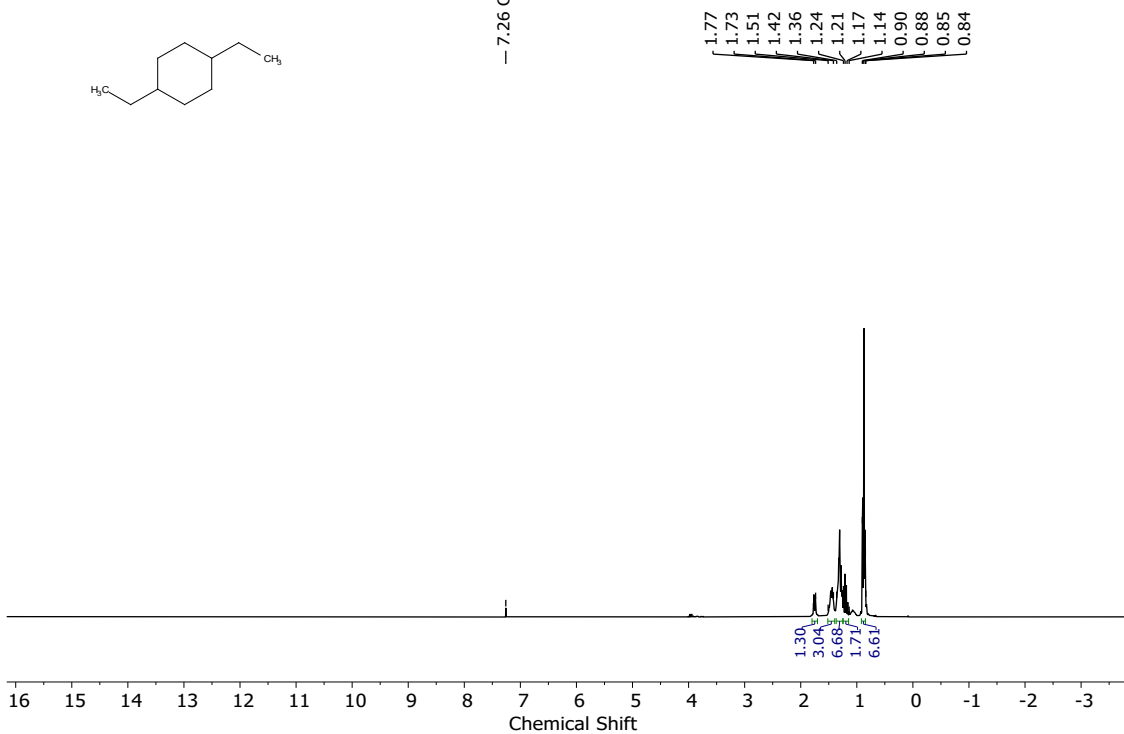27.29
25.99
21.15
11.58

TFE

TFE

270 250 230 210 190 170 150 130 110 90 70 50 30 10 -10
Chemical Shift
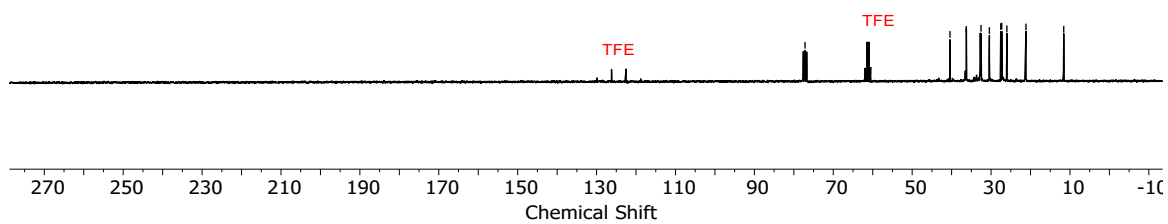
Figure S33 ^{13}C NMR of **6d** (CDCl$_3$, 100 MHz)

23

SDC-ArH-64

−7.26 CDCl3

1.73
1.64
1.31
1.10
0.92
0.88
0.84
0.81

10.22
14.00
3.78

16 15 14 13 12 11 10 9 8 7 6 5 4 3 2 1 0 -1 -2 -3
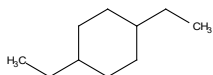Chemical Shift
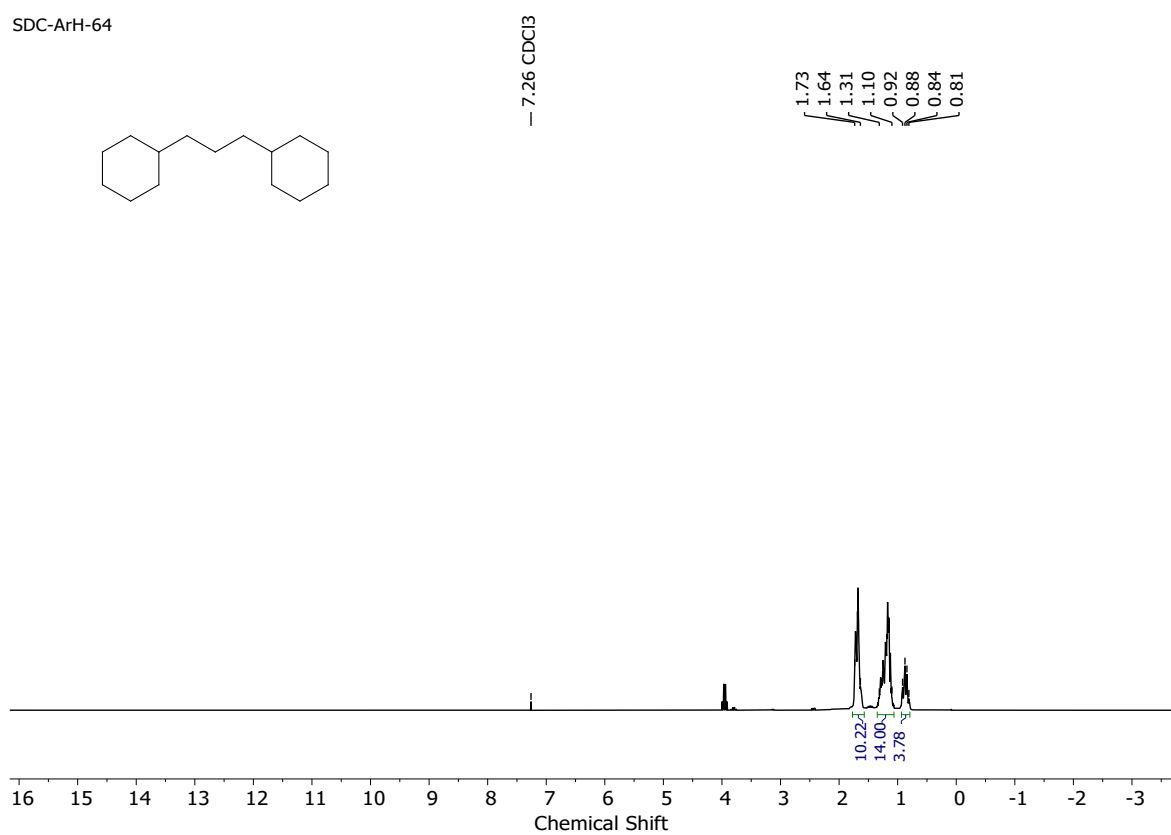
Figure S34 ^{1}H NMR of **7d** (CDCl$_3$, 400 MHz)

SDC-ArH-64

−77.16 CDCl3

38.05
37.92
33.67
26.98
26.67
24.26

38.05
37.92
33.67
26.98
26.67
24.26

38 36 34 32 30 28 26 24
Chemical Shift

20 210 200 190 180 170 160 150 140 130 120 110 100 90 80 70 60 50 40 30 20 10 0 -10
Chemical Shift
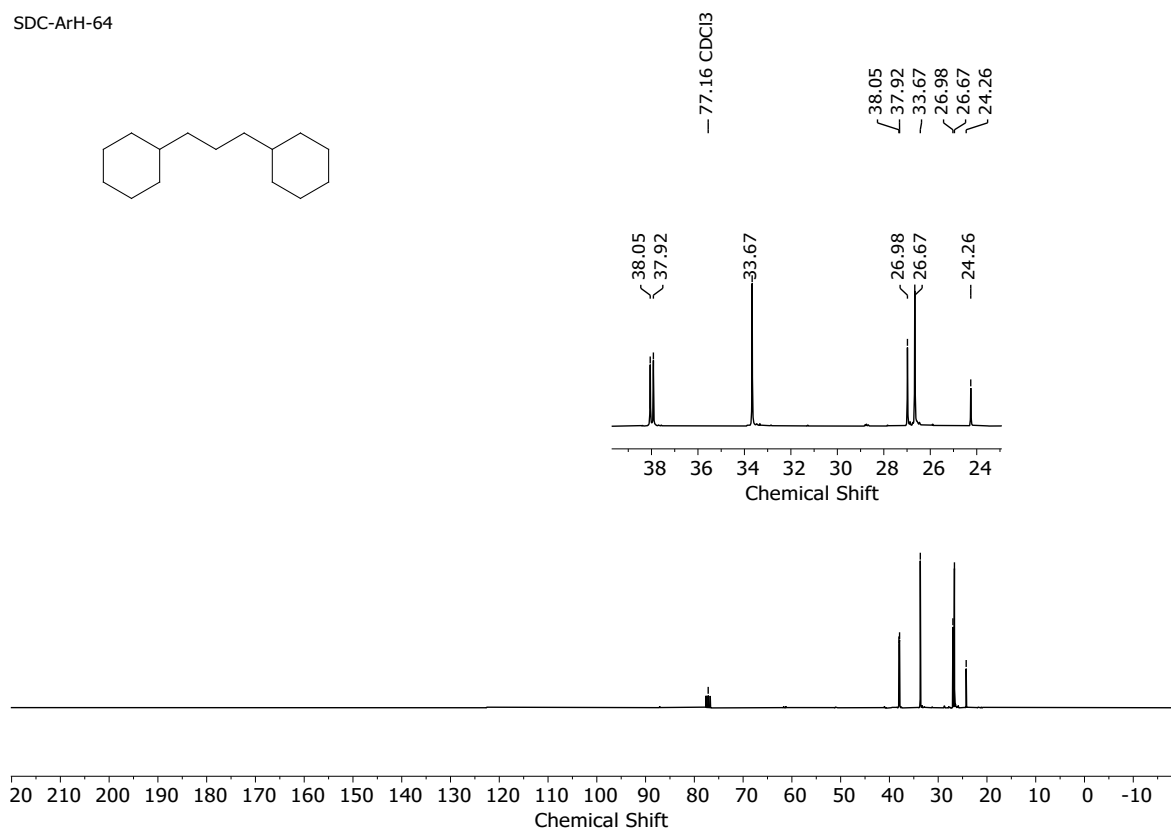
Figure S35 ^{13}C NMR of **7d** (CDCl$_3$, 100 MHz)

24

SDC-ArH-65

—7.26 CDCl3

1.77
1.73
1.51
1.42
1.36
1.24
1.21
1.17
1.14
0.90
0.88
0.85
0.84

1.30
3.04
6.68
1.71
6.61

16 15 14 13 12 11 10 9 8 7 6 5 4 3 2 1 0 -1 -2 -3
Chemical Shift
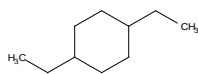
Figure S36 ^{1}H NMR of **8d** (CDCl$_3$, 400 MHz)

SDC-ArH-65

—77.16 CDCl3

39.89
37.53
33.14
30.27
28.74
27.10
12.07
11.70

20 210 200 190 180 170 160 150 140 130 120 110 100 90 80 70 60 50 40 30 20 10 0 -10
Chemical Shift
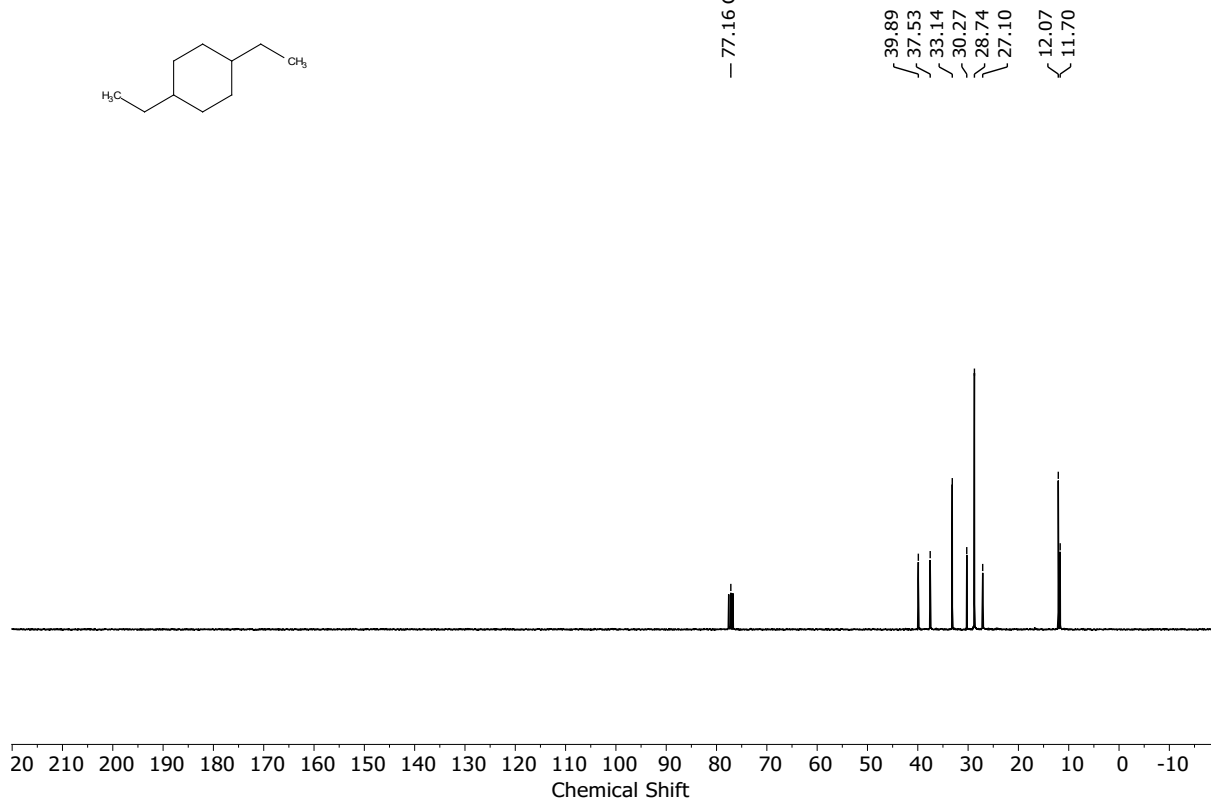
Figure S37 ^{13}C NMR of **8d** (CDCl$_3$, 100 MHz)

25

SDC-ArH-75

— 7.26 CDCl3

1.75
1.58
1.50
1.17
0.92
0.84

1.96
9.27
1.61
5.16

16 15 14 13 12 11 10 9 8 7 6 5 4 3 2 1 0 -1 -2 -3

Chemical Shift
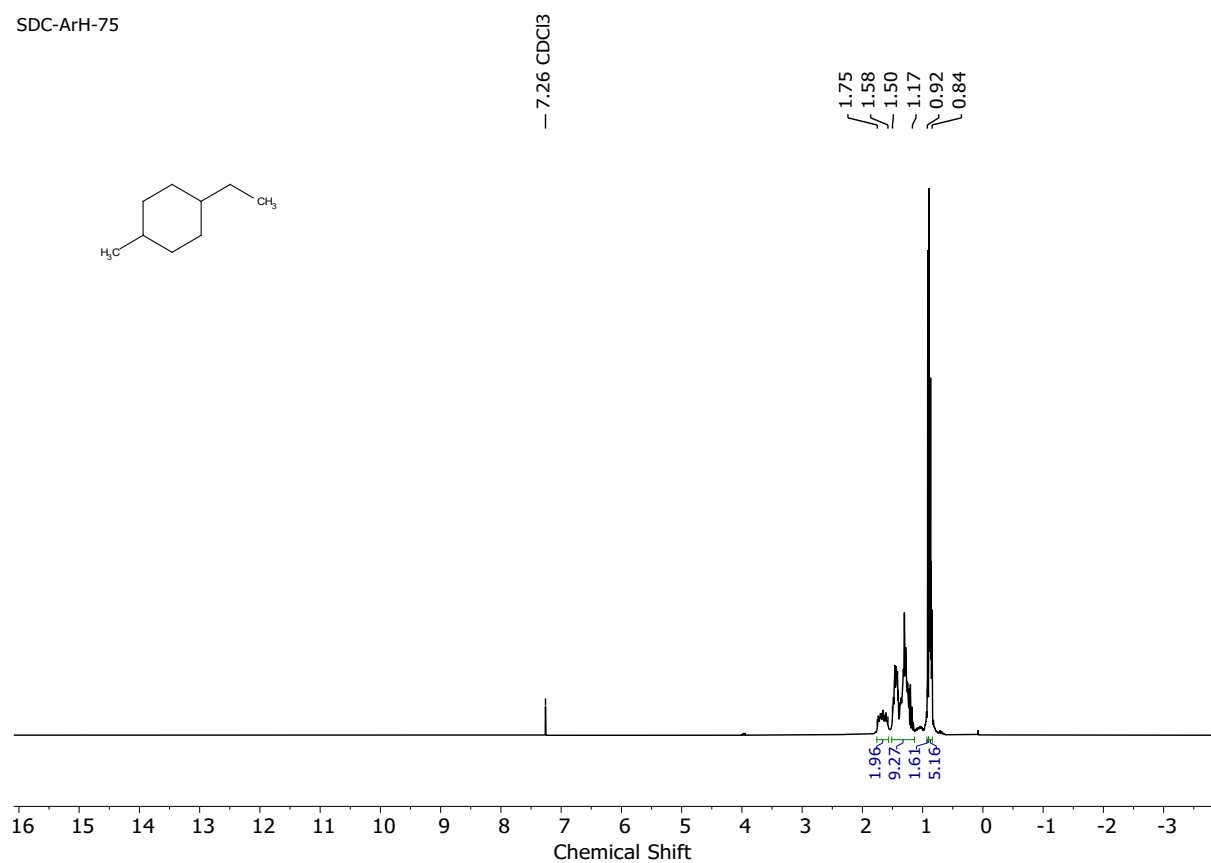
Figure S38 ^{1}H NMR of **9d** (CDCl₃, 400 MHz)

SDC-ArH-75

— 77.16 CDCl3

39.40
37.31
35.56
33.15
31.01
30.39
30.21
28.57
27.06
22.92
20.40
12.09
11.70

270 250 230 210 190 170 150 130 110 90 70 50 30 10 -1(

Chemical Shift
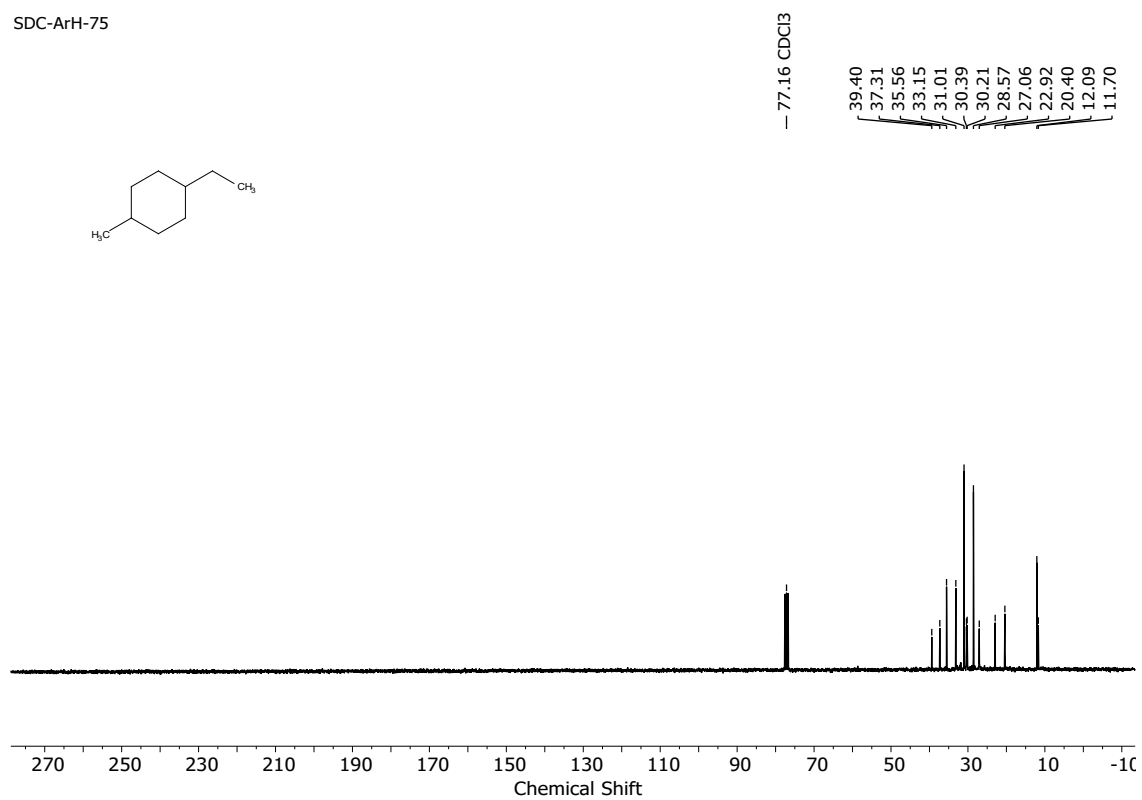
Figure S39 ^{13}C NMR of **9d** (CDCl₃, 100 MHz)

26

— 7.26 CDCl3

1.77
1.65
1.29
1.14
0.92
0.87
0.79

5.55
11.02
5.43
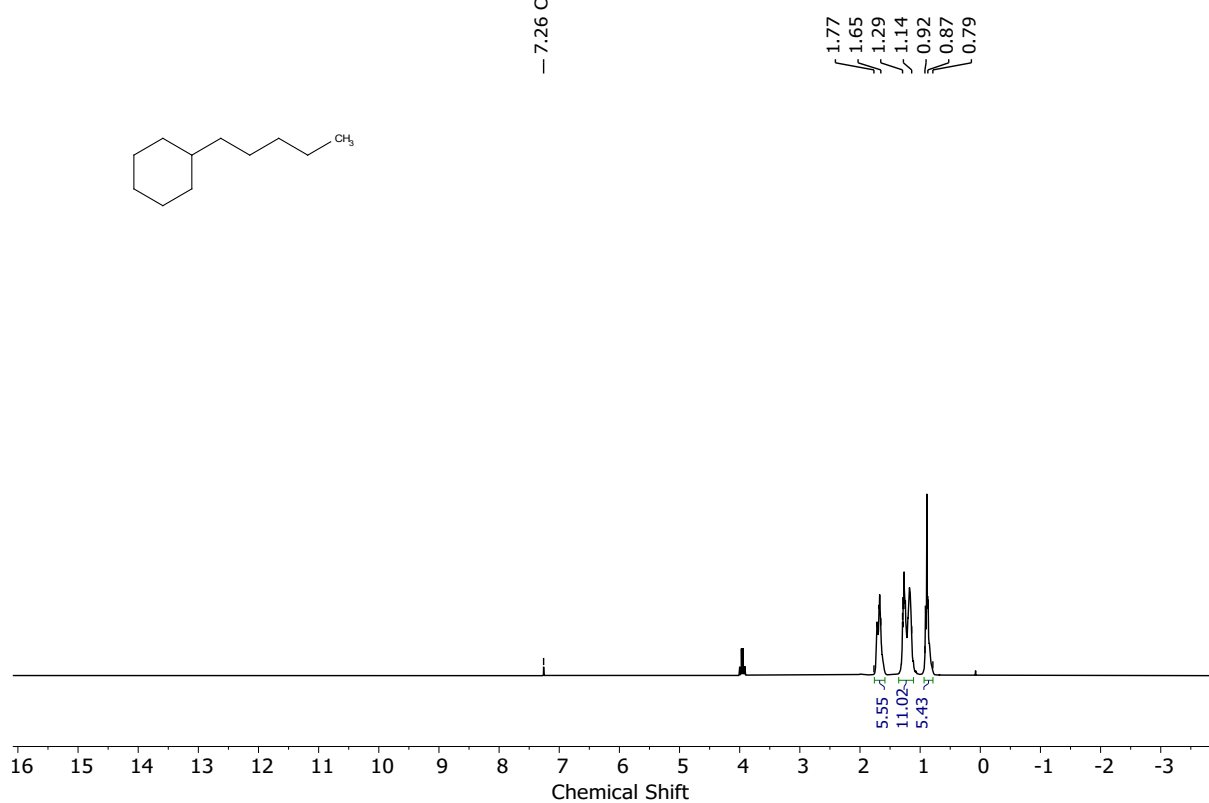
Figure S40 ^{1}H NMR of **14d** (CDCl$_3$, 400 MHz)

— 77.16 CDCl3

37.87
37.45
33.66
29.31
26.95
26.66
23.21
14.30
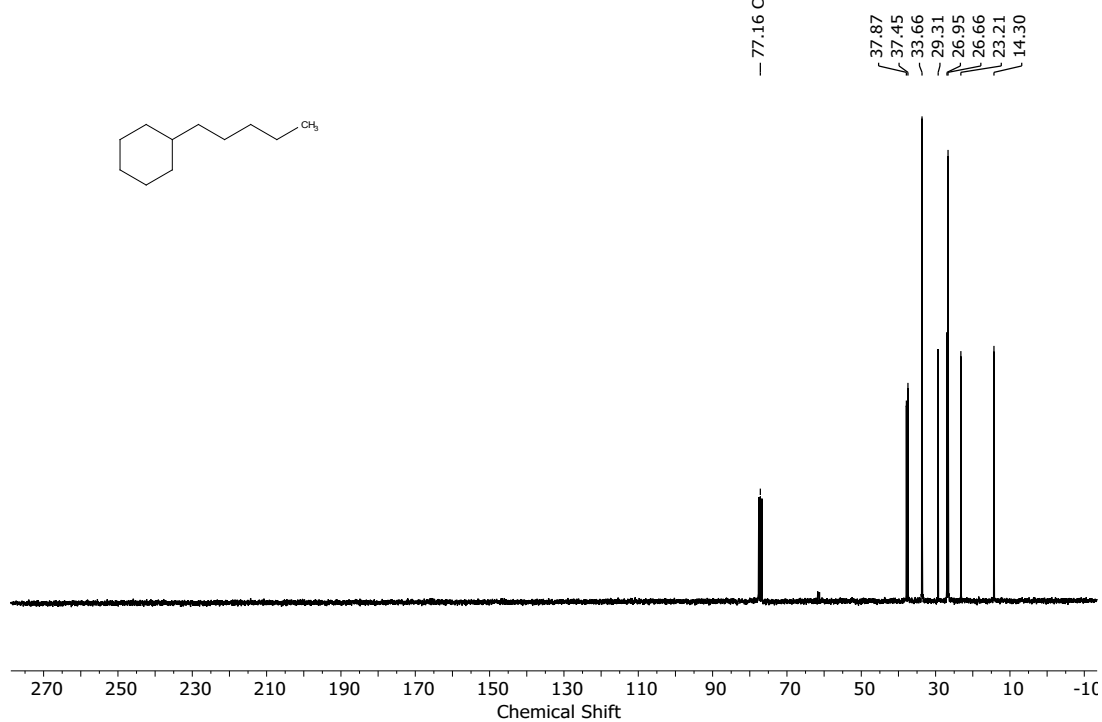
Figure S41 ^{13}C NMR of **14d** (CDCl$_3$, 100 MHz)

27

SDC-ArH-106

− 7.26 CDCl3

2.13
1.90
1.75
1.62
1.49
1.08
0.91
0.81
0.70
0.62

0.82
3.27
6.39
5.88
1.64

16 15 14 13 12 11 10 9 8 7 6 5 4 3 2 1 0 -1 -2 -3

Chemical Shift
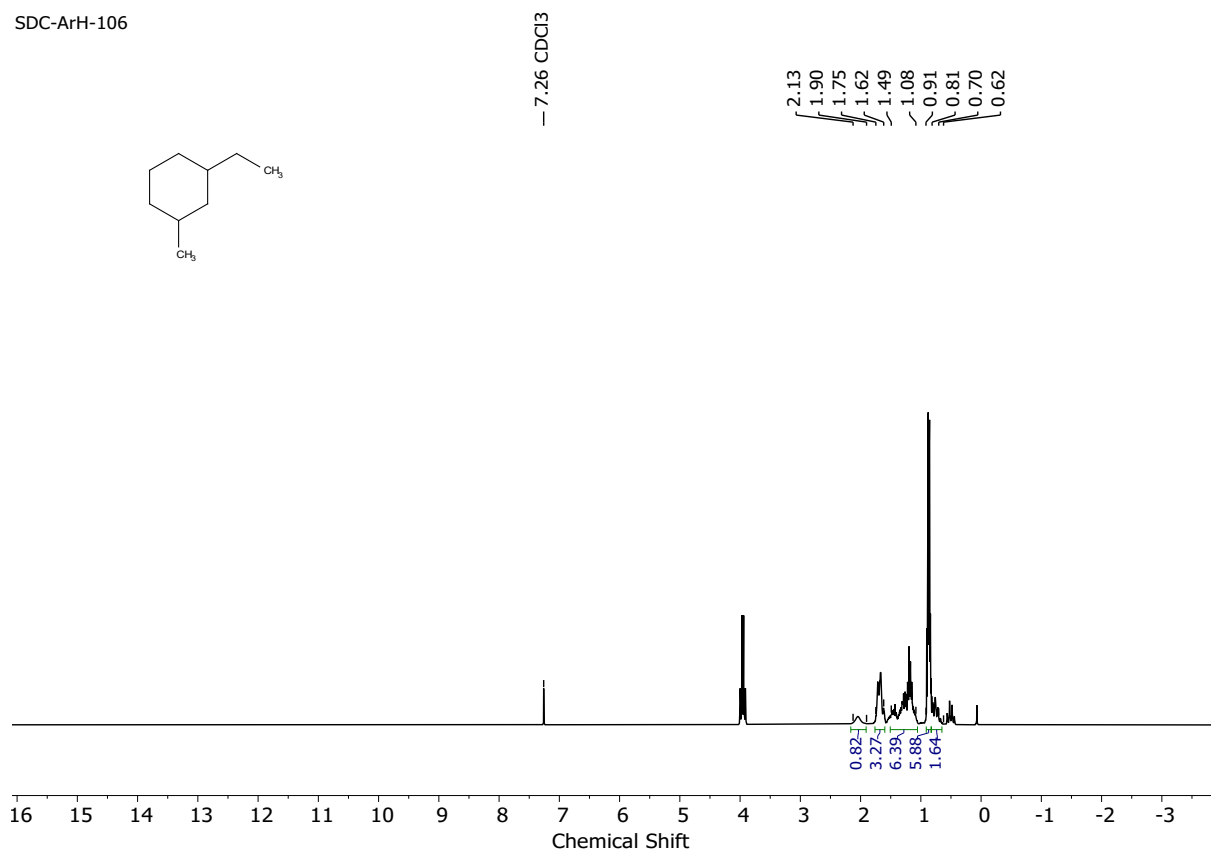
Figure S42 ¹H NMR of **15d** (CDCl₃, 400 MHz)

SDC-ArH-106

−77.16 CDCl3

42.17
39.67
35.17
32.90
32.21
30.36
26.54
23.16
21.04
12.12
11.58

270 250 230 210 190 170 150 130 110 90 70 50 30 10 -10

Chemical Shift
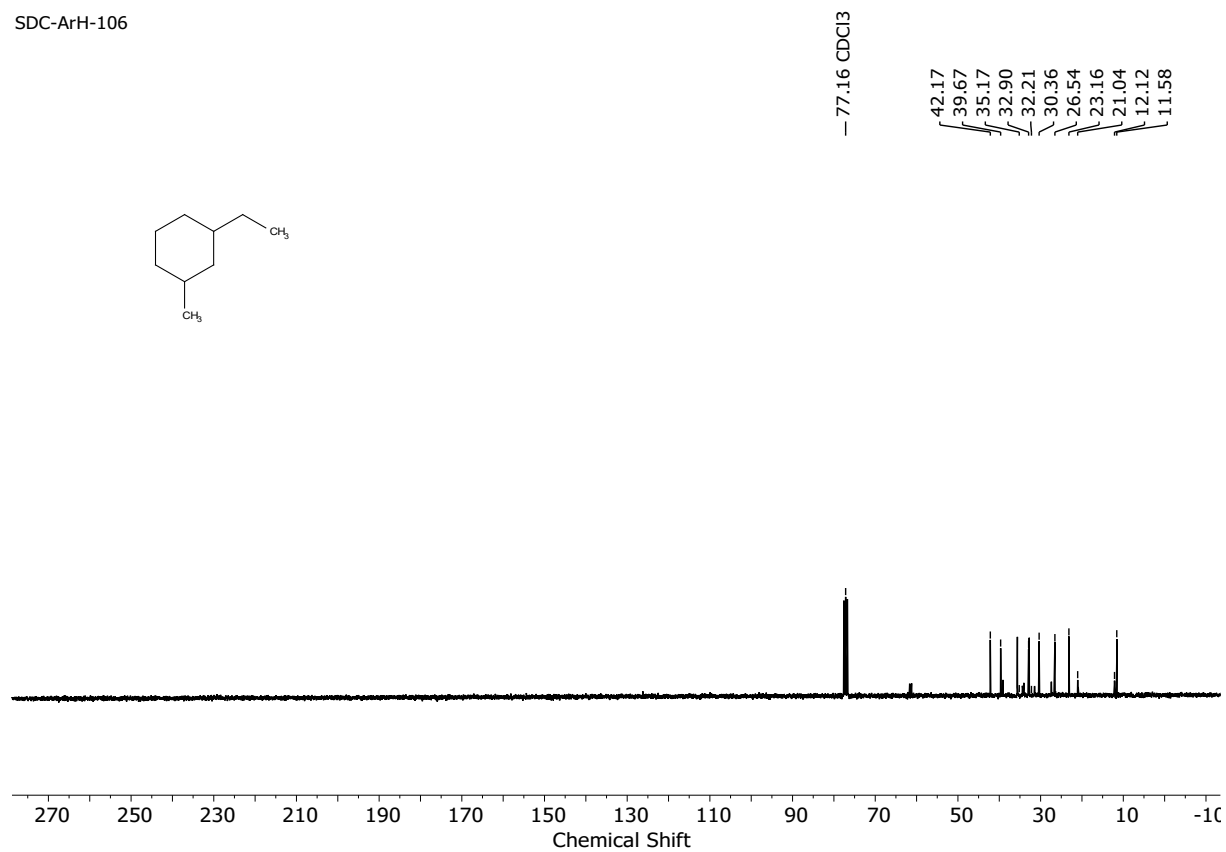
Figure S43 ¹³C NMR of **15d** (CDCl₃, 100 MHz)

28
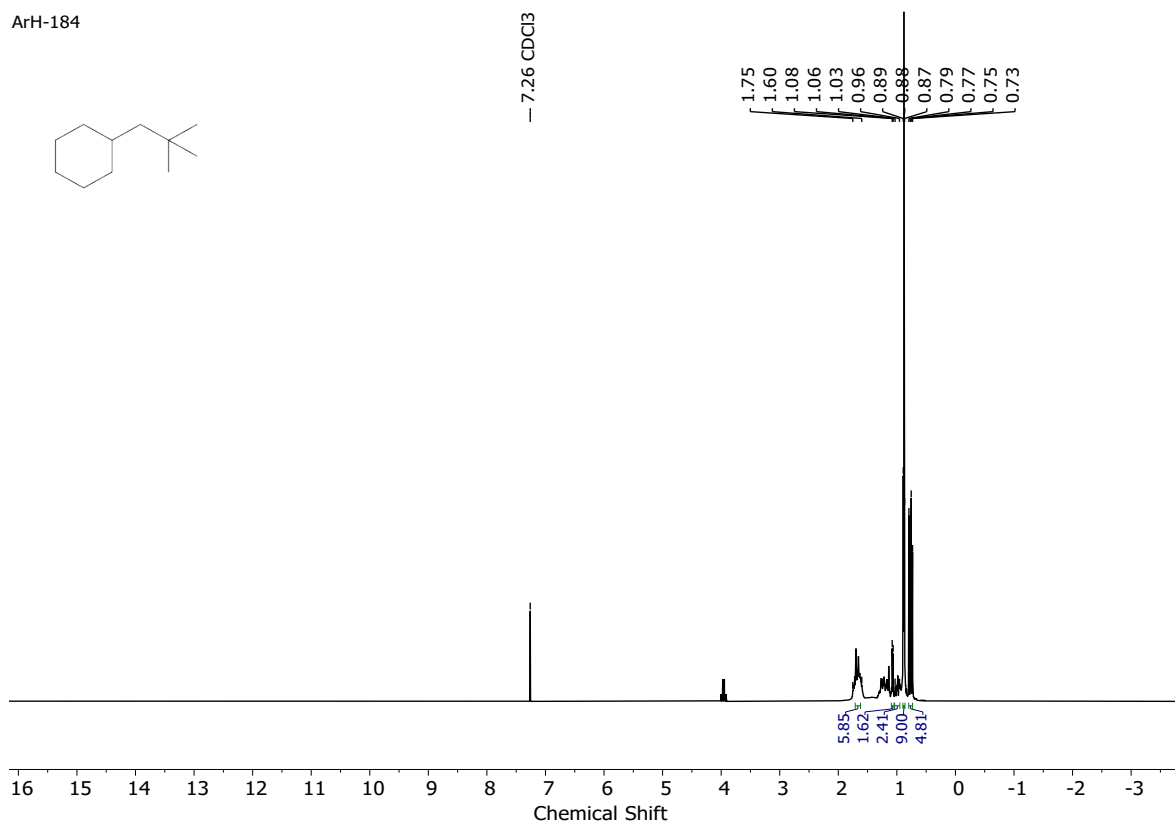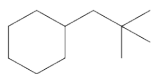
ArH-184

Figure S44 ^{1}H NMR of **17d** (CDCl$_3$, 400 MHz)

ArH-184
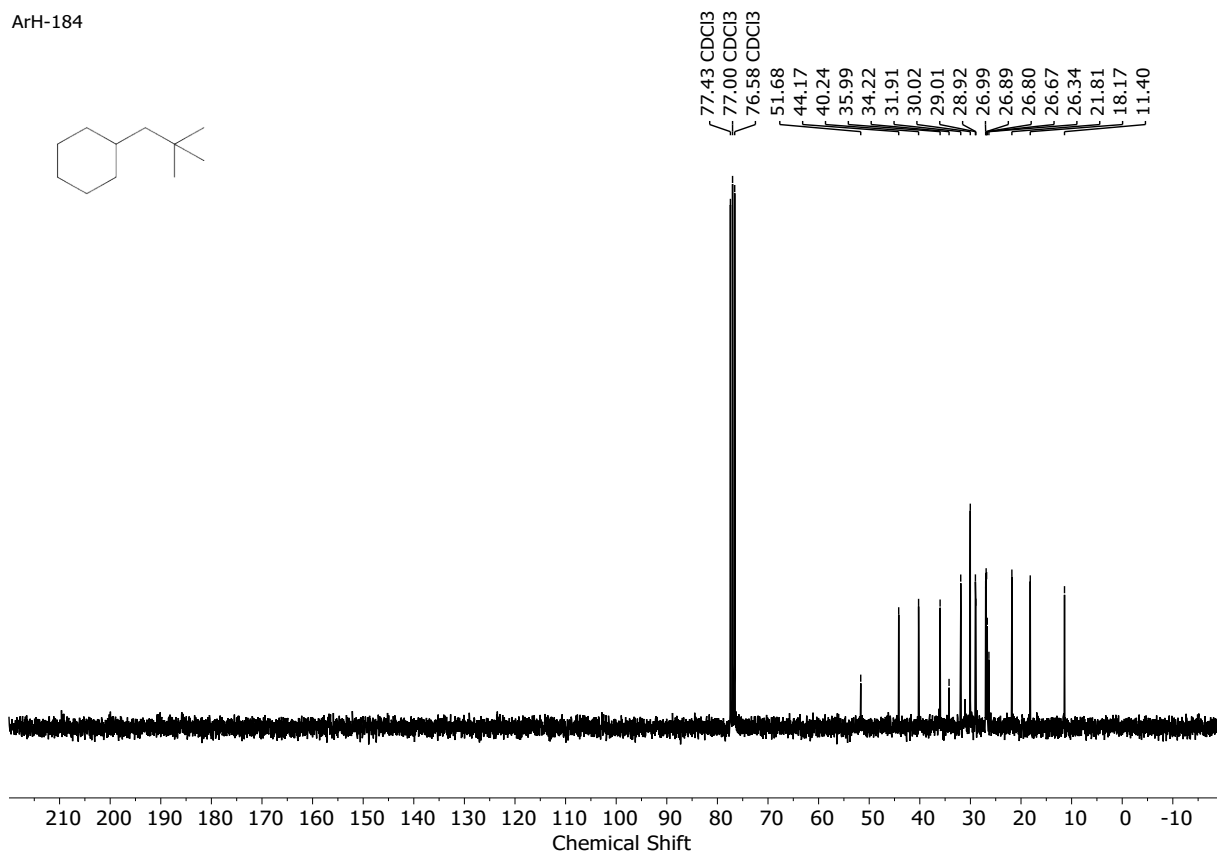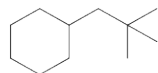
Figure S45 ^{13}C NMR of **17d** (CDCl$_3$, 100 MHz)

SDC-ArH-105

−7.26 CDCl3

2.20
2.18
1.80
1.31
1.21
0.91
0.84
0.82

0.72
7.20
6.74
9.34

16 15 14 13 12 11 10 9 8 7 6 5 4 3 2 1 0 -1 -2 -3
Chemical Shift
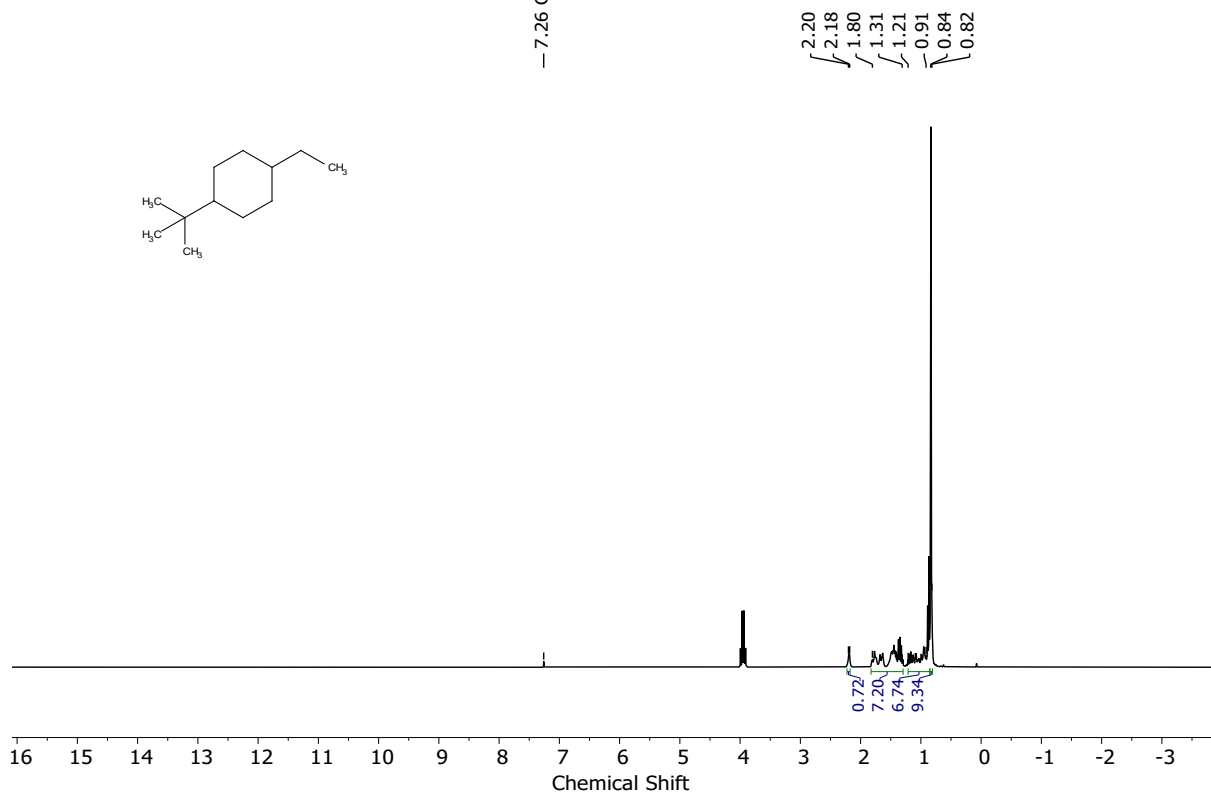
Figure S46 ^{1}H NMR of **18d** (CDCl3, 400 MHz)

SDC-ArH-105

−77.16 CDCl3

48.75
39.74
34.61
33.60
30.48
27.65
23.72
21.79
12.57

270 250 230 210 190 170 150 130 110 90 70 50 30 10 -10
Chemical Shift
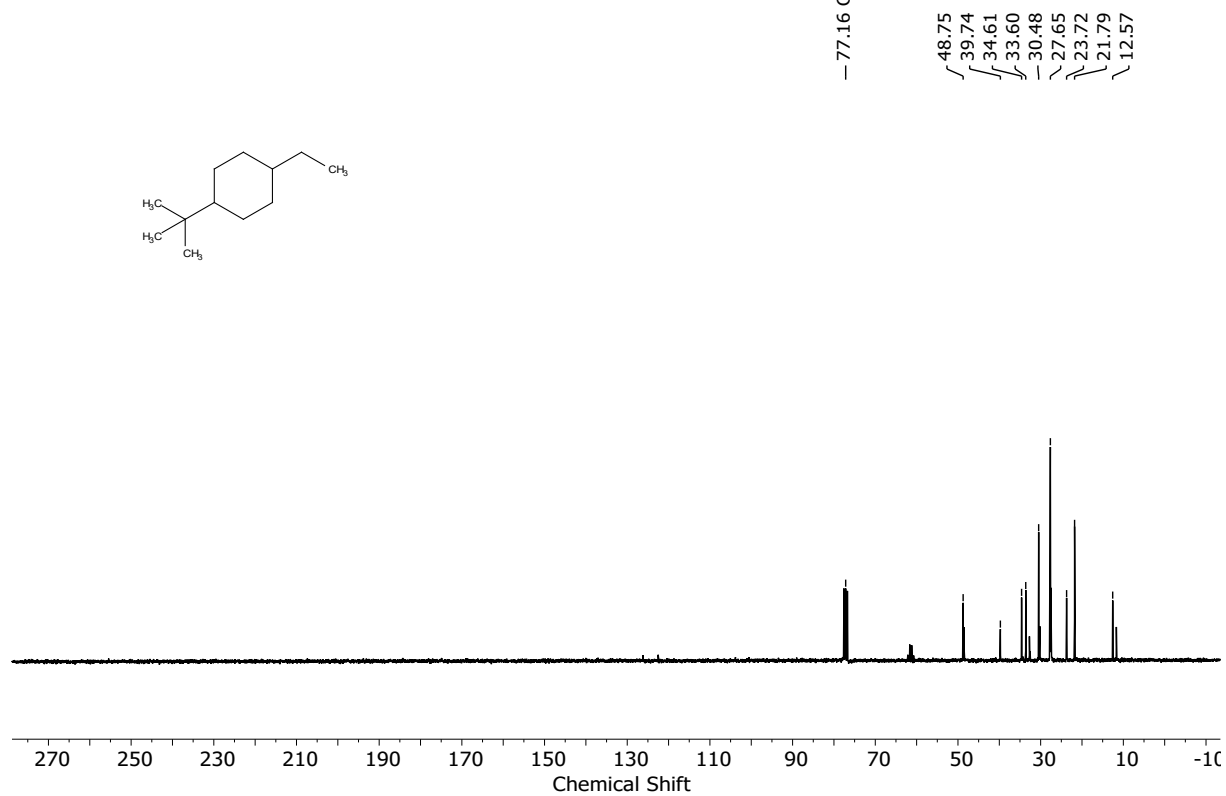
Figure S47 ^{13}C NMR of **18d** (CDCl3, 100 MHz)

30
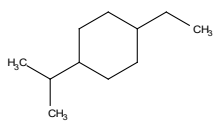
SDC-ArH-111

— 7.26 CDCl3

1.80
1.66
1.55
0.99
0.89
0.80

1.27
11.30
9.43

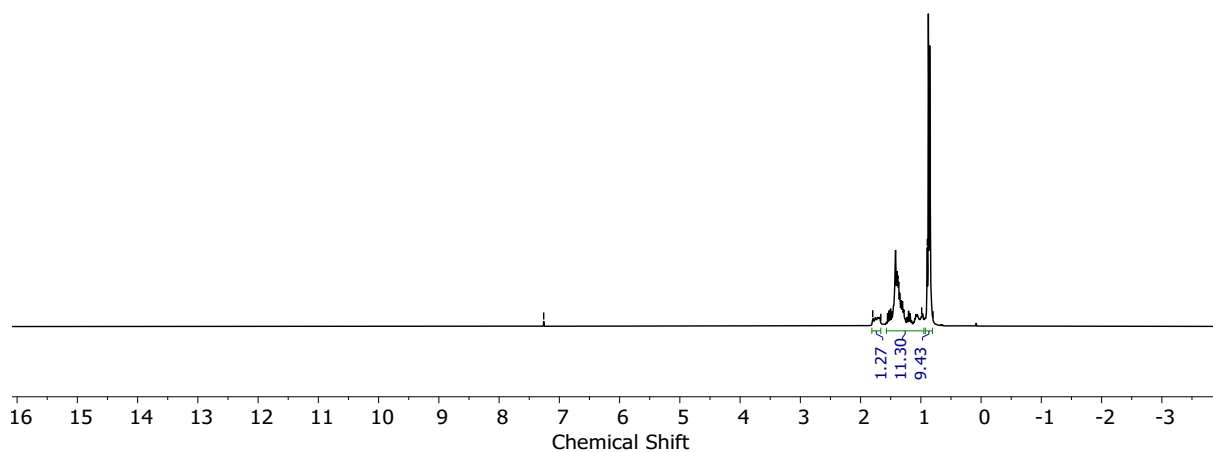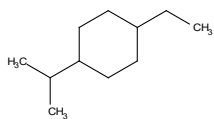16 15 14 13 12 11 10 9 8 7 6 5 4 3 2 1 0 -1 -2 -3

Chemical Shift

Figure S48 ¹H NMR of **19d** (CDCl₃, 400 MHz)

SDC-ArH-111

77.16 CDCl3
44.48
43.32
39.87
36.62
33.33
33.13
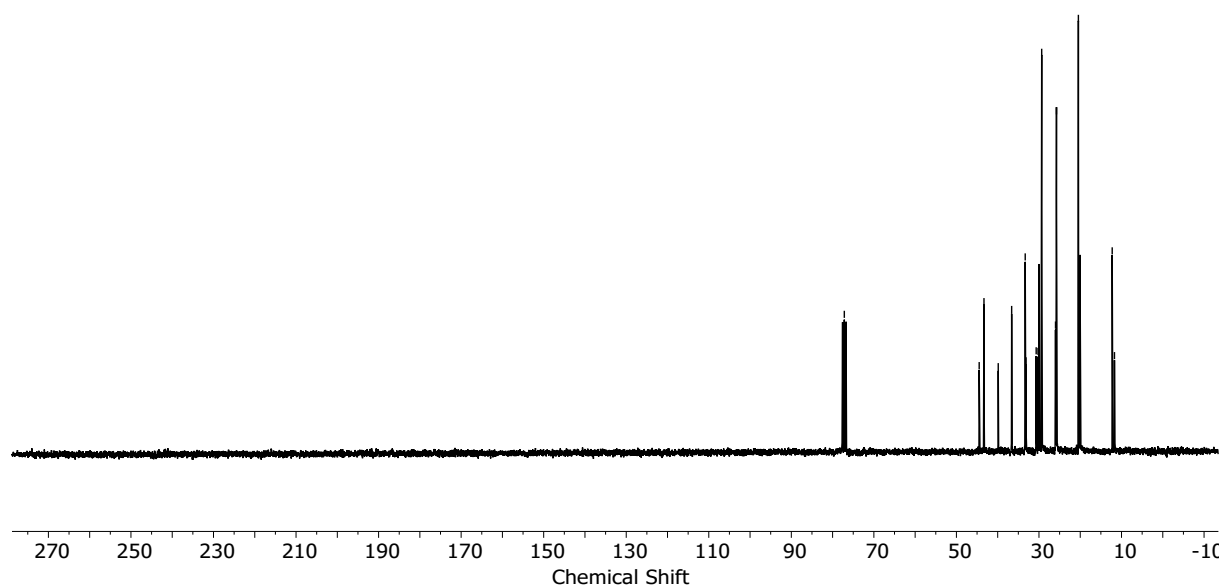30.68
30.23
29.93
29.34
25.99
25.76
20.45
20.01
12.26
11.71

270 250 230 210 190 170 150 130 110 90 70 50 30 10 -10

Chemical Shift

Figure S49 ¹³C NMR of **19d** (CDCl₃, 100 MHz)

31

— 7.26 CDCl3

1.77
1.17
1.13
1.11
1.09
1.07
1.00
0.88
0.84
0.82

11.98
1.51
0.85
9.66

16 15 14 13 12 11 10 9 8 7 6 5 4 3 2 1 0 -1 -2 -3

Chemical Shift
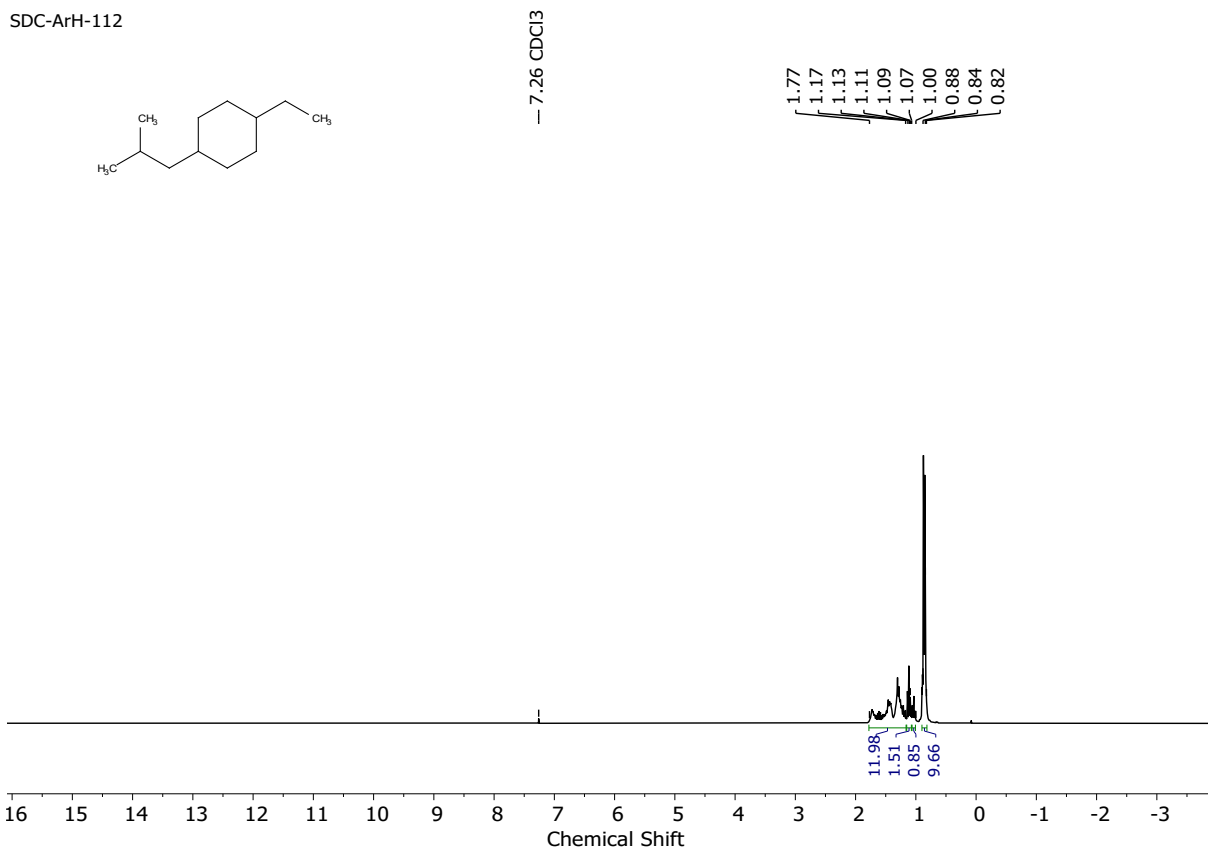
Figure S50 ^{1}H NMR of **20d** (CDCl₃, 400 MHz)

77.16 CDCl3
47.29
43.92
39.88
37.51
35.54
33.75
33.14
32.92
30.27
29.27
28.75
27.06
25.25
24.98
23.07
12.10

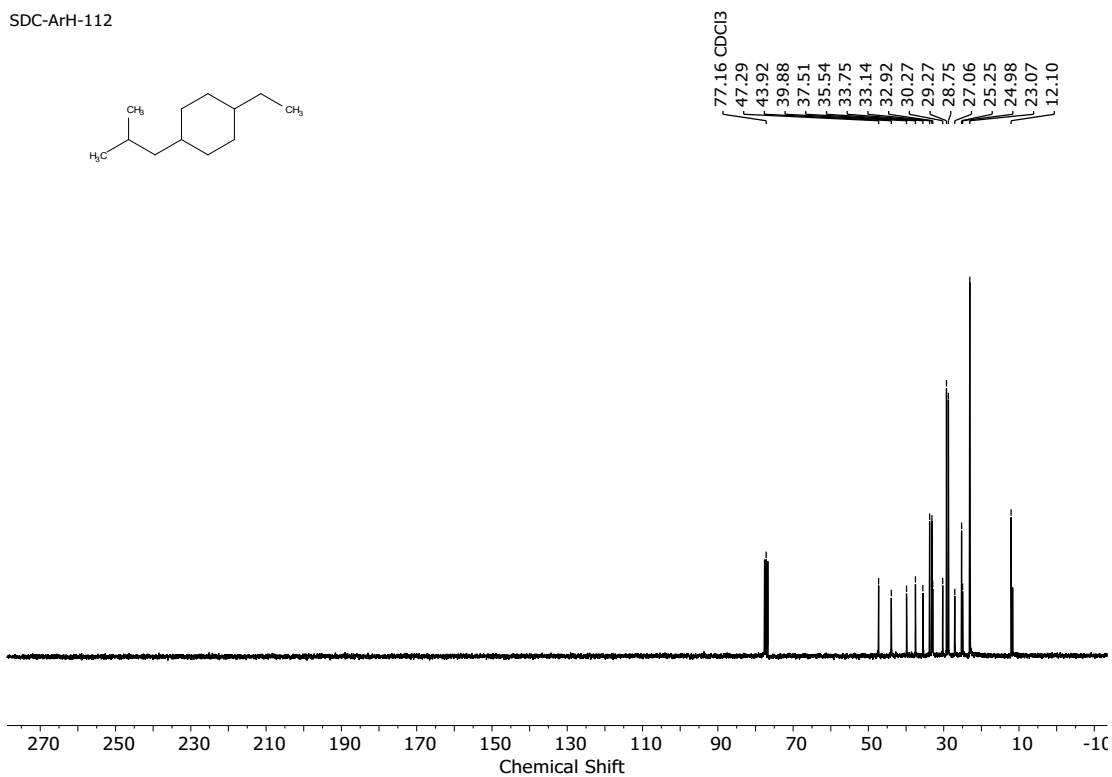270 250 230 210 190 170 150 130 110 90 70 50 30 10 -10

Chemical Shift

Figure S51 ^{13}C NMR of **20d** (CDCl₃, 100 MHz)

SDC-ArH-74
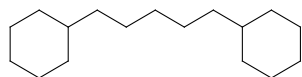
−7.26 CDCl3

1.73
1.63
1.36
1.11
0.96
0.80

10.80
17.12
4.08

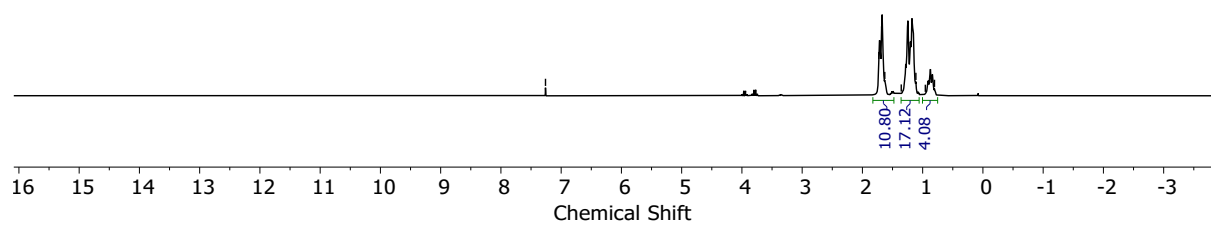16 15 14 13 12 11 10 9 8 7 6 5 4 3 2 1 0 -1 -2 -3
Chemical Shift

Figure S52 ¹H NMR of **28d** (CDCl₃, 400 MHz)

SDC-ArH-74
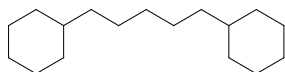
−77.16 CDCl3

37.89
37.76
33.66
30.53
27.11
26.97
26.65

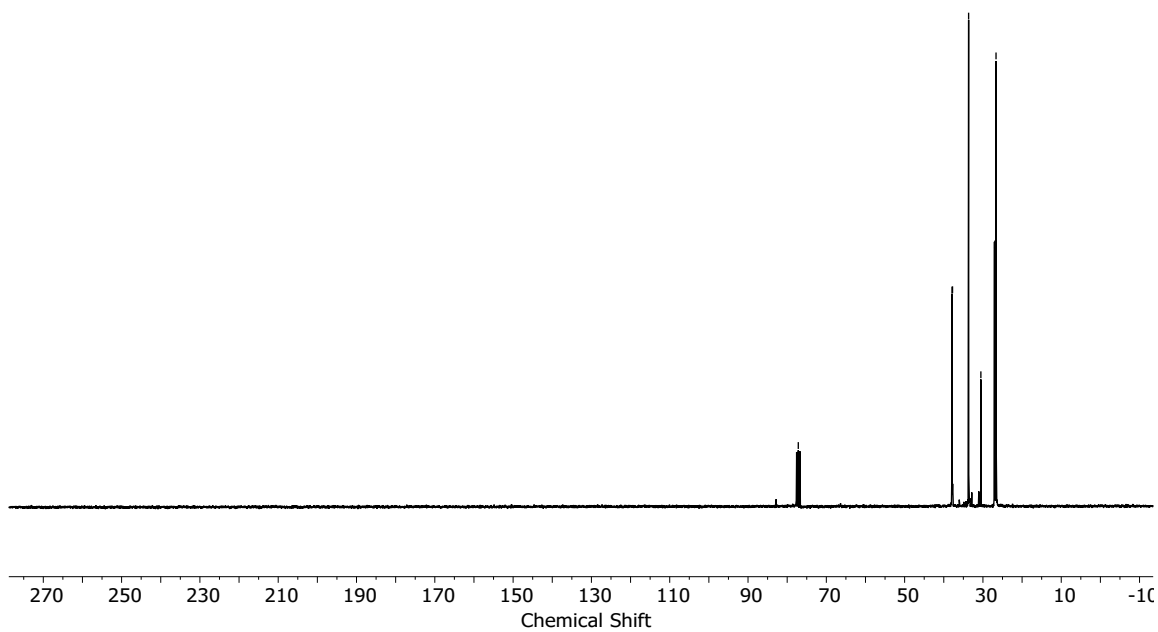270 250 230 210 190 170 150 130 110 90 70 50 30 10 -10
Chemical Shift

Figure S53 ¹³C NMR of **28d** (CDCl₃, 100 MHz)

33
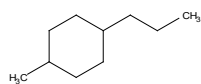
SDC-ArH-108

−7.26 CDCl3

2.24
1.73
1.13
0.92
0.84

0.78
12.51
6.71

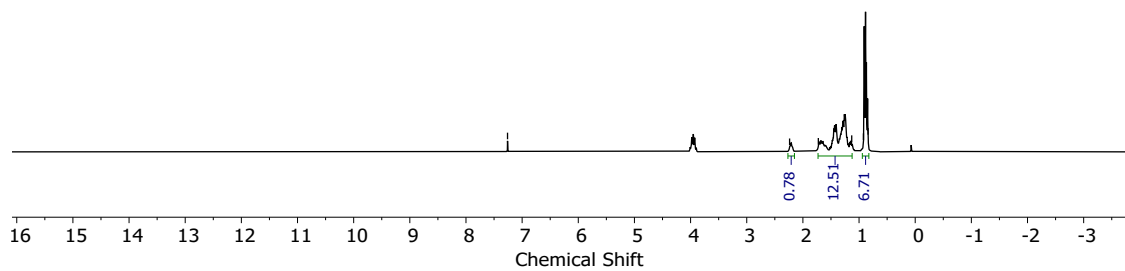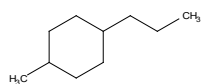16 15 14 13 12 11 10 9 8 7 6 5 4 3 2 1 0 -1 -2 -3

Chemical Shift

Figure S54 ^{1}H NMR of **29d** (CDCl$_3$, 400 MHz)

SDC-ArH-108

−77.16 CDCl3

39.97
37.29
35.56
33.52
31.00
28.94
22.91
20.61
14.54

270 250 230 210 190 170 150 130 110 90 70 50 30 10 -10
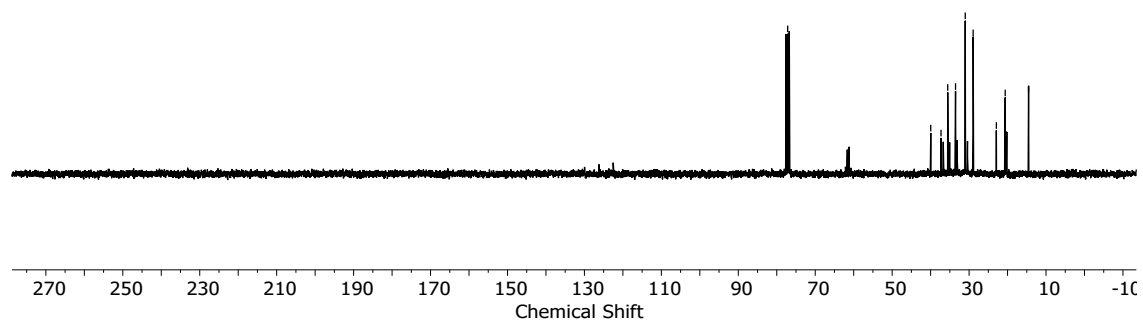
Chemical Shift

Figure S55 ^{13}C NMR of **29d** (CDCl$_3$, 100 MHz)

34

16.NMR of the cyclohexane-alcohol products
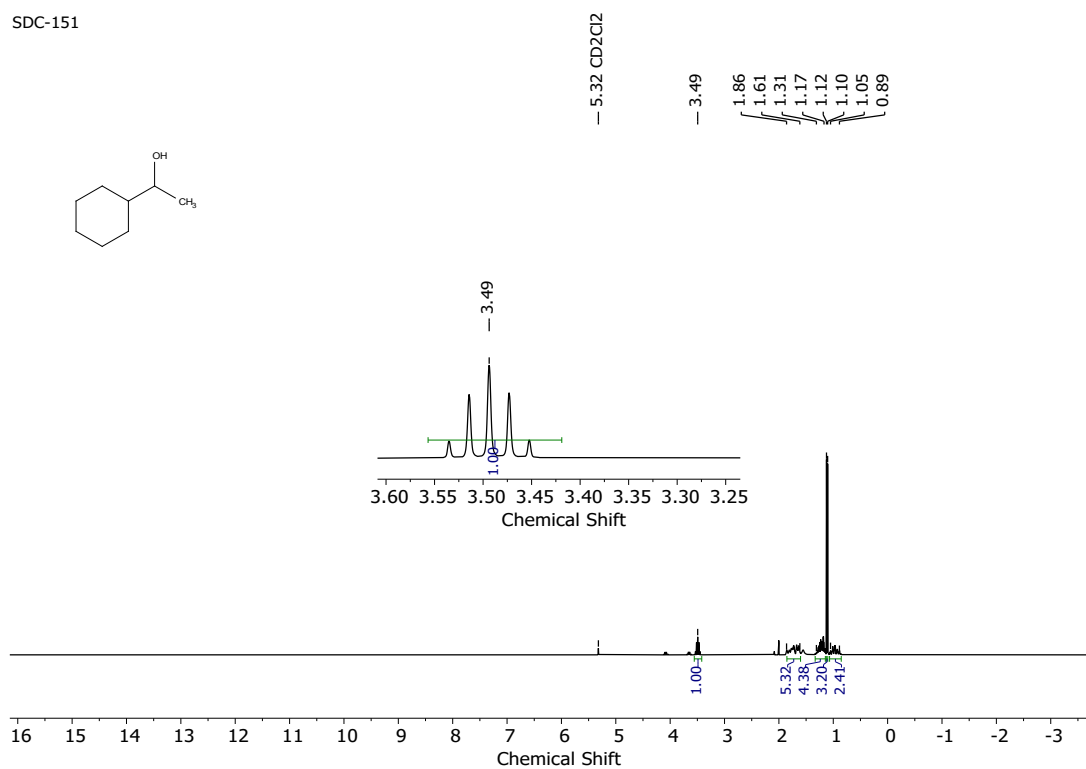
Figure S 56 ^{1}H NMR of **1c** (CD$_2$Cl$_2$, 400 MHz)
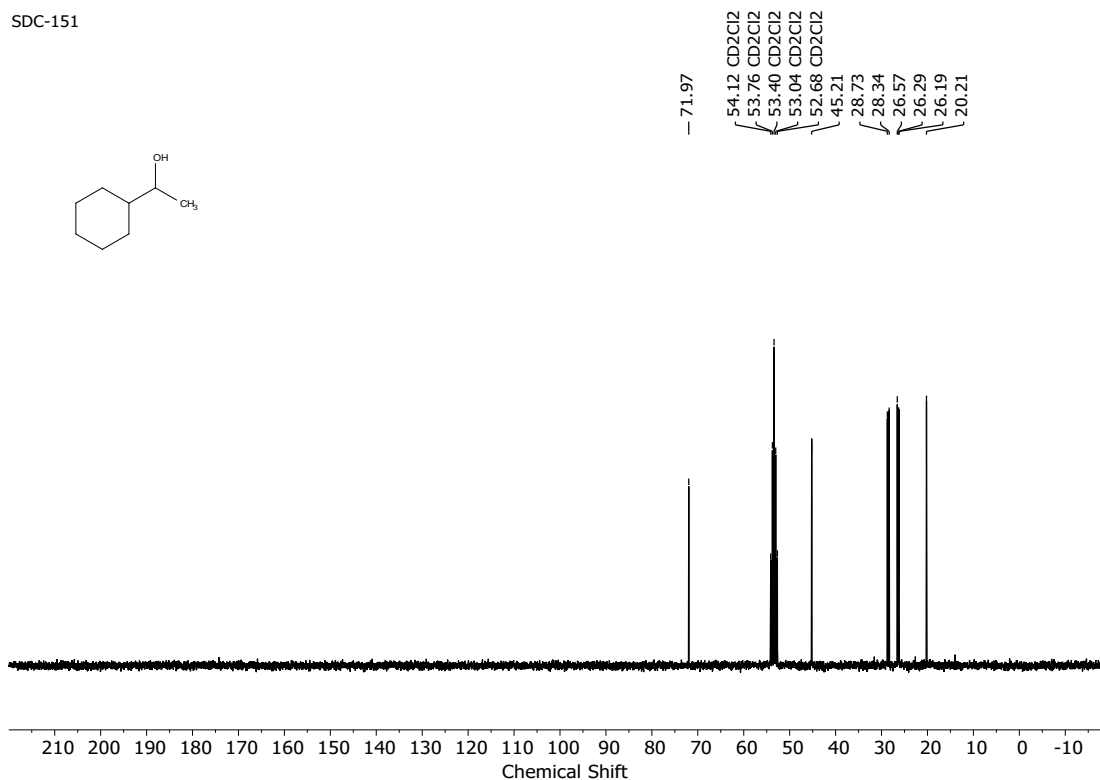
Figure S 57 ^{13}C NMR of **1c** (CD$_2$Cl$_2$, 100 MHz)

SDC-155

—7.26 CDCl3

—3.28

1.80
1.73
1.60
1.50
1.45
1.23
1.15
1.03
0.99
0.95
0.93
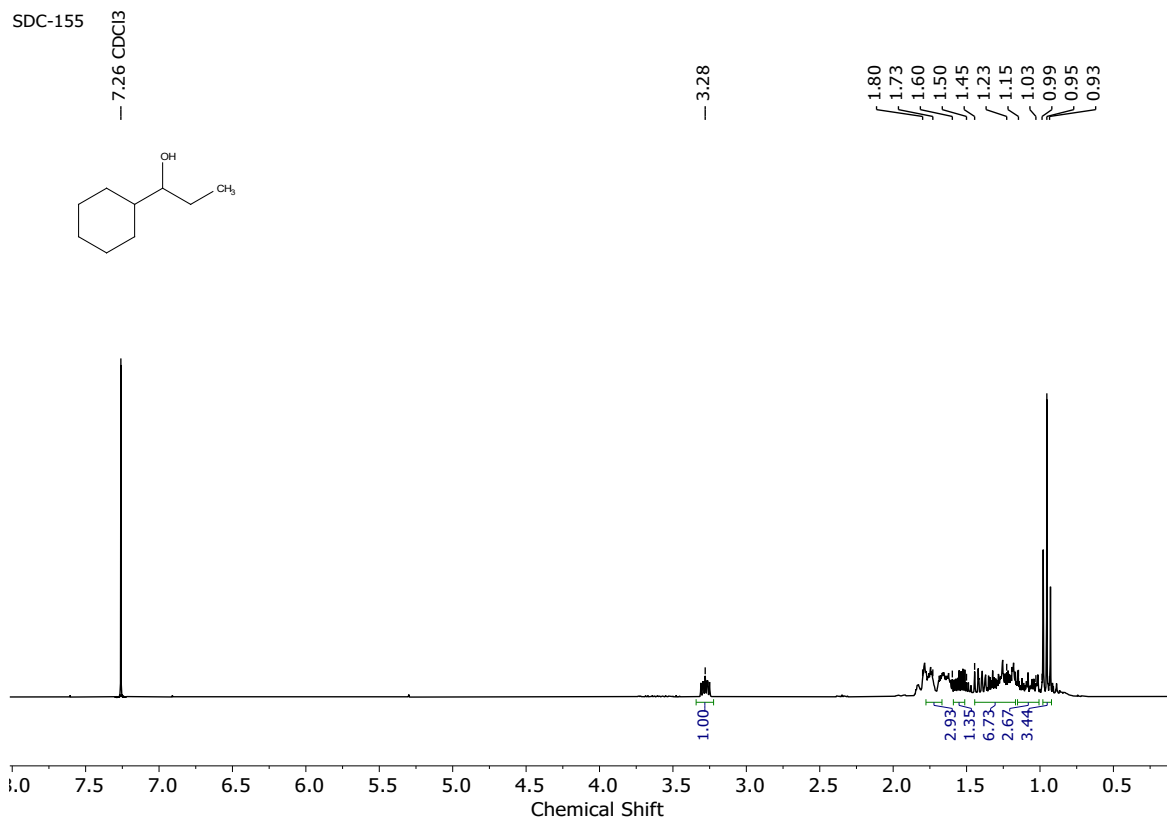
Figure S 58 ^{1}H NMR of **2c** (CDCl$_3$, 400 MHz)

SDC-155

77.73
77.16 CDCl3

43.26
29.42
27.84
26.93
26.68
26.50
26.33
9.60
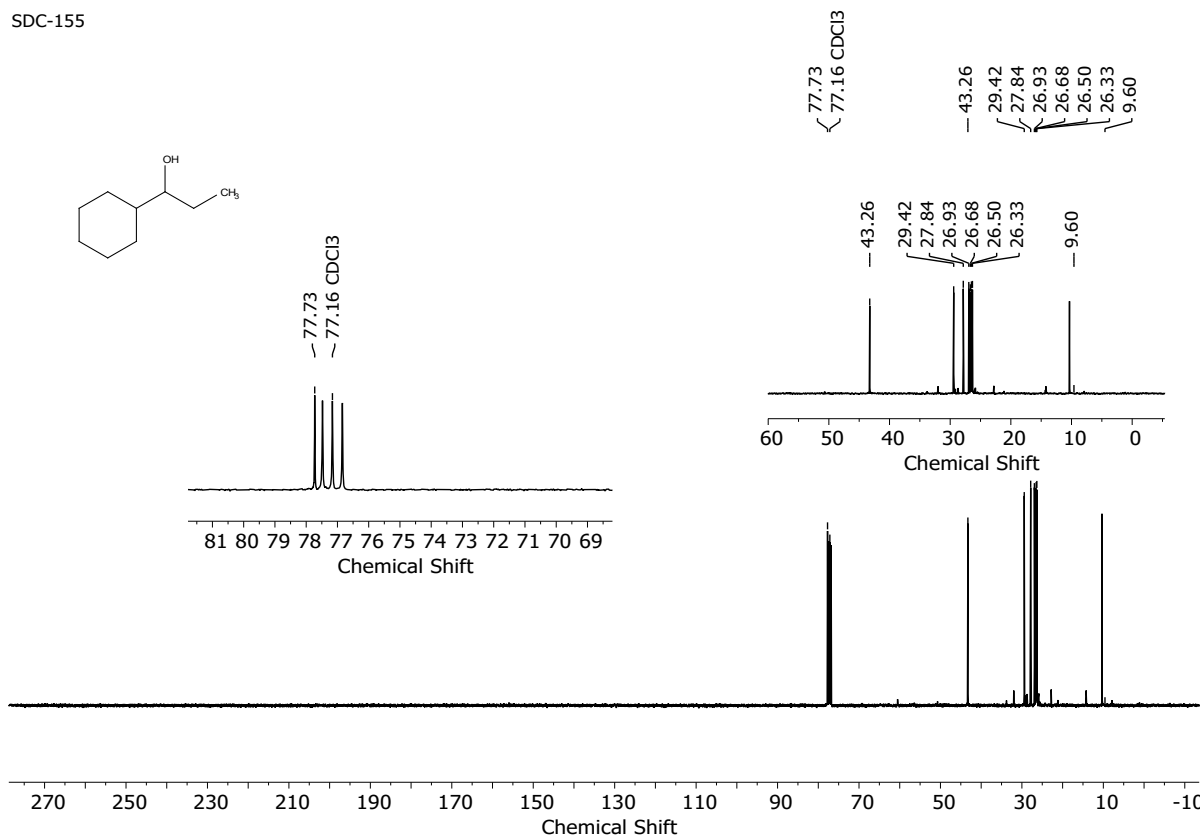
Figure S 59 ^{13}C NMR of **2c** (CDCl$_3$, 100 MHz)

36

SDC-156

~ 7.26 CDCl3

3.04

1.88
1.73
1.69
1.57
1.48
1.35
1.27
1.07
0.93
0.91
0.89

OH

CH₃

CH₃

6.00

0.98   0.94   0.90   0.86   0.82
Chemical Shift

0.93

3.87
3.04
1.82
5.01
6.00

.5   9.0   8.5   8.0   7.5   7.0   6.5   6.0   5.5   5.0   4.5   4.0   3.5   3.0   2.5   2.0   1.5   1.0   0.5
Chemical Shift
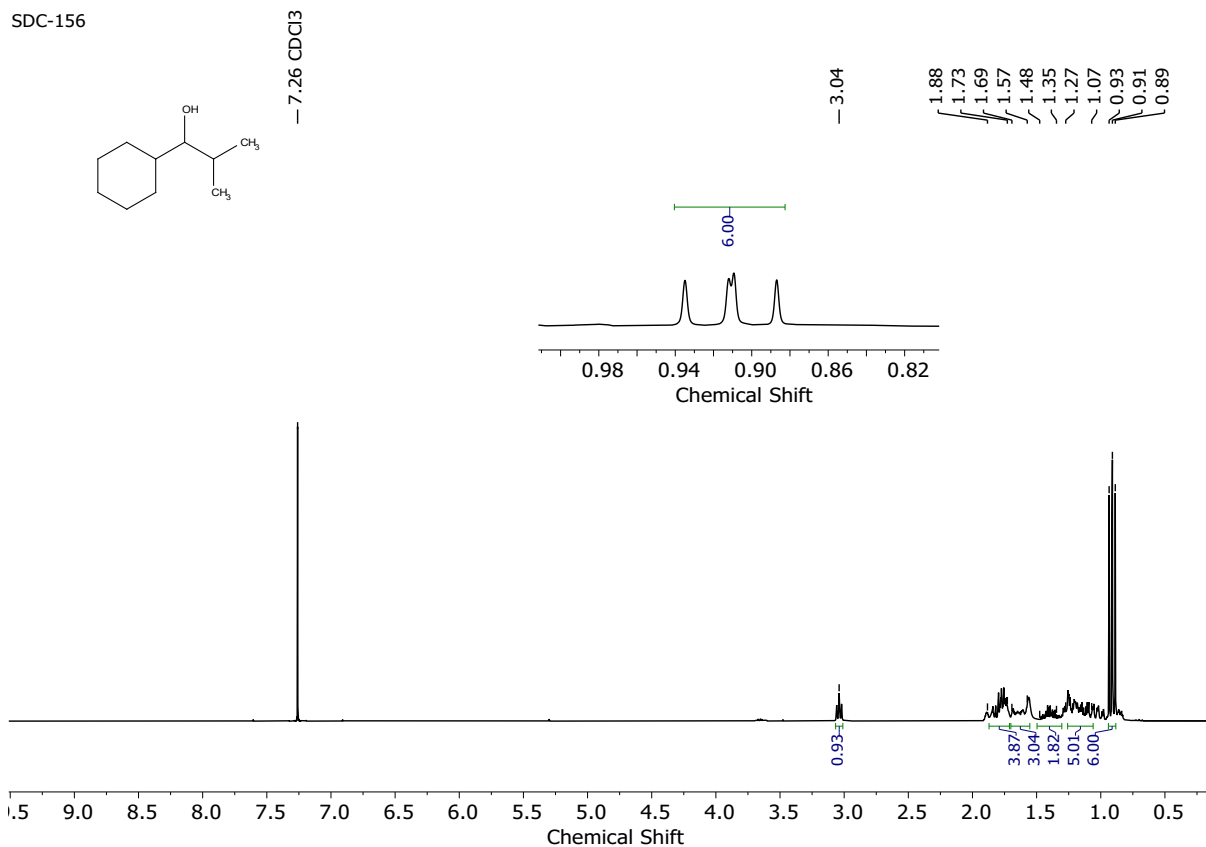
Figure S 60 ¹H NMR of **3c** (CDCl₃, 400 MHz)

SDC-156

~ 81.21
77.16 CDCl3

40.74
30.05
29.89
27.79
26.68
26.58
26.29
20.04
16.67

OH

CH₃

CH₃

40.74
30.05
29.89
27.79
26.68
26.58
26.29
20.04
16.67

70   60   50   40   30   20   10   0
Chemical Shift

270   250   230   210   190   170   150   130   110   90   70   50   30   10   -10
Chemical Shift
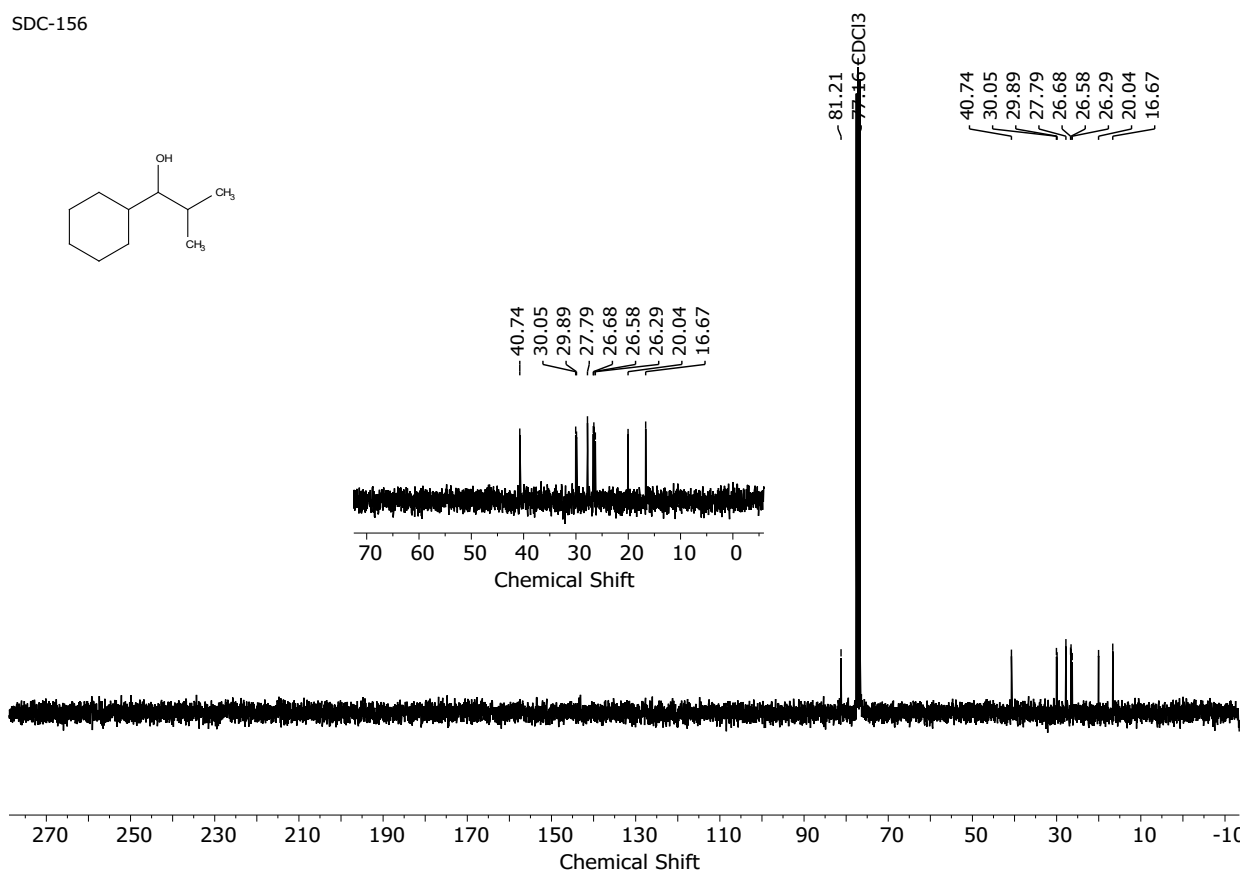
Figure S 61 ¹³C NMR of **3c** (CDCl₃, 100 MHz)

37

SDC-179

—7.26 CDCl3

—3.06

—1.85
1.53
1.47
1.37
1.30
—0.95

OH

0.97

10.62
1.91
10.50

9.5 9.0 8.5 8.0 7.5 7.0 6.5 6.0 5.5 5.0 4.5 4.0 3.5 3.0 2.5 2.0 1.5 1.0 0.5

Chemical Shift
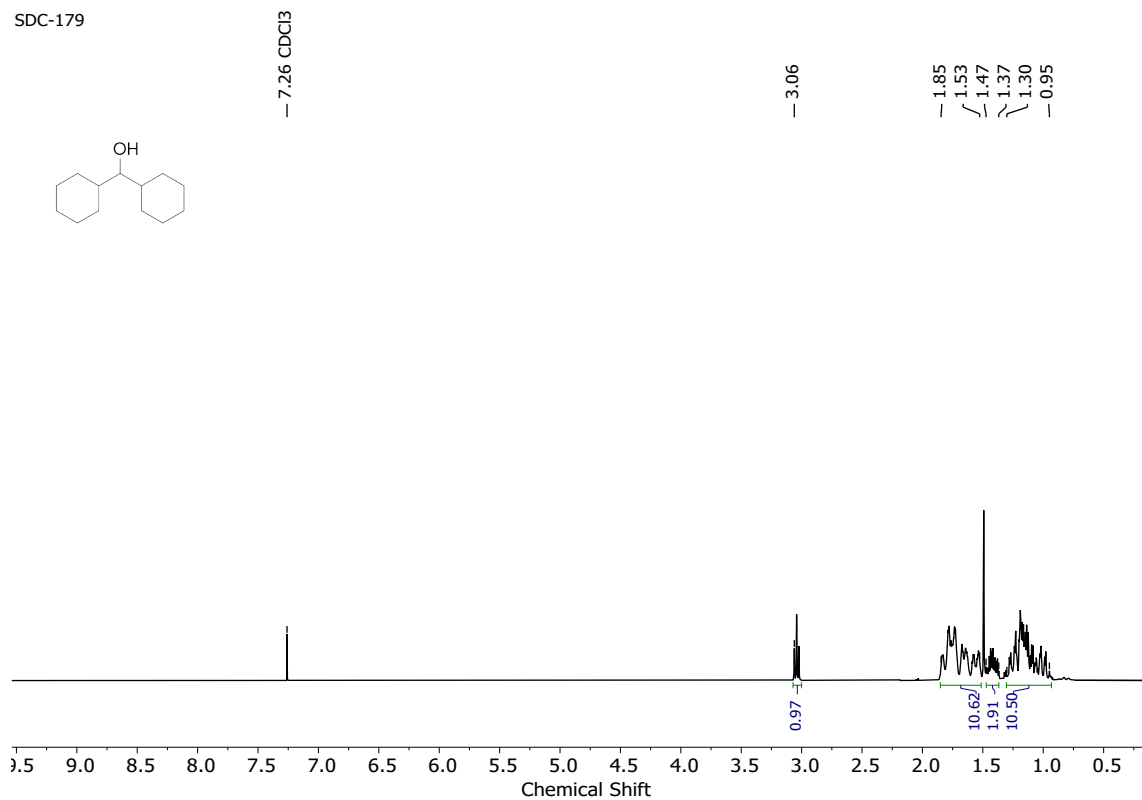
Figure S 62 ¹H NMR of **5c** (CDCl₃, 400 MHz)

SDC-179

—80.58
—77.16 CDCl3

—40.01
30.14
27.47
26.63
26.32

OH

20 210 200 190 180 170 160 150 140 130 120 110 100 90 80 70 60 50 40 30 20 10 0 -10

Chemical Shift
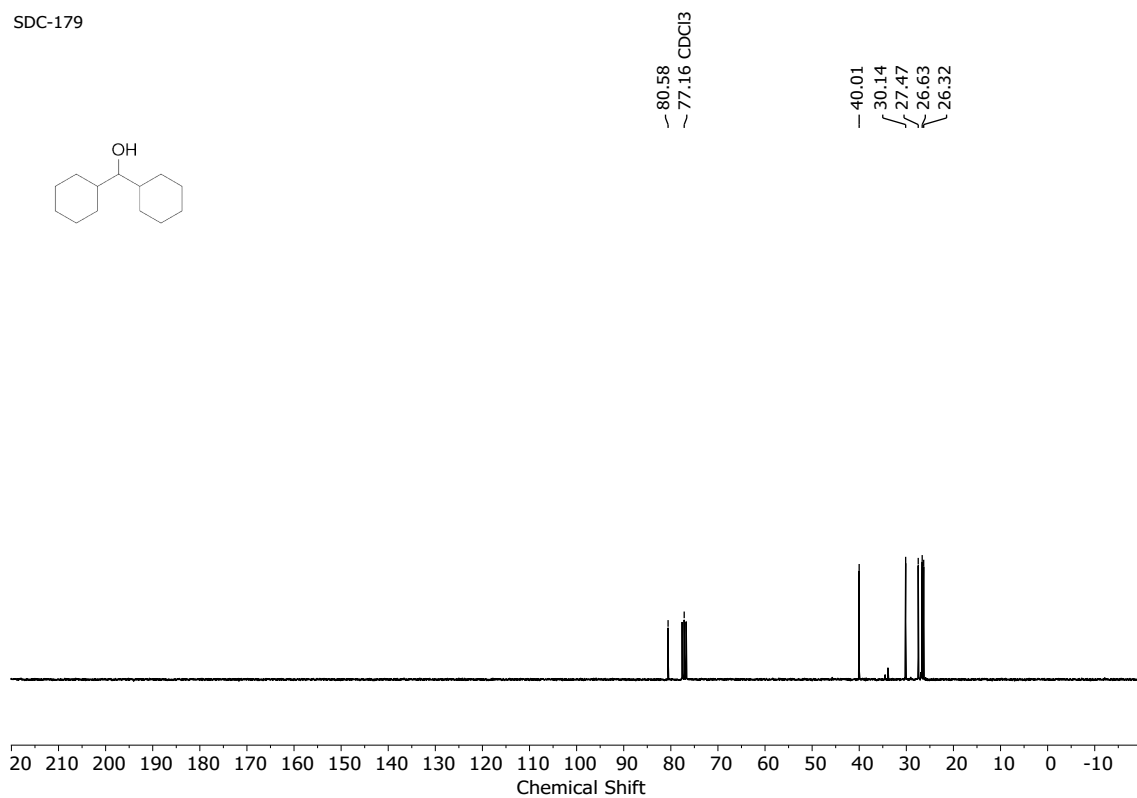
Figure S 63 ¹³C NMR of **5c** (CDCl₃, 100 MHz)

38
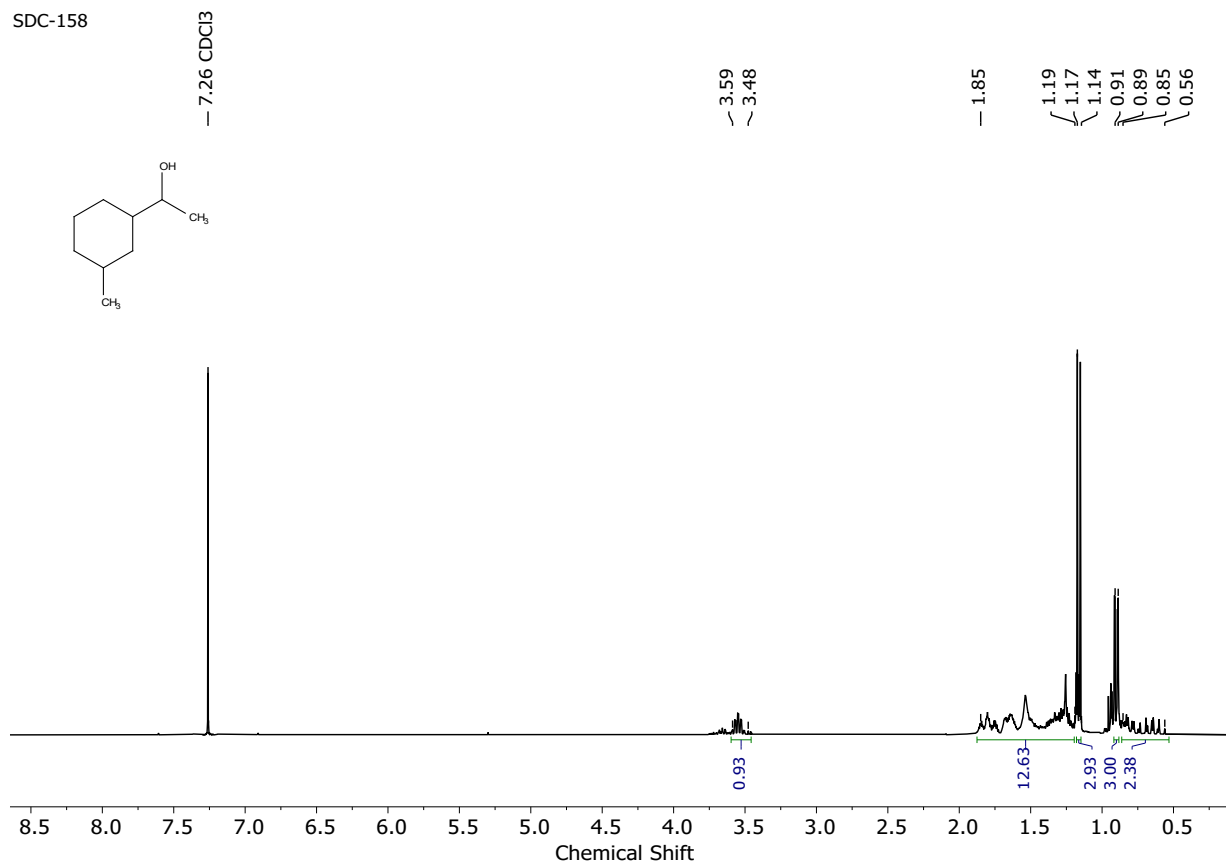
Figure S 64 ^{1}H NMR of **15c** (CDCl$_3$, 400 MHz)

SDC-158

77.16 CDCl3
72.43
44.51
37.69
35.33
27.80
25.89
22.54
20.56

80   75   70   65
Chemical Shift

77.16 CDCl3
72.43

270 250 230 210 190 170 150 130 110 90   70   50   30   10 -10
Chemical Shift
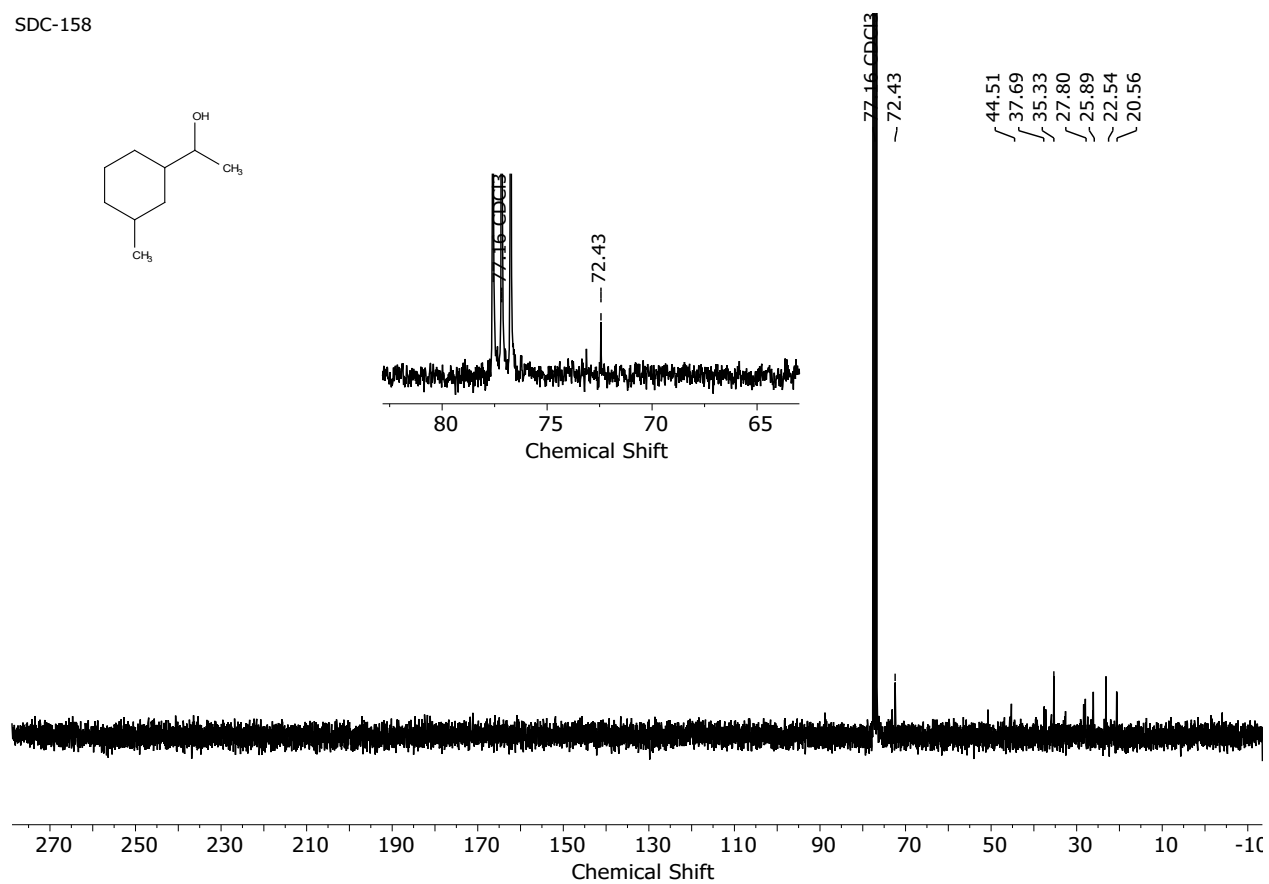
Figure S 65 ^{13}C NMR of **15c** (CDCl₃, 100 MHz)

SDC-182

7.26 CDCl3
3.03
1.79
1.49
1.40
1.19
0.93

0.97
8.81
4.26
9.00

16 15 14 13 12 11 10 9   8   7   6   5   4   3   2   1   0   -1 -2 -3
Chemical Shift
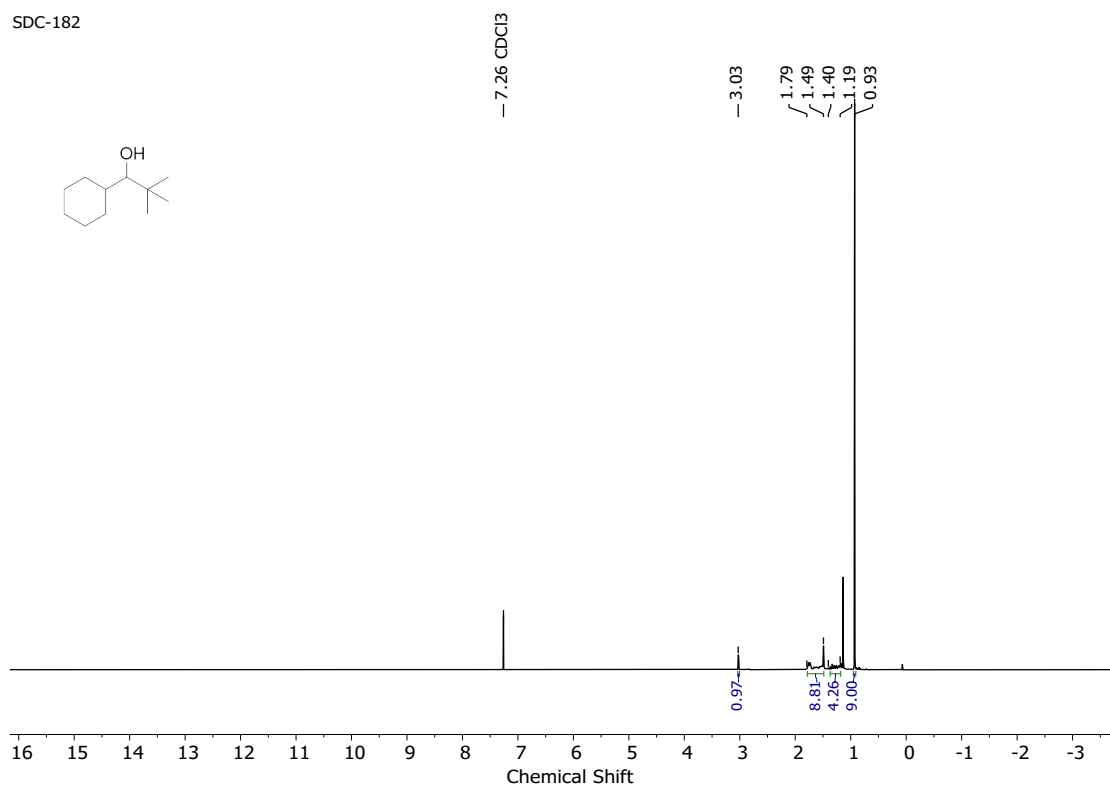
Figure S 66 ^{1}H NMR of **17c** (CDCl₃, 400 MHz)

40

SDC-182

—84.02
—77.16 CDCl3

—39.51
—36.07
—34.04
—27.40
—27.11
—26.53

—39.51
—36.07
—34.04
—27.40
—27.11
—26.53

45 40 35 30 25 20
Chemical Shift

20 210 200 190 180 170 160 150 140 130 120 110 100 90 80 70 60 50 40 30 20 10 0 -10
Chemical Shift
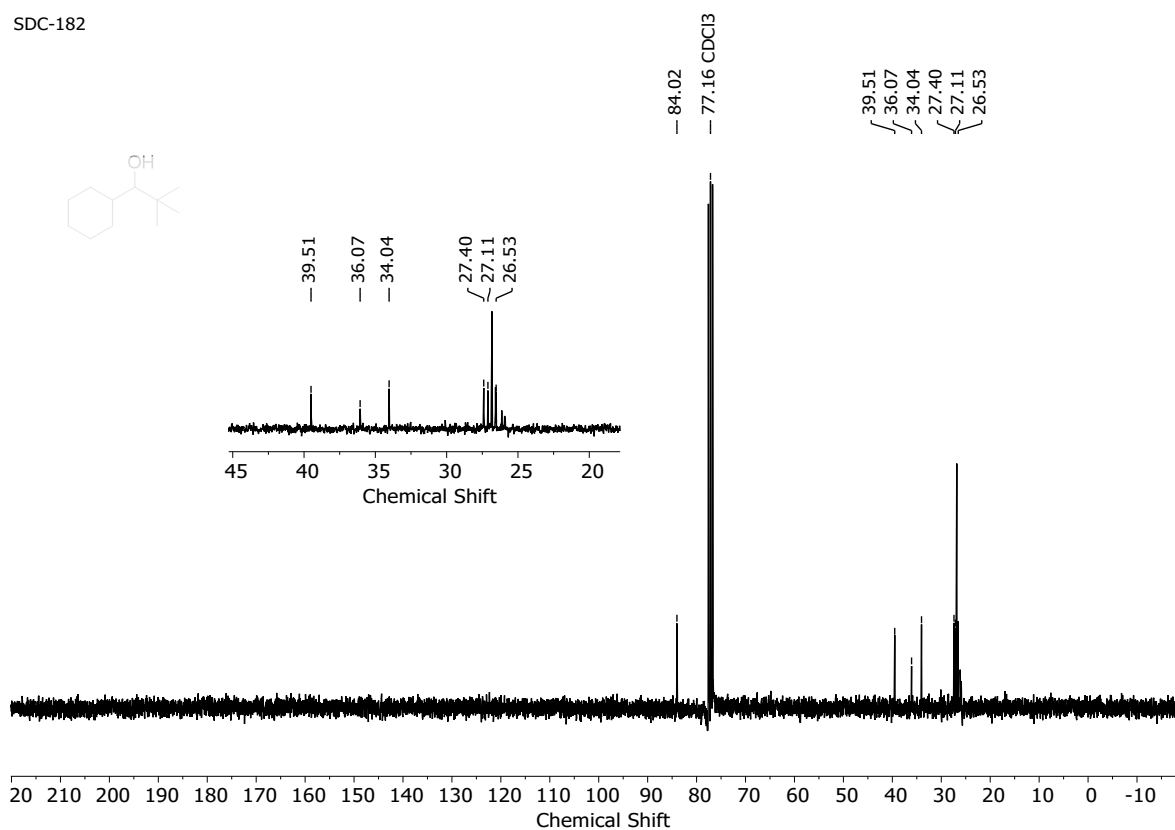
Figure S 67 ^{13}C NMR of **17c** (CDCl$_3$, 100 MHz)

SDC-181

—7.26 CDCl3

—3.93
—3.53
—2.14
—2.03
—1.93
—1.72
—1.58
—1.29
—1.22
—1.19
—1.15
—1.13
—1.08
—0.90
—0.84
—0.82

1.15
1.01
1.25
4.91
6.63
3.21
3.16
8.06
18.55

16 15 14 13 12 11 10 9 8 7 6 5 4 3 2 1 0 -1 -2 -3
Chemical Shift
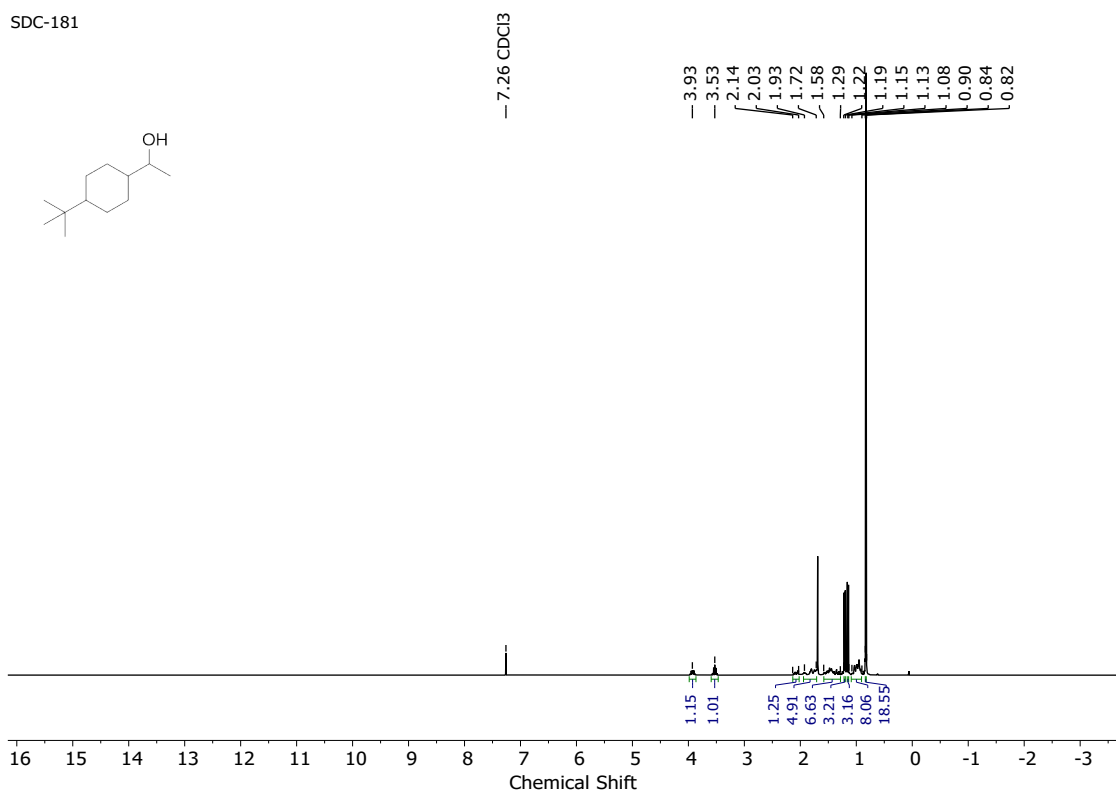
Figure S 68 ^{1}H NMR of **18c** (CDCl$_3$, 400 MHz)

SDC-181

77.45 CDCl3
77.03 CDCl3
76.60 CDCl3
72.31
66.65

48.18
48.11
45.13
41.04
32.58
29.03
28.77
28.54
27.56
27.47
27.07
27.03
26.93
22.22
21.99
21.97
20.50

210 200 190 180 170 160 150 140 130 120 110 100 90 80 70 60 50 40 30 20 10 0 -10
Chemical Shift
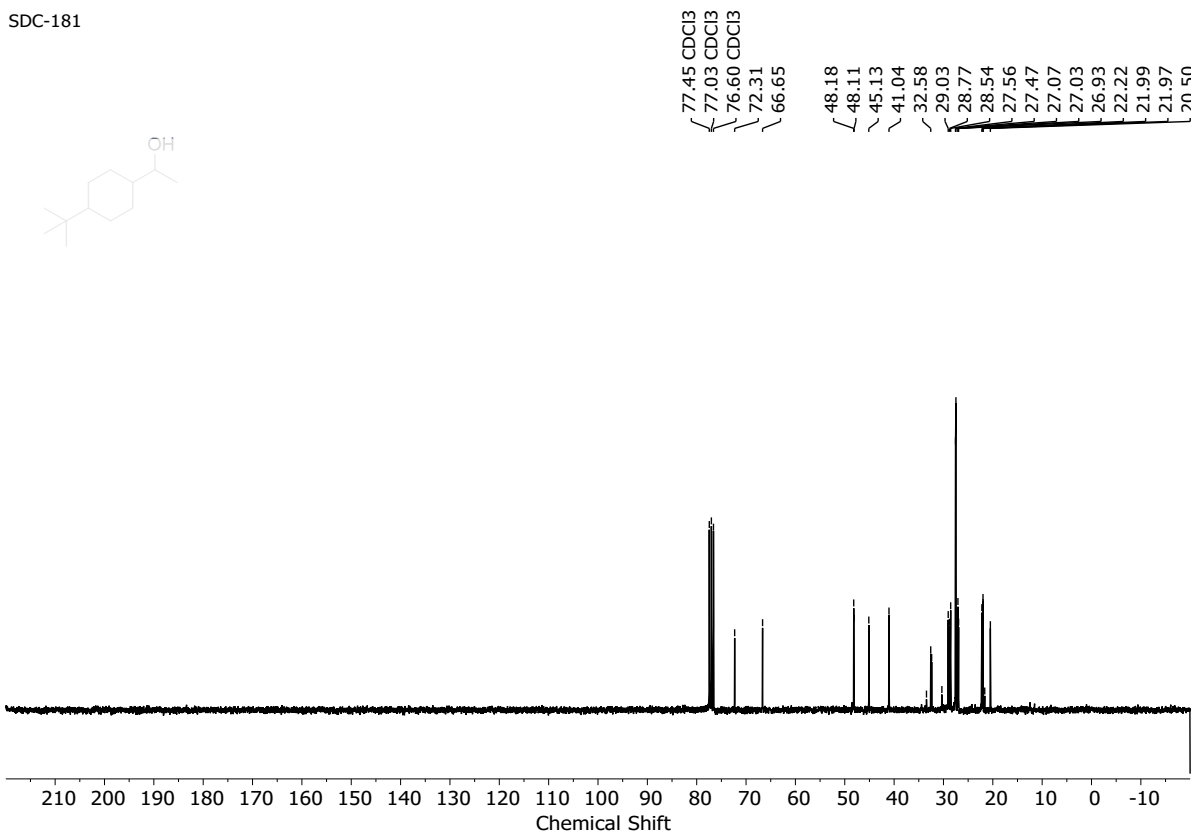
Figure S 69 ^{13}C NMR of **18c** (CDCl₃, 100 MHz)

SDC-183

7.26 CDCl3

3.73
3.54
1.94
1.87
1.77
1.70
1.60
1.51
1.44
1.37
1.19
1.17
1.14
0.93
0.87
0.86
0.85
0.84

16 15 14 13 12 11 10 9 8 7 6 5 4 3 2 1 0 -1 -2 -3
Chemical Shift

1.00
0.48
0.49
1.50
2.76
3.13
8.09
1.52
2.24
0.88
2.99
9.83
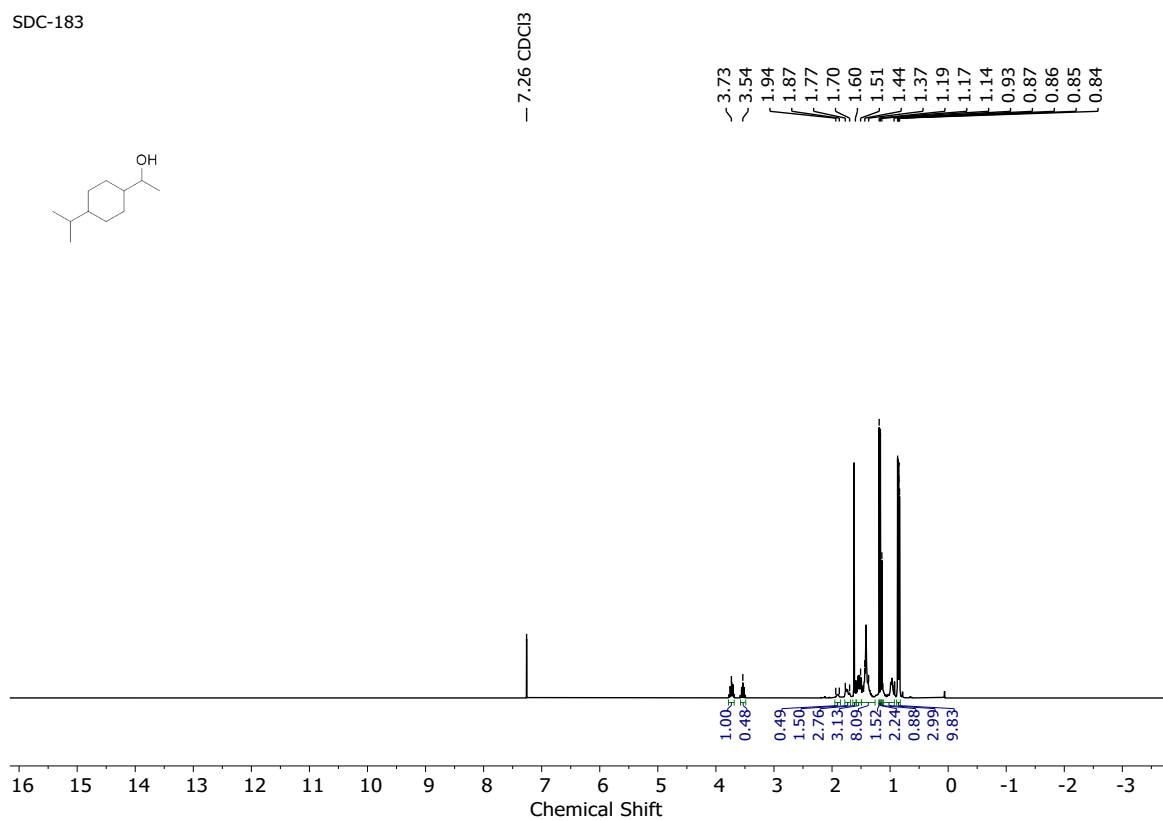
Figure S 70 ^{1}H NMR of **19c** (CDCl₃, 400 MHz)[2]

77.45 CDCl3
77.02 CDCl3
76.60 CDCl3
72.32
69.57

45.24
44.07
43.39
42.08

29.45
29.34
29.05
28.76
28.46
26.42
26.26
25.71
24.71
21.20
20.52
19.83
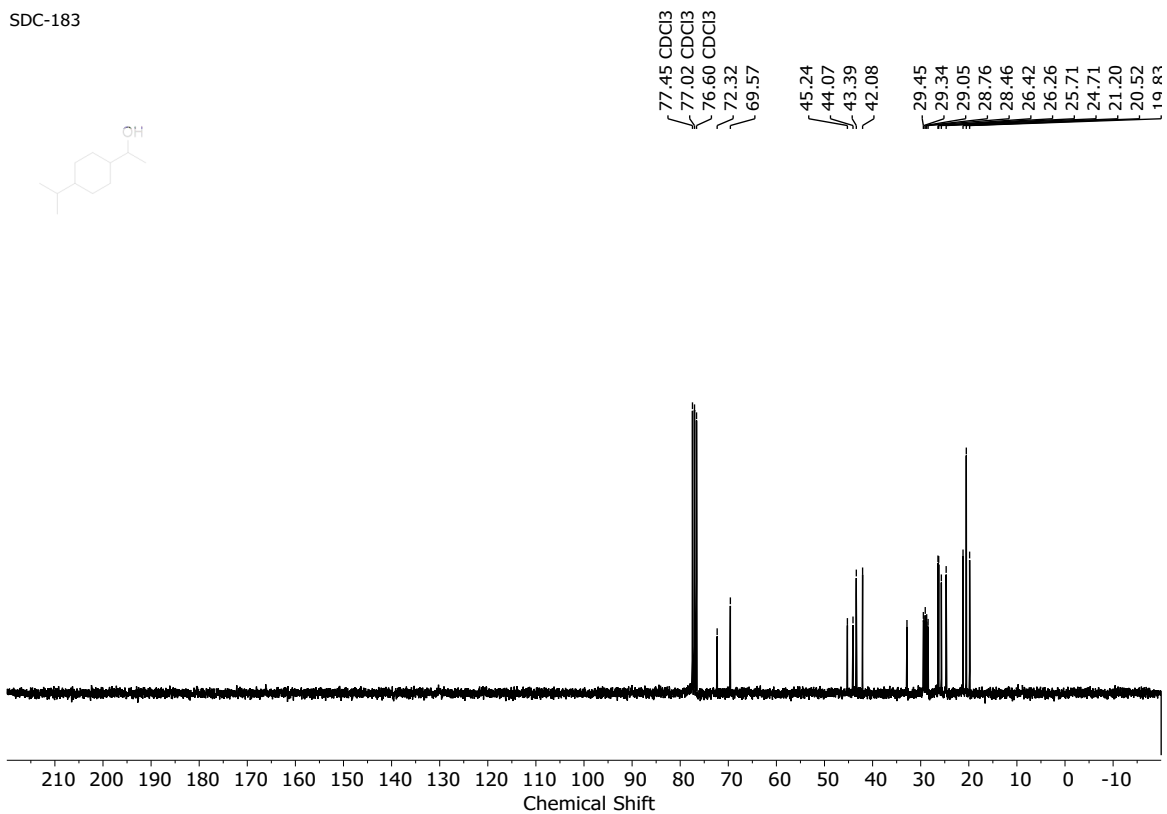
Figure S 71 ^{13}C NMR of **19c** (CDCl$_3$, 100 MHz)[2]

— 7.26 CDCl3

— 3.92

1.80
1.62
1.45
1.34
1.31
1.21
1.19
1.17
1.06
0.82

1.00

6.44
2.23
2.73
3.14
2.38
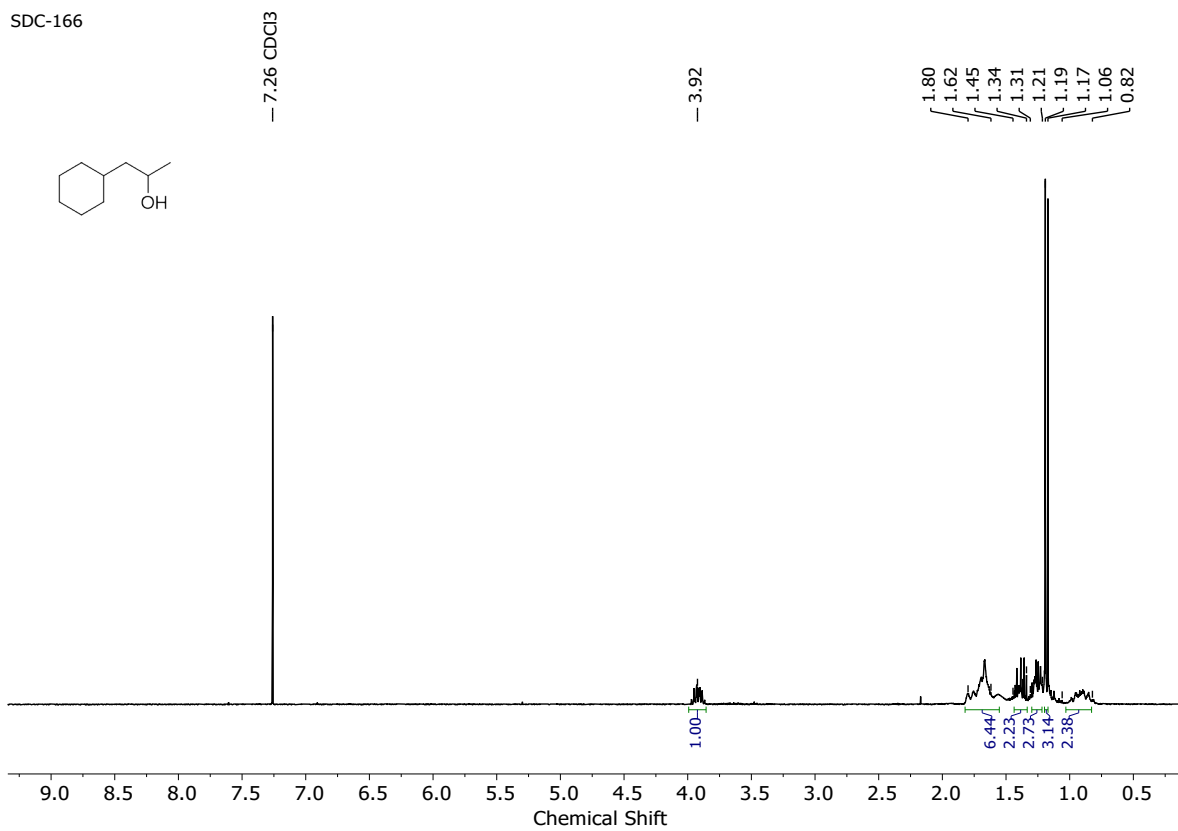
Figure S 72 ^{1}H NMR of **22c** (CDCl$_3$, 400 MHz)

43
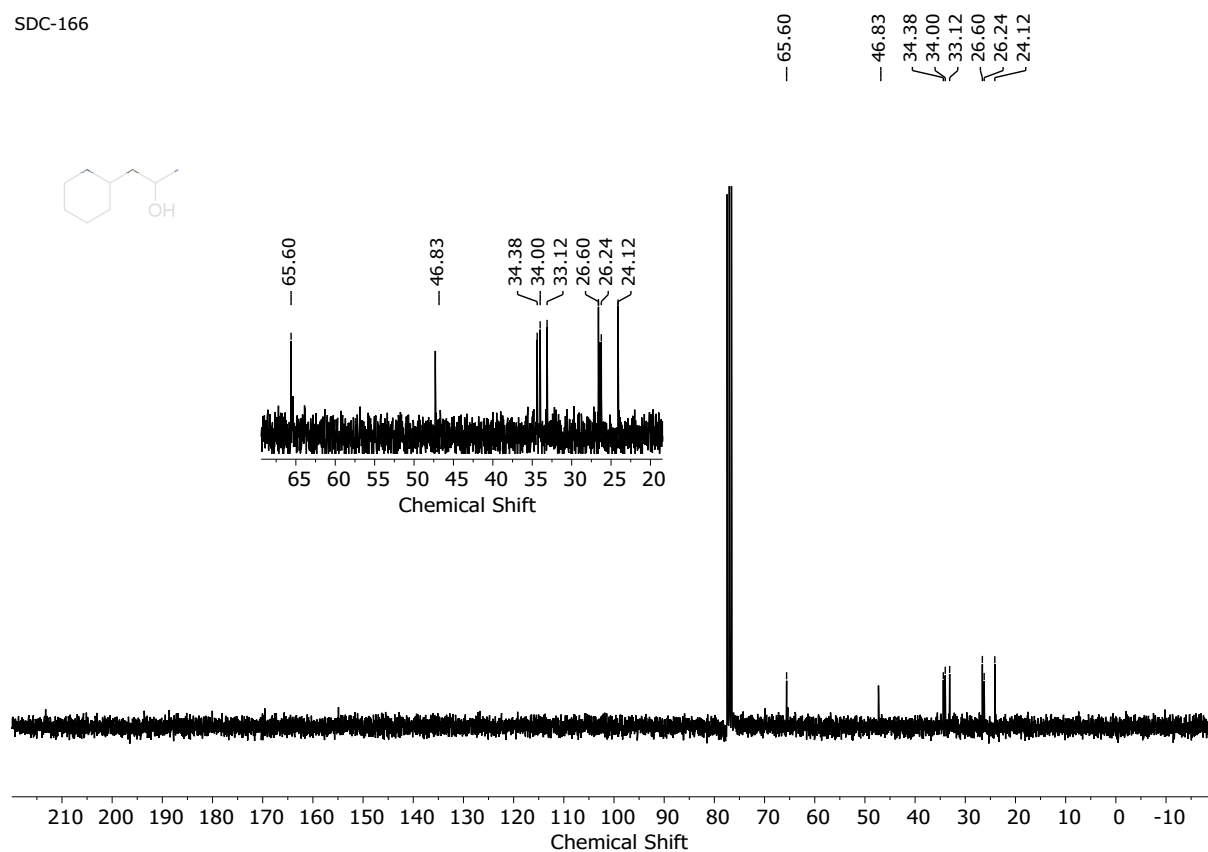
Figure S 73 ^{13}C NMR of **22c** (CDCl$_3$, 100 MHz)

17. Snapshot of a typical HDO experiment

a) RhCl$_3$ in TFE after stirring for 10-15 minutes

b) RhNPs

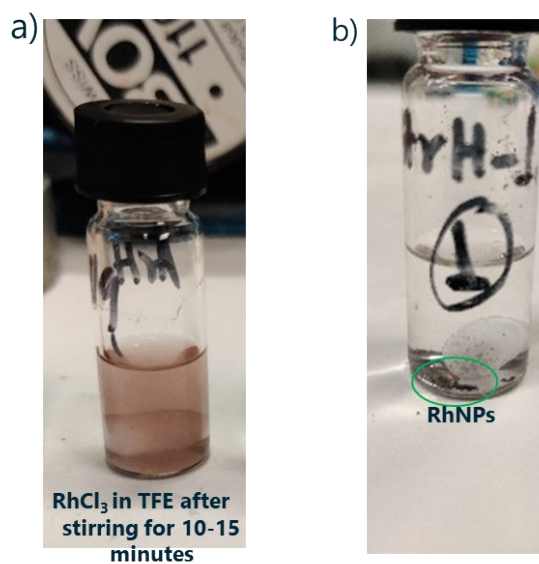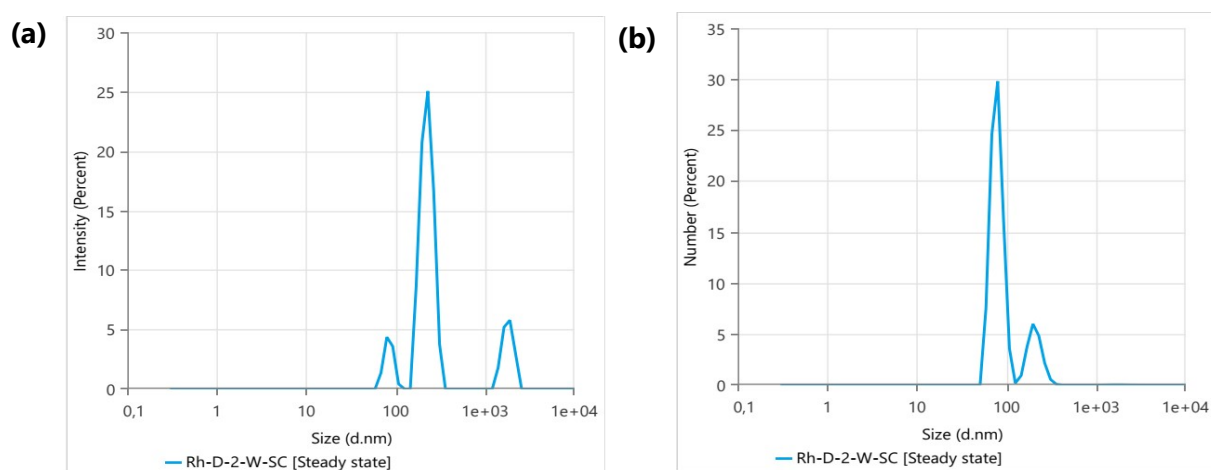*Figure S 74* Visualization of a typical hydrodeoxygenation experiment.

18. DLS analyses

The RhCl$_3$ solution (in TFE) has been prepared following the optimized reaction condition using acetophenone as a model substrate and after 1 hour of the reaction, an aliquot of sample has been taken for DLS measurements.

(a)

(b)

Figure S 75 DLS analysis of the insitu formed RhNPs (after 1 hr of the reaction, TFE, HDO condition), (a) Size distribution by Intensity, (b) Size distribution by Number, *Z (avg. in nm) = 179.8.*

19. STEM before and after 1h of catalysis

In order to investigate the formation of nanoparticles different reaction solutions of $RhCl_3$ have been prepared using acetophenone as substrate and following the optimized HDO reaction conditions. As solvents, water, ethanol, and TFE have been used. Scanning transmission electron microscopy (STEM) analysis was done before catalysis after stirring the respective solutions for 10-15 min, and after 1h hour under reaction conditions. Preparation of the grids was done by transfer of a drop of the solution onto the grid and subsequent evaporation of the solvent under ambient atmosphere without any external auxiliaries applied.

Before the reaction, no Rh nanoparticles have been observed in water or in ethanol. After evaporation, mainly Cl containing materials could be observed. Exemplary images of the trifluoroethanol solution before the reaction are shown in Figure S 76.
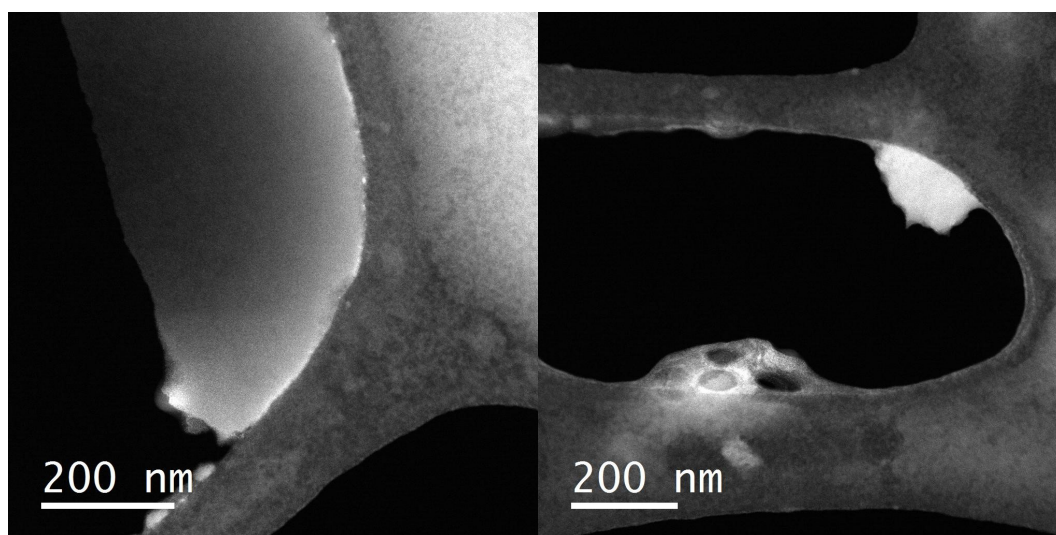

Figure S 76 Selected HAADF-STEM images after evaporation of a solution of $RhCl_3$ and acetophenone in trifluoroethanol under optimized HDO conditions before the reaction. No Rh particles could be observed in this case.

After 1 hour of reaction, the aqueous as well as the solution in TFE showed tiny black particles, which were already visible with the naked eye. Moreover, in the TFE solution a phase separation was visible with the black particles being exactly located at the interface between the immiscible phases. This was also reflected in the preparation of the TEM grid, and it was not possible to grasp some of the black particles out of the solution. However, the aqueous solution showed a more unique behaviour and all visible components of the solution could be deposited on the grid. It turned out that Rh particles were present besides the Cl⁻ containing materials that have already been observed in the two fresh samples discussed above. Selected HAADF-STEM images of this material are shown in Figure S 77, respective EDX spectra in Figure S 78.
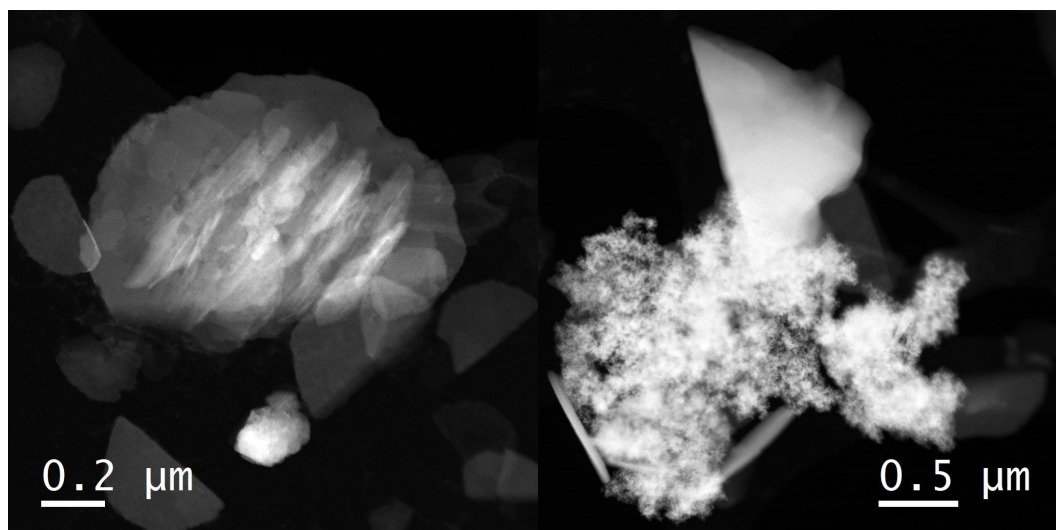
Figure S 77 Selected HAADF-STEM images after evaporation of a solution of RhCl₃ and acetophenone in trifluoroethanol (TFE) under optimized HDO conditions after 1h of reaction. Note that Rh is only visible in the right image.
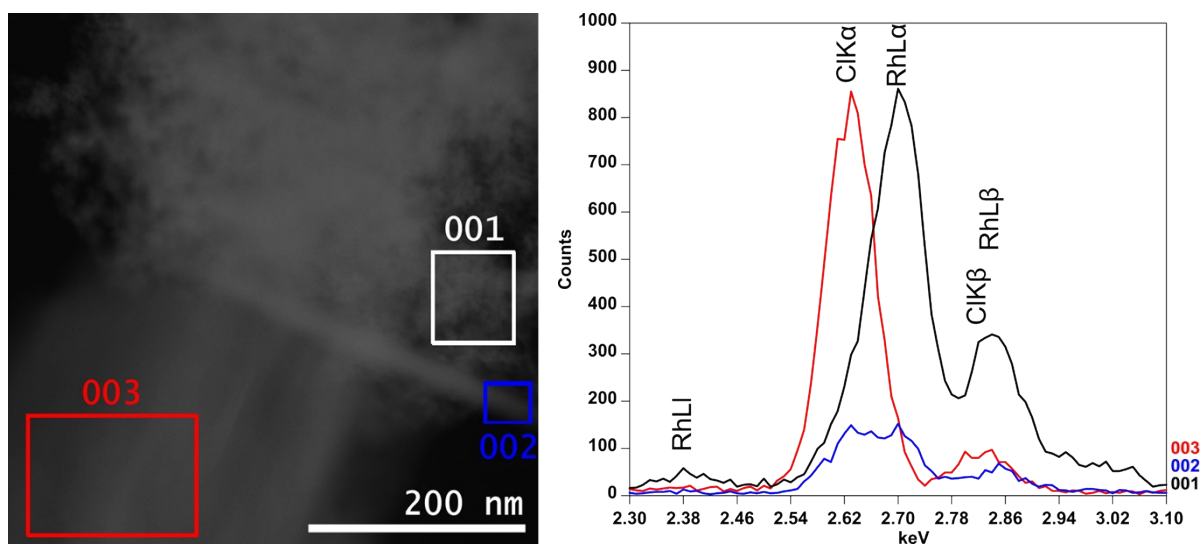
Figure S 78 Enlarged selected EDX spectra of the marked areas of the material, obtained after evaporation of a solution of RhCl₃ and acetophenone in water after 1h reaction, (left) are shown on the right. It can be clearly seen that area 001 contains exclusively Rh, while area 003 comprises only Cl and area 002 has both elements.

20. Reference

[1]   J. H. Scofield, *Journal of Electron Spectroscopy and Related Phenomena* **1976**, *8*, 129-137.

[2]   G. A. B. Vieira, T. L. G. Lemos, M. C. de Mattos, M. d. C. F. de Oliveira, V. M. M. Melo, G. de Gonzalo, V. Gotor-Fernández, V. Gotor, *Tetrahedron: Asymmetry* **2009**, *20*, 214-219.